ABSTRACT

Title of Dissertation: DEVELOPMENT AND CHARACTERIZATION OF EPSTEIN-BARR VIRUS (EBV) ANTIBODIES AND TESTING THEIR EFFICACY IN A HUMANIZED MOUSE MODEL

JungHyun Rachel Kim,
Doctor of Philosophy, 2022

Dissertation directed by: Dr. Jeffrey Cohen
Medical Virology Section,
Laboratory of Infectious Diseases,
National Institute of Allergy and Infectious Diseases,
National Institutes of Health

Epstein-Barr virus (EBV) is one of the most prevalent human viruses with more than 90% of the adult population infected with EBV. EBV is well-known to cause infectious mononucleosis, but also is associated with several B cell lymphomas and epithelial cell carcinomas. In bone marrow or solid organ transplant patients and individuals with X-linked lymphoproliferative disease,

primary EBV infection can lead to life-threatening complications. There is no licensed vaccine and even if one is available, these immunocompromised individuals might not respond well to the vaccine. Thus, an effective vaccine and therapeutic are both needed. Here, I have evaluated the efficacy of (a) EBV hyperimmune globulin isolated from healthy plasma donors with high EBV gp350 antibody and EBV B cell neutralizing titers, (b) several EBV gp350, gH/gL and gp42 monoclonal antibodies (mAbs) isolated from human plasma or vaccinated monkeys, (c) a bispecific antibody targeting both gH/gL and gp42, and (d) gH/gL and gH/gL/gp42 nanoparticle vaccines in a humanized mouse model. Animals that received hyperimmune globulin showed protection from EBV infection at a similar level as that seen in animals receiving intravenous immunoglobulin. However, humanized mice that received gH/gL mAb B10 or gp42 mAb A10 showed increased survival and reduced viremia compared to animals that received other gH/gL or gp42 mAbs. These two mAbs also demonstrated protection from development of EBV B cell lymphomas in animals. Humanized mice that received bispecific antibody derived from gH/gL mAb B10 and gp42 mAb A10 showed similar protection against EBV as animals that received the combination of the two antibodies. Passive transfer of IgG isolated from mice immunized with a gH/gL or gH/gL/gp42 nanoparticle vaccine showed reduction in viremia and no development of EBV lymphomas compared to mice that received IgG from naïve mice. These findings suggest that development of vaccines or therapeutics targeting gH/gL and/or gp42 may provide protection in healthy individuals and severely immunocompromised individuals from EBV infection and B cell lymphoma.

# DEVELOPMENT AND CHARACTERIZATION OF EPSTEIN-BARR VIRUS (EBV) ANTIBODIES AND TESTING THEIR EFFICACY IN A HUMANIZED MOUSE MODEL

by

JungHyun Rachel Kim

Dissertation submitted to the faculty of the Graduate School of the
University of Maryland, College Park in partial fulfillment
of the requirements for the degree of
Doctor of Philosophy
2022

Advisory Committee:
Xiaoping Zhu, PhD, Chair
Jeffrey Cohen, MD
Yanjin Zhang, PhD
Margaret Scull, PhD
Jeffrey DeStefano, PhD, Dean's Representative

# Dedication

I dedicate this dissertation to my husband, my parents, my parents-in-law, and my sister for their endless love and support.

# Acknowledgements

First and foremost, I would like to acknowledge my mentor, Dr. Jeffrey Cohen who has provided a tremendous support and guidance during all of my times in his lab. He is truly an inspiring mentor and passionate person. I will never forget all of patience and effort he has put in to guide me to become a mature scientist.

I also like to thank Dr. Wei Bu who has spent enormous efforts and supports to guide me in a right direction in every aspect. I've seen and learned numerous qualities to become a good scientist like him. All of his advises on my research as well as career pathways helped me to broaden my perspectives.

I appreciate all of my committee- Dr. Xiaoping Zhu, Dr. Jeffrey DeStefano, Dr. Yanjin Zhang, and Dr. Margaret Scull for their thoughtful guidance and feedback. I especially thank Dr. Zhu for all of his support and mentoring as an on-campus advisor.

I also appreciate all Cohen lab members who have been supporting my work with great advises and ideas. I especially thank Dr. Kennichi Dowdell with his help on flow cytometry and animal injections on multiple projects. His advises on my work and career pathways helped me expand my knowledge on the field.

Lastly, I cannot express my gratitude enough to my family members. Special thanks to my husband who encouraged me to pursue a Ph.D. degree and supported me with absolute love during my doctoral study. Thank you to my parents with their unconditional love and support on everything I do. Thanks to my sister who encouraged me whenever I struggled and was in need for a pep talk. I could not come this far without all of them.

This work was supported by the intramural research program of the National Institute of Allergy and Infectious Diseases, NIH.

# Table of Contents

# List of Tables

# List of Figures

# List of Abbreviations

| | |
|---|---|
| ADCC | Antibody-dependent cellular cytotoxicity |
| ADCP | Antibody-dependent cellular phagocytosis |
| AUC | Area under the curve |
| BART | BamHI-A region rightward transcript |
| BL | Burkitt lymphoma |
| BLT | Bone marrow, liver, and thymus |
| CDC | Complement-dependent cytotoxicity |
| CH | Constant domain of heavy chain |
| CL | Constant domain of light chain |
| CR2 | Complement receptor 2 |
| DNA | Deoxyribonucleic acid |
| DPBS | Dulbecco's phosphate-buffered saline |
| EBER | EBV-encoded small RNA |
| EBNA | EBV nuclear antigen |
| EBV | Epstein-Barr virus |
| ELISA | Enzyme-linked immunoassay |
| Fab | Fragment antigen binding domain |
| FBS | Fetal bovine serum |
| Fc | Fragment crystallizable domain |
| FcRn | Neonatal Fc receptors |
| FDA | Food and Drug Administration |
| GFP | Green fluorescent protein |
| GRU | Green Raji unit |
| GCSF | Granulocyte colony stimulating factor |
| GVHD | Graft-verse-host disease |
| HCMV | Human cytomegalovirus |
| H&E | Hematoxylin & Eosin |

| | |
|---|---|
| HHV-4 | Human herpesvirus 4 |
| HIS | Human immune system |
| HL | Hodgkin's lymphoma |
| HLA | Human leukocyte antigen |
| HSC | Hematopoietic stem cell |
| HVS | Herpesvirus saimiri |
| IgG | Immunoglobulin G |
| IVIG | Intravenous immunoglobulin |
| KIH | Knobs-into-holes |
| KSHV | Kaposi's sarcoma herpesvirus |
| LCL | Lymphoblastoid cell lines |
| LCV | Lymphocryptovirus |
| LIPS | Luciferase immunoprecipitation system |
| LMP | Latent membrane proteins |
| LPD | Lymphoproliferative disease |
| mAbs | Monoclonal antibodies |
| MAC | Membrane attack complex |
| MBL | Mannose-binding lectin |
| NK | Natural killer |
| NP | Nanoparticle |
| NPC | Nasopharyngeal carcinoma |
| PAGE | Polyacrylamide gel electrophoresis |
| PBL | Peripheral blood leucocyte |
| PBMC | Peripheral blood mononuclear cell |
| PBS | Phosphate buffered saline |
| PCR | Polymerase chain reaction |
| PKR | RNA-dependent protein kinase |
| PTLD | Post-transplant lymphoproliferative disease |
| qPCR | Quantitative polymerase chain reaction |
| RDV | Rhadinovirus |

| | |
|---|---|
| SCID | Severe combined immunodeficiency |
| SEC | Size-exclusion chromatography |
| SDS | Sodium dodecyl-sulfate |
| TCL | T-cell lymphoma |
| TNRF | Tumor-necrosis factor receptor |
| VH | Variable domain of heavy chain |
| VL | Variable domain of light chain |
| VLP | Virus-like particle |
| XLPD | X-linked lymphoproliferative disease |

# Chapter 1. Introduction

## 1.1 Epstein-Barr Virus

### 1.1.1 Classification and structure

Epstein-Barr virus (EBV), also known as human herpesvirus 4 (HHV-4), was the first tumor virus found in humans and belongs to the gammaherpesvirus subfamily (Munz 2019). Gammaherpesvirus can be further divided into two genera: Lymphocryptovirus (LCV) and Rhadinovirus (RDV). LCV contains EBV and rhesus lymphocryptovirus, whereas RDV contains herpesvirus saimiri (HVS) and Kaposi's sarcoma herpesvirus (KSHV) (Edelman 2005). Substantial homology is seen in the nucleotide sequences of viruses within the gammaherpesvirus subtypes, but not much homology with alpha- or betaherpesviruses (Longnecker, Kieff, Cohen, 2013). The EBV genome is a linear, double-stranded ~172 kbp DNA which encodes ~80 proteins. DNA is encapsidated in an icosahedral nucleocapsid which in turn is covered with an envelope (**Figure 1.1**). Several glycoproteins protrude from the envelope and tegument proteins are present between the nucleocapsid and the envelope (Shannon-Lowe et al., 2014). EBV is divided into two strains: type 1 and type 2. The two strains are classified based on the sequence of the EBV nuclear antigen 2 (EBNA2) gene where only 55% of protein sequence is identical between the two strains (Lucchesi et. al., 2008). Type I EBV is found worldwide but type 2 is predominant in Africa and less frequent in Europe and the United States. Type 1 EBV can also efficiently produce immortalized lymphoblastoid cell lines (LCLs) from B cells but type 2 is less efficient at producing LCLs (Lucchesi et. al., 2008).

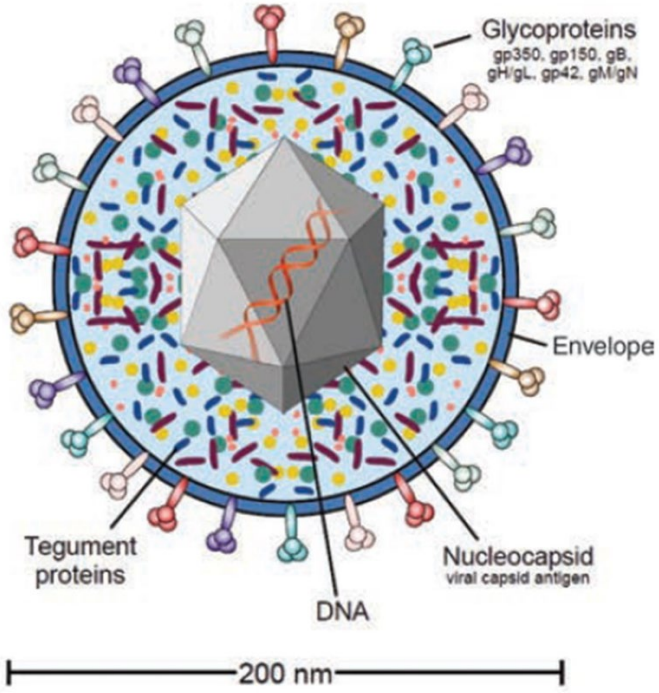


**Figure 1.1. Diagram of EBV virion.**
Linear, double stranded DNA is encapsidated in the nucleocapsid and surrounded by an envelope. Tegument proteins are between the nucleocapsid and the envelope and various glycoproteins are shown as spikes on the surface of the envelope. This figure was published in Gewurz BE, Longnecker L, Cohen JI. Epstein-Barr Virus. In: Knipe DM, Howley PM, Cohen JI, Damania B, Whelan SPJ, Enquist L, Freed EO. Fields Virology, 7th edition. Philadelphia, Wolters Kluwer 2022, 324-388.

### 1.1.2 Epidemiology

EBV is one of the most prevalent viruses in humans and more than 90% of adults are infected with EBV (Cohen et al., 2011). EBV is well-known to cause infectious mononucleosis and is also associated with ~200,000 new cases of cancer each year worldwide. These cancers include B cell lymphomas such as Burkitt and Hodgkin lymphoma, and epithelial cell malignancies such as nasopharyngeal and gastric carcinomas (Cohen et al., 2011). In immunocompromised patients undergoing solid organ or bone marrow transplant, EBV infection is responsible for >70% of cases of post-transplant lymphoproliferative disorder (PTLD) (San-Juan et al., 2014). In solid organ transplantation patients, the higher risk of developing a PTLD is

in first two years after transplantation (Wistinghausen, Gross, and Bollard, 2013). This time frame for development of PTLD is even shorter for patients undergoing bone marrow transplantation which is usually within one year of transplantation (Fujimoto and Suzuki, 2020). Also, the frequency of PTLD in EBV seronegative persons is 24- to 33-fold higher after transplant than in EBV seropositive persons (Preiksaitis and Cockfield, 1998). EBV infection can also be fatal to individuals with certain primary immunodeficiencies such as boys with X-linked lymphoproliferative disorder (Cohen, 2015). Currently, there is no licensed prophylactic or therapeutic vaccine.

### 1.1.3 Viral entry and spread

There are two major cell types that EBV infect in vivo: B cells and epithelial cells (**Figure 1.2**). During B cell infection, EBV glycoprotein 350/220 first attaches to B cells via complement receptor 2 (CR2), also known as CD21 (Fingeroth et al., 1984). gp350 and gp220 are encoded from the same mRNA, but gp220 is generated from a single splice variant. Both gp350 and gp220 contain the domain that binds to CR2. Binding of gp350/220 to CR2 allows EBV to attach to the cells. EBV gH/gL/gp42 forms a heterotrimer which binds to HLA class II on B cells (Spriggs et al., 1996). Binding of the gH/gL/gp42 complex to the B cell activates EBV gB, to fuse viral and plasma membranes together to allow virions to enter the cells (McShane and Longnecker, 2004).

In epithelial cell infection, BMRF2 plays a similar role as gp350/220 where BMRF2 tethers the viral membrane to host cell plasma membrane by binding to integrins on the plasma membrane (Tugizov et al., 2003). This binding activates gH/gL to bind to ephrin receptor A2 and

integrin receptors on the target cells and allows gB to fuse the viral and host cell plasma membranes together (Zhang et al., 2018).

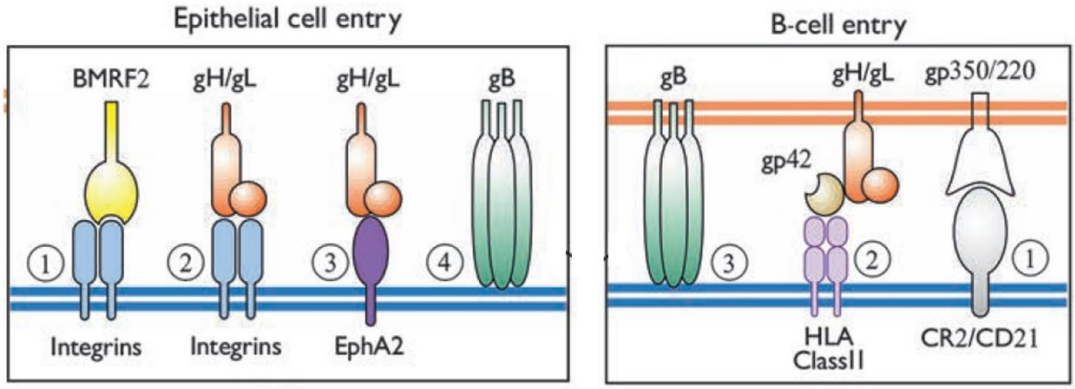


**Figure 1.2. EBV B cell and epithelial cell entry.**
During epithelial cell entry, BMRF2 attaches to cells, and gH/gL bind to integrins and Ephrin A2 receptors on epithelial cells. For B cell entry, gp350/220 attaches to cells, and gH/gL, gp42, and gB interact with each to allow virus entry. This figure was published in Gewurz BE, Longnecker L, Cohen JI. Epstein-Barr Virus. In: Knipe DM, Howley PM, Cohen JI, Damania B, Whelan SPJ, Enquist L, Freed EO. Fields Virology, 7th edition. Philadelphia, Wolters Kluwer 2022, 324-388.

In humans, EBV is spread mainly through contact with saliva from infected persons (Cohen, 2000). During primary infection, virus particles in the saliva infect epithelial cells in the oropharynx followed by virus replication in epithelial cells and infection of resting, naïve B cells that traffic through the oropharynx (**Figure 1.3**). EBV can also directly infect resting, naïve B cells in the tonsillar crypts. Some of the infected B cells undergo lytic infection and actively spread infectious virus particles, but most B cells become latently infected. The EBV genome remains as an episome that does not produce infectious viral particles but has the potential to reactivate anytime. One interesting aspect of EBV is its ability to immortalize B cells. EBV infected latent B cells can proliferate indefinitely as LCLs in vitro (Longnecker, Kieff, Cohen, 2013).

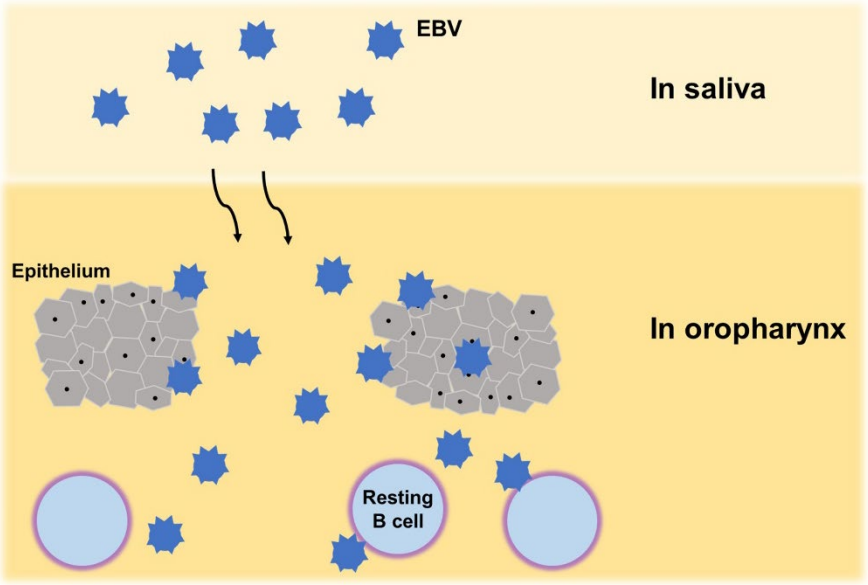


**Figure 1.3. Diagram of EBV primary infection.**
EBV particles in the saliva enters through the oropharynx and infect epithelial cells and nearby resting B cells. Infected B cells either go through lytic infection or become latently infected cells.

### 1.1.4 Latent infection

One of the most interesting aspects of gammaherpesvirus is its establishment of latent infection in B cells. After primary infection, the viral genome resides in the host's memory B cells for the lifetime by staying silently with a limited expression of a subset of viral latent genes (Young and Murray, 2003; Hatton et al., 2014). In cell culture, persistent presence of viral genome in the host cells can be accomplished by immortalization of EBV as LCLs (Young and Murray, 2003). During latency, EBV genomes express EBV-encoded nuclear antigens (EBNA-1, 2, and 3A-3C), latent membrane proteins (LMP1 and LMP 2A and 2B), EBNA-leader protein (EBNA-LP), EBV-encoded small RNAs (EBER1 and 2), and non-transcribed BART (BamHI-A region rightward transcript) RNAs (Kang and Kieff, 2015). After primary infection, latent infection can be divided into three types depending on the pattern of viral gene expression

(**Table 1.1**). Different patterns of latent gene expression are critical for growth and survival of EBV-associated malignancies. Type 1 latency is most common in Burkitt lymphoma tumors while type 2 latency is commonly found in nasopharyngeal carcinomas (Kang and Kieff, 2015). Type 0 latency, in which some viral RNAs, but no viral protein expression is found in healthy persons previously infected with EBV. Type 3 latency is found in post-transplant lymphoproliferative disease tissues.

| Latency | EBERs | EBNA-1 | EBNA-2 | EBNA-3 | EBNA-LP | LMP1 | LMP2 | Disease |
|---|---|---|---|---|---|---|---|---|
| 0 | + | - | - | - | - | - | - | Blood in healthy EBV seropositive individuals |
| 1 | + | + | - | - | - | - | - | Burkitt lymphoma, gastric carcinoma |
| 2 | + | + | - | - | - | + | + | Nasopharyngeal carcinoma, Hodgkin lymphoma |
| 3 | + | + | + | + | + | + | + | Post-transplant lymphoproliferative disease |

**Table 1.1. EBV latency gene expression patterns.**
Different latency genes are expressed in each type of latency and these types are often specific to certain diseases.

### 1.1.5 Latent genes

EBNA-1 is expressed in latency types 1-3 and required for episome replication and maintenance of the episomal genome when EBV infected B cells divide (Kang and Kieff, 2015; Young and Murray, 2003). EBNA1 is the only gene that is expressed during both lytic and latent infection (Sivachandran et al., 2012). Recently, research demonstrated that EBNA-1 may have an important role in multiple sclerosis (Lanz et al., 2022).

EBNA-2 and EBNA-LP are known to be co-expressed and involved in activation of viral and cellular gene transcription by working cooperatively (Kang and Kieff, 2015). These two genes are essential for B-cell transformation in LCLs (Cohen et al., 1989; Mannick et al., 1991).

EBNA-3A, -3B, and 3-C regulate host transcription and have the same promoter and similar gene structures (Kang and Kieff, 2015). All three EBNA-3s are coactivators of EBNA-2, but EBNA-3C can also function as a corepressor (Lin et al., 2002). EBNA-3B is the only gene that is dispensable while EBNA-3A and 3C are essential for B-cell transformation in vitro (Kang and Kieff, 2015).

LMP-1 is a major EBV-encoded oncogene and is critical for EBV-induced B-cell transformation in vitro (Young and Murray, 2003). LMP1 can function as a tumor-necrosis factor receptor (TNFR) and activates various signaling pathways such as NF-κB or JAK/STAT pathways (Paine et al., 1995; Gires et al., 1999). LMP-2A and 2B are both non-essential for B cell transformation but LMP-2A promotes B-cell growth by blocking B-cell receptor signaling and induction of lytic infection (Miller et al., 1995; Longnecker, 2000). LMP-2B interferes and negatively regulates LMP-2A by promoting the switch from latent to lytic EBV replication (Rechsteiner et al., 2008).

EBER1 and 2 are expressed in all types of latency and are the most abundantly expressed EBV genes in latently infected cells (Young and Murray, 2003; Kang and Kieff, 2015). EBERs use host RNA polymerase III to transcribe (Rosa et al., 1981). EBERs show resistance to IFNα-induced apoptosis by inhibiting RNA-dependent protein kinase (PKR) (Nanbo and Takada, 2002). PKR is a mediator of the antiviral effects of the interferons and inhibition of PKR could be an antiviral strategy against viral persistence (Clemens et al., 1994).

## 1.2 Antibody

### 1.2.1 Overview

Monoclonal antibodies (mAbs) have been developed to treat many diseases. Antibodies are secreted from B cells to mediate humoral immunity when the body is exposed to foreign substances such as viruses or bacteria (Xu et al., 2014). Antibodies can recognize diverse and specific foreign pathogens. There are two forms of antibodies: membrane-bound antibodies and secreted antibodies (**Figure 1.4**). Membrane-bound antibodies are on the surface of B cells and have a C-terminal transmembrane domain that is anchored on the plasma membrane (Abbas et al., 2011). These antibodies can function as receptors for specific antigens. Secreted antibodies are present in the tissues, blood, and mucosal sites and prevent entry of pathogens into cells and help to eliminate pathogen-infected cells. Secreted antibodies are involved in Fc-mediated effector functions such as antibody-dependent cellular cytotoxicity (ADCC) and antibody-dependent cellular phagocytosis (ADCP).

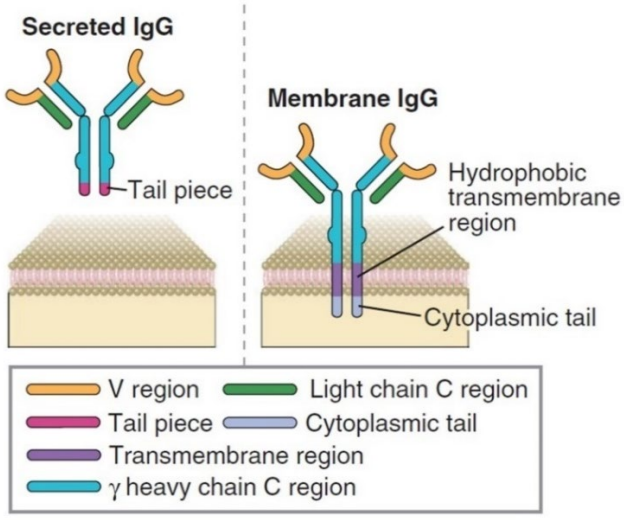


**Figure 1.4. Two forms of antibodies.**
Antibodies can be present in secreted or membrane forms. In secreted antibodies, the heavy chain ends with tail piece while in membrane antibodies, the C-terminal transmembrane domain is anchored on the plasma membrane of B cells. This figure was published in Abbas AK, Lichtman AH, Pillai S. Antibodies and Antigens. Cellular and Molecular Immunology, 7th edition. Philadelphia, Elsevier Saunders 2012, 89-107.

### 1.2.2 Structure of antibodies

The structure of a typical antibody is composed of two heavy chains and two light chains with an identical symmetry on each side to form a heterodimer (Litman et al., 1993) (**Figure 1.5**). Light chains of human immunoglobulin can be divided into two functionally similar classes, κ or λ; both classes are composed of a constant domain (CL) and a variable domain (VL) (Chiu et al., 2019). The heavy chain of human immunoglobulins can be divided into 5 isotypes, IgA, IgD, IgE, IgG, and IgM, and each isotype has different functions (Brezski and Georgiou, 2016). IgA, IgD, and IgG have three constant domains (CH) and one variable domain (VH) and IgE and IgM have four CHs and one VH (Chiu et al., 2019). IgM, the first antibody produced after encounter with an antigen, is found as a pentamer and activates the complement system (Janeway et al., 2001). IgA is secreted as monomers, dimers, and trimers and is involved in mucosal immunity (Woof and Kerr, 2005). IgE is found in monomers and involved in immunity to parasites and can cause hypersensitive reactions to allergens (Sutton et al., 2019). IgG is most abundant antibody in humans and found in monomers. IgG can clear pathogens by neutralization, opsonization, complement activation, and cell-mediated cytotoxicity (Forthal 2014). The function of IgD is still unknown.

IgG can further be divided into two fragment antigen binding domains (Fabs) and one fragment crystallizable (Fc) domain (**Figure 1.5**). The Fab fragments are composed of VL-CL paired with VH-CH1 and the Fc fragment contains CH2-CH3 segments. Fab and Fc fragments are linked by a hinge region that allows Fabs to be flexible and proteases can cleave this region into Fab and Fc fragments (Stanfield and Wilson, 2014). Each Fab fragment has identical antigen-binding sites that can bind a specific target antigen and the Fc region can trigger

different effector functions by binding to various receptors on cells (e.g. macrophages, NK cells) (Chiu et al., 2019).

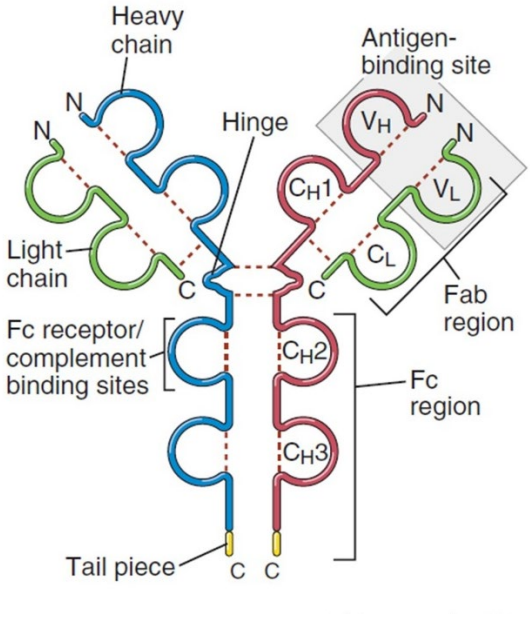


**Figure 1.5. Structure of an antibody.**
An antibody is composed of heavy and light chains which each contain variable and constant regions. An antibody can also be cleaved into Fab and Fc fragments by proteases. This figure was published in Abbas AK, Lichtman AH, Pillai S. Antibodies and Antigens. Cellular and Molecular Immunology, 7th edition. Philadelphia, Elsevier Saunders 2012, 89-107.

The function of Fab and Fc domains was identified by proteolytic cleavage of IgG into multiple fragments. When papain is added to an IgG, it digests the hinge region between the CH1 and CH2 domains of the heavy chain leading to three fragments, two Fab fragments and one Fc fragment (**Figure 1.6**). If pepsin is added to the IgG, it cleaves a region below the hinge region and produces one $F(ab')_2$ fragment with the rest of heavy chain digested in pieces.

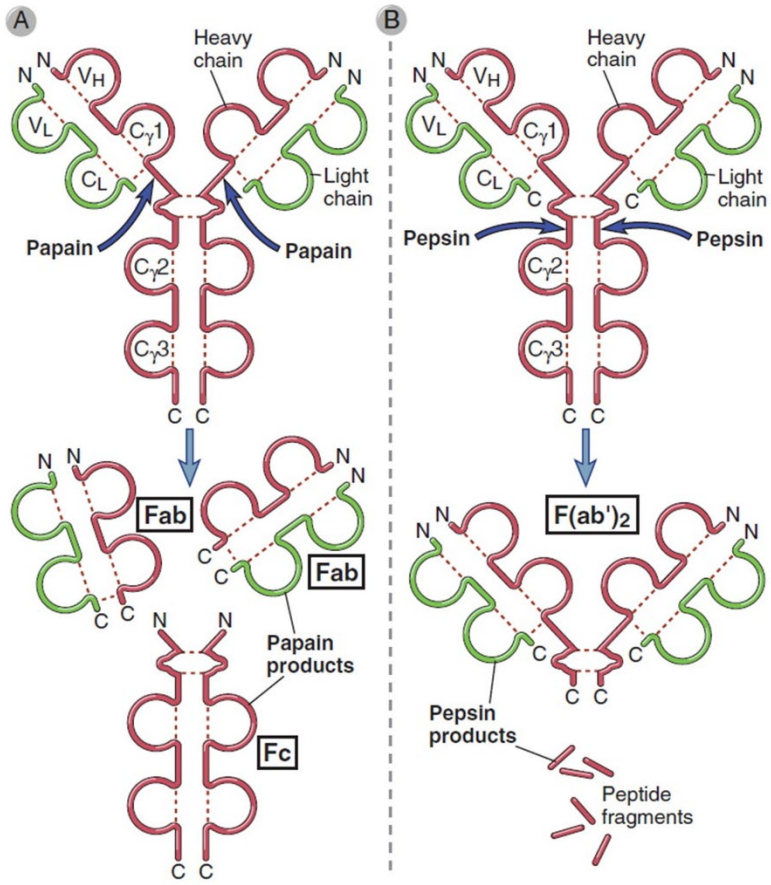


**Figure 1.6. Cleaved fragments of IgG.**
Digestion with papain produces two Fab fragments and one Fc fragment while pepsin produces one $F(ab')_2$ fragment with the rest of heavy chain digested in peptide fragments. This figure was published in Abbas AK, Lichtman AH, Pillai S. Antibodies and Antigens. Cellular and Molecular Immunology, 7th edition. Philadelphia, Elsevier Saunders 2012, 89-107.

### 1.2.3 Half-life of antibodies

The half-life of antibodies in the blood differs based on their isotypes. IgE has the shortest half-life of 2 days in the circulation, while IgA has a half-life of 3 days and IgM of 4 days (Abbas et al., 2011). IgG has the longest half-live of 21 to 28 days in humans. The long half-life of IgG is due to its ability to bind to neonatal Fc receptor (FcRn). FcRn transports maternal IgG through the placenta to the fetus (Roopenian et al., 2007). Circulating IgG in the

blood gets endocytosed into early endosomes (**Figure 1.7**). To prevent IgG from degradation due to acidic conditions in the endosome, IgG binds to FcRn and recycles back out to the extracellular space as an IgG-FcRn complex. The neutral pH condition of the extracellular space allows IgG to fall off from the complex and circulates again back into the blood. To increase the half-life of mAbs developed as therapeutics, several of mutations at the Fc fragment of IgG were discovered to increase their binding to FcRn. The LS mutation (M428L / N434S) in an IgG Fc fragment is one of the widely used mutations to increase the half-live of the IgG molecule (Ko et al., 2014).

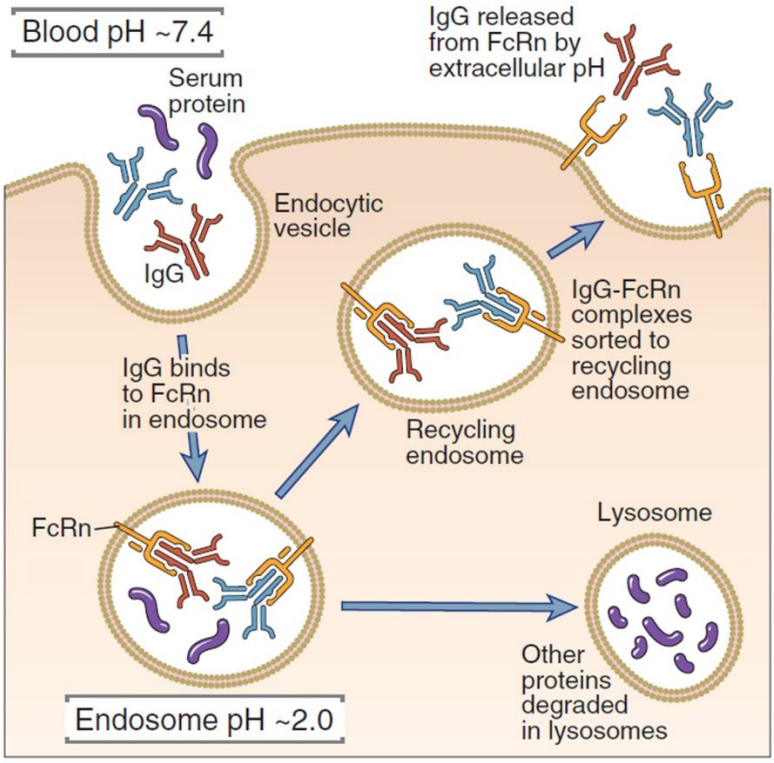


**Figure 1.7. Recycling of IgG by FcRn to increase half-life of antibodies.**
IgG binds to the FcRn in the endosome to prevent degradation due to low pH condition in the endosome. IgG-FcRn complexes are recycled back into blood and IgG is released. This figure was published in Abbas AK, Lichtman AH, Pillai S. Antibodies and Antigens. Cellular and Molecular Immunology, 7th edition. Philadelphia, Elsevier Saunders 2012, 89-107.

### 1.2.4 Monoclonal antibodies

The discovery of monoclonal antibodies (mAbs), antibodies that produce a single specificity and target one epitope on the antigen, by tumor cells led to a significant advancement in clinical medicine. Development of a method to produce one specific antibody in a large quantity allowed mAbs to be used as medical diagnostics and therapeutics. Currently, there are more than 100 FDA-approved mAbs (Mullard 2021) in various formats. Traditional canonical antibodies are the most commonly approved forms, but other formats such as antibody-drug conjugates or fragments have also been approved.

### 1.2.5 Bispecific antibodies

Lately, efforts to develop bispecific antibodies have been increasing. Unlike traditional mAbs where both arms of an antibody target one epitope, bispecific antibodies can be engineered to target two different epitopes, either on the same antigen or different antigens (Brinkmann and Kontermann, 2017). Initially, bispecific antibodies were developed for cancer therapy, but development has been widening to other fields such as chronic inflammatory diseases, autoimmunity, neurodegeneration, bleeding disorders, and infections (Brinkmann and Kontermann, 2017). Currently, there are more than 110 types of bispecific antibodies in various stages of clinical trials (Ma et al., 2021). Advantages of bispecific antibodies are that they can promote higher binding specificity by interacting with two different epitopes compared to one and they can also simultaneously block receptors at different pathways of infection (Fan et al., 2015). Bispecific antibodies may also reduce the cost of manufacturing as only one product needs to be manufactured compared to two mAbs (Sedykh et al., 2018). Unlike traditional mAbs, bispecific antibodies can be assembled into numerous formats as they require two different heavy chains and two different light chains (Brinkmann and Kontermann, 2017). The format of

bispecific antibodies can be largely divided into an asymmetric or a symmetric architecture (Brinkmann and Kontermann, 2017). The presence or absence of a Fc region and mutations in the Fc region adds more possibilities to assemble into different formats. Active studies are ongoing to find a way to increase the possibility of pairing heavy and light chains into the desired product. One common technology used in the field is the so-called "knobs-into-holes" (KIH) structure (**Figure 1.8**). By introducing mutations in the CH3 domains of each heavy chain, this increases the chance of forming heterodimers between two heavy chains like knobs into holes (Krah et al., 2018). Despite the intense effort to find methods to produce bispecific antibodies, it is still difficult to manufacture products that are homogenous and that stably express with high purity (Fan et al., 2015). Currently, there are only four FDA-approved bispecific antibodies (Ma et al., 2021).

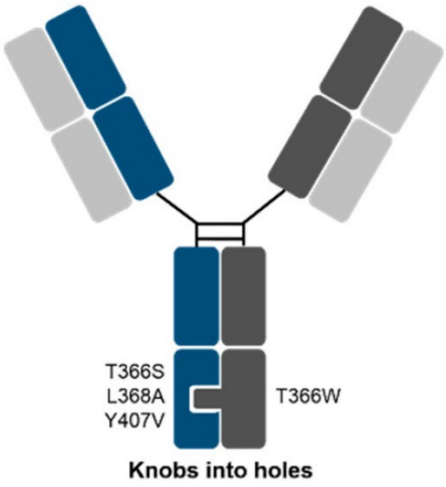


**Figure 1.8. Bispecific antibody with knobs-into-holes mutations.**
Three mutations on the CH3 domain of antibody 1 and one mutation on the CH3 domain of antibody 2 increase the chance of two heavy chains to form heterodimers. This figure was published in Krah, S., Kolmar, H., Becker, S., and Zielonka, S. (2018). Engineering IgG-like bispecific antibodies-an overview. *Antibodies*. 7, 28.

### 1.2.6 Bispecific mAb in CrossMAb format

CrossMAb technology is the crossover of the antibody heavy and light chain domains in one of the Fab arms of a bispecific IgG to enable a correct assembly of heavy and light chains (**Figure 1.9**). There are three types of crossovers. First, CrossMAb$^{Fab}$ exchanges the complete Fab domain of heavy and light chains but can also form side products that include a non-functional monovalent antibody by the VH-CH1 and VL-CL domains and Fab from the 2 parental antibodies. Second, CrossMAb$^{VH-VL}$ exchanges variable regions of heavy and light chains. This crossover type can also produce a side product called Bence-Jones proteins where a normal light chain with variable and constant regions is paired with a crossed Fab-arm (VL-CH1). Finally, CrossMAb$^{CH1-CL}$ exchanges a constant domain of a light chain with a CH1 domain of a heavy chain. This is the only type that does not produce a side product.

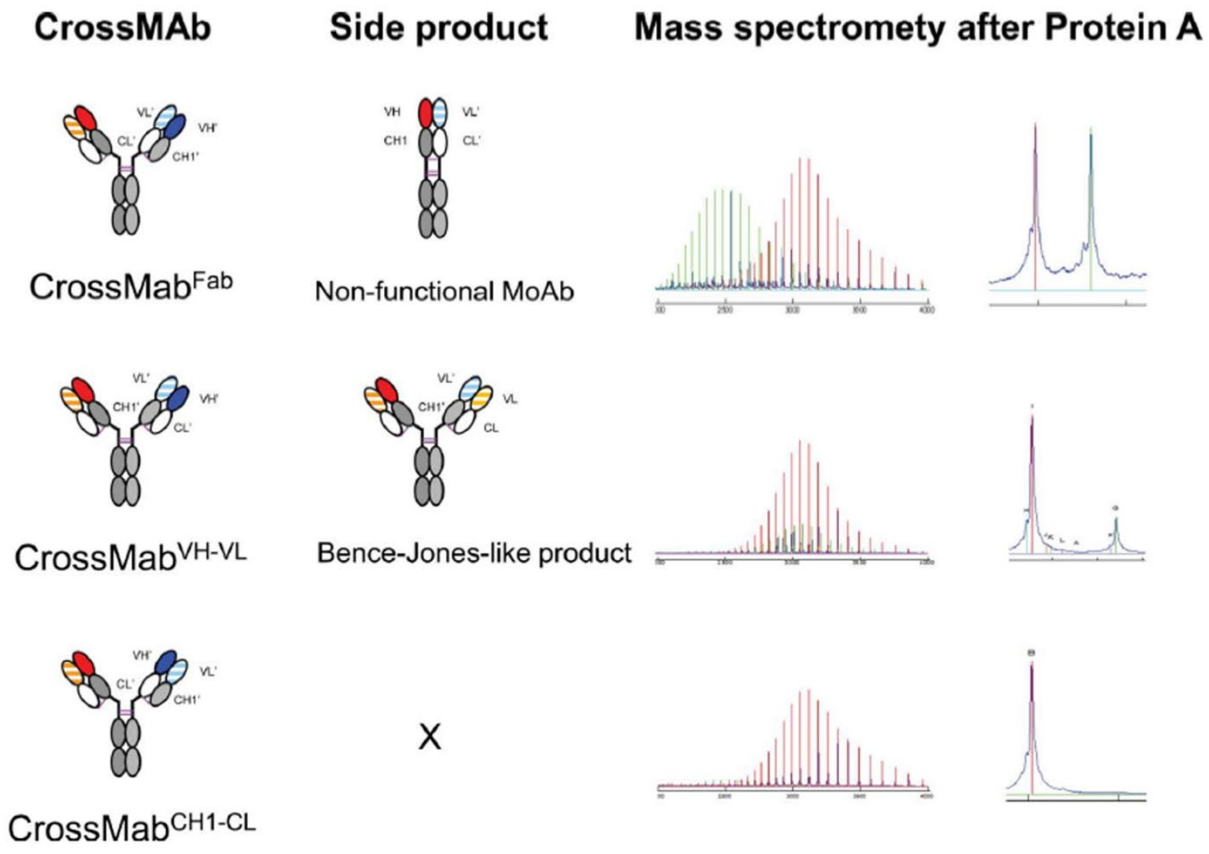


**Figure 1.9. Types of bispecific CrossMAb formats.**
Only one arm of the antibody is manipulated, and the other arm has conventional mAb format. CrossMAb$^{Fab}$ and CrossMAb$^{VH\text{-}VL}$ form sides products while CrossMAb$^{CH1\text{-}CL}$ does not product a side product. This figure was published in This figure was published in Klein, C., Schaefer, W., and Regula, J.T. (2016). The use of CrossMAb technology for the generation of bi- and multispecific antibodies. *MAbs*. 8(6):1010-20.

### 1.3 Antibody effector functions

An antibody's most common function is to prevent infection by neutralization of the pathogen via its antigen binding sites located in its Fab fragments (Abbas et al., 2011); however, there are other effector functions mediated by the Fc fragment of an antibody to eliminate antigens: antibody-dependent cellular phagocytosis (ADCP), antibody-dependent cellular cytotoxicity (ADCC), and complement-dependent cytotoxicity (CDC). Different effector functions of an antibody facilitate a stronger defense system against pathogens to protect the host.

#### 1.3.1 Neutralization

The simplest function of antibodies is to directly neutralize infection caused by microbes. Antigen-binding regions of the antibodies are only required to neutralize antigens so experimentally, Fab or F(ab)2 fragments without Fc fragments are capable of neutralizing antigens in vitro (Lu et al., 2018). Since the Fc region is not required, any isotype of antibodies can neutralize antigens. There are several mechanisms for antibodies to neutralize infection. The most common mechanism is to block attachment of microbes to host cells (Stanfield and Wilson, 2014). Microbes often enter host cells via particular microbial surface molecules which bind to membrane receptors of the host (Abbas et al., 2011). Bulky antibodies that are bound on the microbial surface molecule will prevent microbes from binding to host cell receptors. Antibodies can also neutralize pathogens by inhibiting or inducing conformational changes of the surface molecule of microbes (Stanfield and Wilson, 2014). For example, in influenza virus, conformational changes must occur in hemagglutinin to fuse membranes together (Carr and Kim,

1993). Anti-influenza antibodies have been discovered that block these conformational changes and have been shown to protect mice from lethal challenge (Dreyfus et.al., 2012).

### 1.3.2 Antibody-dependent cellular phagocytosis

ADCP is a process of killing microbes such as virus particles by opsonization and phagocytosis via interaction between the Fc domain of antibody and Fc receptors on immune receptor cells (Kamen et al., 2019; Tay et al., 2019) (**Figure 1.10**). When Fab regions of IgG detect and bind to an antigen, this allows the Fc region of IgG to bind to Fc receptors on the phagocytes. Fc receptors signals phagocytes to activate phagocytosis and subsequently destroy the ingested pathogens. Among different Fc receptors, FcγRI (CD64) has highest affinity to human IgG1, IgG3, and IgG4 (Tay et al., 2019). This receptor is mainly present on the surface of macrophages and neutrophils, two cell types that promote phagocytosis. A clinical trial of a human cytomegalovirus (HCMV) vaccine in postpartum women showed that vaccination induced low titers of neutralizing antibodies, but more robust titers of antibodies that mediated ADCP (Nelson et al., 2018).

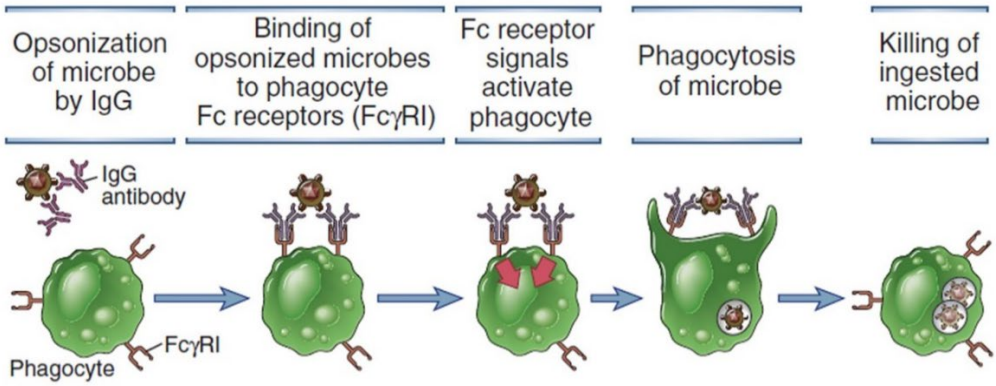


**Figure 1.10. Mechanism of antibody-dependent cellular phagocytosis.**
IgG antibodies first bind to microbes via Fab fragment. This binding allows FcγRI on the phagocytes to bind to Fc fragment of IgG and initiate phagocytosis, leading to destruction of ingested microbes. This

figure was published in Abbas AK, Lichtman AH, Pillai S.Effector Mechanisms of Humoral Immunity. Cellular and Molecular Immunology, 7th edition. Philadelphia, Elsevier Saunders 2012, 269-292.

### 1.3.3 Antibody-dependent cellular cytotoxicity

ADCC is a mechanism that kills infected cells with antibodies in conjunction with the activity of NK cells (**Figure 1.11**). When infected cells are present, antibodies bind to viral proteins on the surface of the cells via their Fab region. This allows the Fc region of an antibody to cross-link the Fc receptor on NK cells and allows the NK cells to secrete granzymes and perforin to lead to death of the infected cells (Lu et al., 2018). The main Fc receptor on NK cells is FcγRIIIA (CD16). CD16 binds to clusters of IgG-antigen complex on the infected cell surface, but not circulating monomeric IgG. Therefore, unlike ADCP, ADCC can only occur on infected cells and not on cell-free virus particles. ADCC has been reported as a key effector function for antibody protection against various infectious pathogens such as HIV-1, Ebola, and Dengue (Li et al., 2014; Liu et al., 2017; Laoprasopwattana et al., 2007)

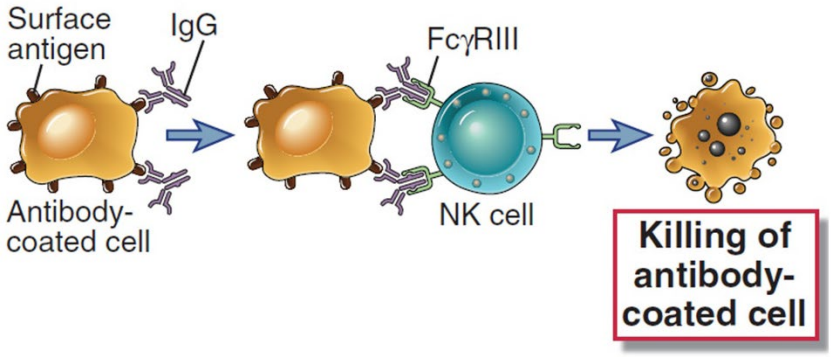


**Figure 1.11. Mechanism of antibody-dependent cellular cytotoxicity.**
The Fab fragment of IgG binds to surface antigens on the infected cells and activates cross-linking of the Fc fragment of IgG with FcγRIIIA on NK cells. Granzymes and perforin secreted from NK cells lead to killing of infected cells. This figure was published in Abbas AK, Lichtman AH, Pillai S.Effector Mechanisms of Humoral Immunity. Cellular and Molecular Immunology, 7th edition. Philadelphia, Elsevier Saunders 2012, 269-292.

### 1.3.4 Complement-dependent cytotoxicity

CDC is activated by recruitment of complement when pentameric IgM or IgG that forms stable hexameric complexes detects pathogens (Lu et al., 2018) (**Figure 1.12**). Complement can be activated by the classical pathway where C1q is recruited to antigen-antibody immune complexes or through the lectin pathway where mannose-binding lectin (MBL) is recruited to antibody-opsonized material (Lu et al., 2018). Complement can also be activated by the alternative pathway where neither C1q nor MBL are involved. Once the complement cascade is activated by any of these three pathways, the products of complement activation attach to antigen bound IgM or IgG and promote phagocytosis, inflammation, and/or cell lysis (Lu et al., 2018) and clear the pathogen. A monoclonal antibody, rituximab, which is widely used in treatment of B-cell malignancies and B-cell related diseases has been shown to trigger CDC and ADCC of B cells (van Meerten et al., 2006).

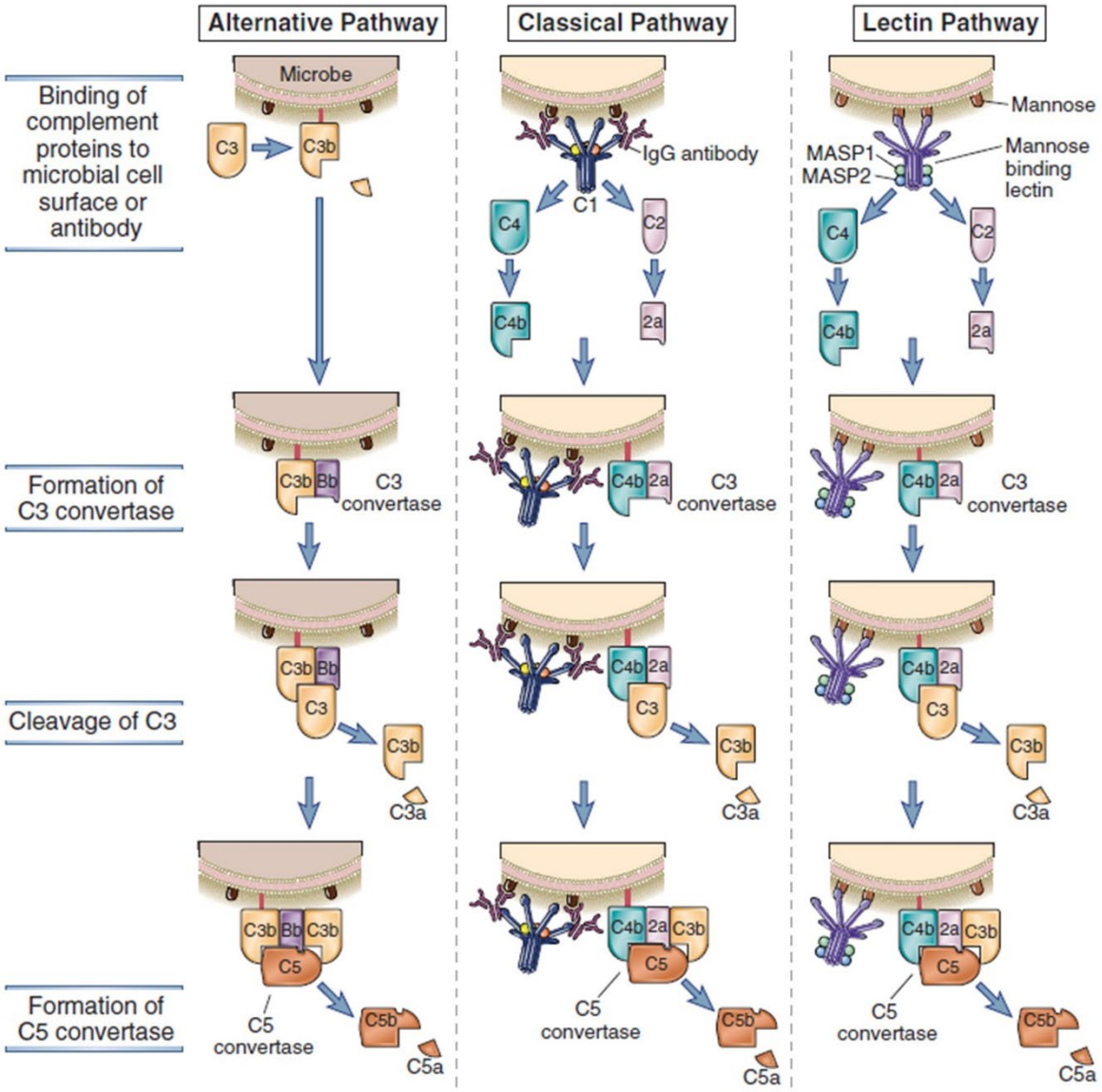


**Figure 1.12. Three pathways of complement system activation.**
The cascade of component activation in classical, lectin, or alternative pathways leads to formation of membrane attack complex (MAC) and promote cell lysis. This figure was published in Abbas AK, Lichtman AH, Pillai S.Effector Mechanisms of Humoral Immunity. Cellular and Molecular Immunology, 7th edition. Philadelphia, Elsevier Saunders 2012, 269-292.

## 1.4 Humanized mouse models

### 1.4.1. Types of humanized mouse models

Small animals such as mice and rats have been widely used in biomedical research but due to EBV's host tropism, there are limitations on finding a small animal model that can be infected with EBV.To overcome this barrier, humanized mice have been engrafted with human cells or tissues that are susceptible to various human pathogens. There are several methods to make a humanized mouse (**Figure 1.13**). Using immunodeficient mice, humanized mice can be generated in three ways: engraftment with human peripheral blood mononuclear cells (PBMCs), human fetal tissues, or hematopoietic stem cells (HSCs) (Allen et. al., 2019). Mice engrafted with human PBMCs are the most direct way to create humanized mice easily (Allen et al., 2019). This model can be established in a short time and human T cells are highly expanded, but mice often develop severe graft-verse-host disease (GVHD) and therefore are not suitable for long-term in vivo studies (Yong et al., 2018; Ito et al., 2017). Another humanized mouse model often used is engraftment of mice with a combination of human fetal bone marrow, liver, and thymus (BLT). The BLT model is made by inserting human fetal liver and thymus under the kidney capsule of the mice along with intravenous injection of $CD34^+$ HSCs from the same fetal liver (Ito et al., 2017). Although this model has highest level of human cell reconstitution among the three models, generation of this model takes time as surgical implantation is required and there are ethical issues of using human fetal samples (Yong et al., 2018). Lastly, mice engrafted with HSCs, also called humanized human immune system (HIS) mice, are the most commonly used model (Ito et al., 2017). Before engrafting immunodeficient mice with HSCs, mice need to be preconditioned with sublethal levels of X-ray irradiation or treated with radiomimetic drugs to deplete mouse hematopoietic cells (Allen et al., 2019). HSCs can be obtained from human umbilical cord blood, bone marrow, fetal liver, or peripheral blood after using granulocyte

colony stimulating factor (GCSF) to mobilize the cells from the bone marrow. This model results in mice containing human T and B cells (Yong et al., 2018). An advantage of this model is that the B and T cells that develop from HSCs undergo negative selection during differentiation which generate a naïve immune system which is tolerated by the mouse host (Yong et al., 2018; Pearson et al., 2008). A disadvantage is that cell differentiation takes time and contains low levels of human red blood cells, polymorphonuclear leukocytes, and megakaryocytes (Yong et al., 2018).

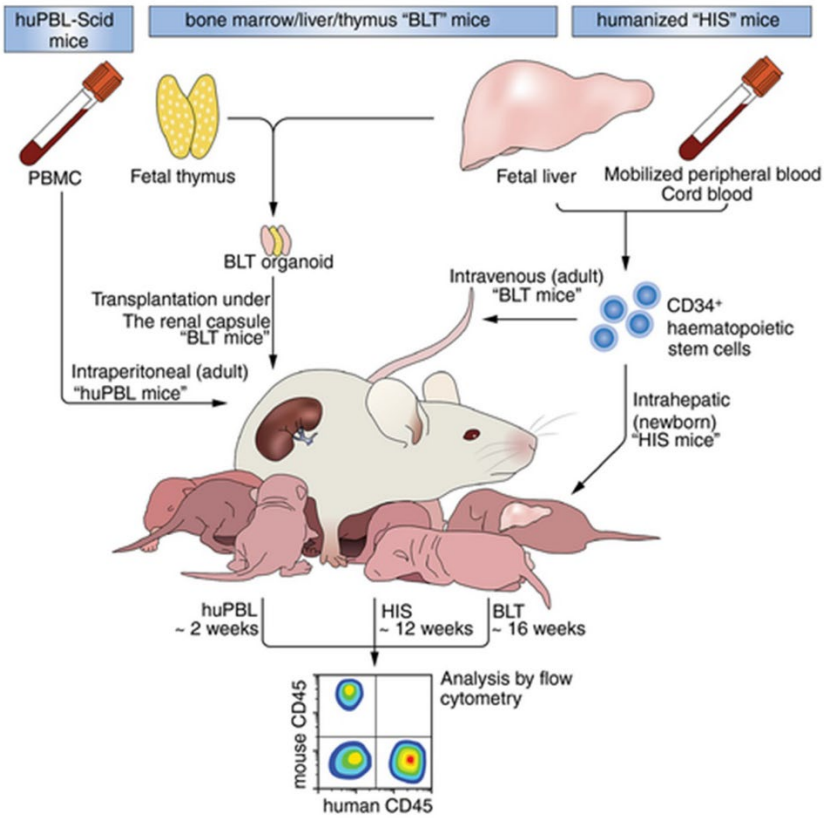


**Figure 1.13. Generation of humanized mouse models.**
Humanized mice can be categorized into human peripheral blood leucocyte (huPBL) mice, bone marrow/liver/thymus (BLT) mice, and humanized human immune system (HIS) mice. This figure was published in Skelton, J.K, Ortega-Prieto, A.M., and Dorner, M. (2018). A hitchhiker's guide to humanized mice: new pathways to studying viral infections. *Immunology*. 154(1):50-61.

### 1.4.2. Humanized mouse model for EBV infection

Humans are the only natural host for EBV (Fujiwara et al., 2015) so there are limitations on finding a small animal model when studying EBV infection. The cotton-top tamarin is susceptible to EBV infection and has been previously used in preclinical studies, but they are an endangered species, thus can no longer be used (Fujiwara et al., 2015). Rhesus monkeys can be infected with rhesus lymphocryptovirus (sometimes referred to as rhesus EBV) (Cho et al., 1999). Although rhesus lymphocryptovirus is very closely related to EBV, there is only 49% amino acid similarity between EBV and rhesus lymphocryptovirus gp350 (Herrman et al., 2016). Currently, the most widely used small animal model in EBV research is humanized mice. Humanized mice, like humans, have been shown to develop both lytic and latent EBV infection. After severe combined immunodeficiency (SCID) mice were inoculated with EBV-seronegative donor PBMCs and then infected with EBV, 67% of the mice developed EBV-positive PTLD-like lesions (Haque et al., 2006). In mice strain NOD/Shi-scid Il2rg$^{null}$ (NOG) or NOD/LtSz-scid Il2rg$^{-/-}$ (NSG) engrafted with human HSCs, signs of B cell lymphoproliferative disease (LPD) after infection with high doses of EBV were similar to EBV-associated LPD found in immunocompromised patients (Yajima et al., 2008). These mice developed viremia, splenomegaly, and lymphoma in the spleen, liver, kidney, and/or adrenal glands with similar latent gene expression and histopathology as immunocompromised patients. Humanized mice infected with EBV generally show peak viral loads in the peripheral blood at week 4-to-6 post infection which is similar to primary EBV infection in humans (Munz, 2017). Humanized mice infected with low doses of EBV showed transiently detectable viral DNA in the peripheral blood with no apparent signs of disease, but EBER-positive B cells were detected in the spleen and liver up to ~7 months after infection (Fujiwara et al., 2015). This asymptomatic and persistent infection mirrors EBV latency in humans.

Although humanized mice show similar features to those found in EBV infection in humans, there is a caveat to this model. As humanized mice are engrafted with human HSCs, they have human B and T cells, but not human epithelial cells (Munz, 2017). Lytic infection through epithelial cells in oropharynx is an important entry route of EBV infection in humans but having mouse epithelial cells prevents EBV infection through this route. Infecting humanized mice with EBV via intravenous injection does not replicate the natural route infection in humans and evaluating EBV therapeutics may be limited by the model. Another difficulty of using a humanized mouse model in EBV research is that although these mice reproduce EBV-associated B-cell LPD, there are other EBV-associated malignancies that have not been observed in this animal model (Fujiwara et al., 2015). EBV is associated with Burkitt lymphoma, Hodgkin lymphoma, gastric carcinoma, and nasopharyngeal carcinoma but there are no studies yet showing humanized mice can develop these types of cancers.

In summary, EBV infection is associated with various diseases despite being one of the most prevalent viruses in humans. There is no FDA approved vaccine or therapeutic and active research to discover one is needed. In this dissertation, the following questions will be explored: i) what is the most appropriate humanized mouse model to evaluate efficacy of EBV therapeutics? ii) what is the most effective EBV mAb that can protect humanized mice from EBV infection and development of lymphoma? iii) can a bispecific antibody provide better protection of humanized mice from EBV infection than a single monoclonal antibody? To answer these questions, comparisons of different humanized mouse models that are suitable for antibody efficacy studies will be discussed in chapter 2. Using an optimized humanized mouse model (chapter 2), discovery and characterization of an EBV hyperimmune globulin (chapter 3),

EBV mAbs (chapter 4), and a bispecific mAb (chapter 5) to find the best candidate(s) to prevent EBV infection and development of lymphoma will be reported.

# Chapter 2. Evaluation of humanized mouse models for EBV infection studies

An additional author contributed on the work in this chapter: Wang Y

**Abstract**

EBV is nearly ubiquitous in adults. In addition to causing infectious mononucleosis, EBV is associated with B cell lymphomas and epithelial cell malignancies including nasopharyngeal carcinoma and gastric carcinoma. There are no licensed vaccines or therapeutics. Since humans are the only natural host of EBV, the virus does not infect B cells or epithelial cells of small animals and there is not a suitable small animal model to study EBV infection. Recently, humanized mice that are engrafted with human PBMCs or $CD34^+$ hematopoietic cells and have human lymphocytes, has been used in EBV studies. Here, I have examined different mouse strains, both SCID mice injected with human PBMCs from EBV seronegative donors and commercially available humanized mice for their ability to develop viremia and B cell lymphomas after challenge with EBV. I also optimized the titer of the EBV challenge virus to find the best conditions to use to evaluate the efficacy of EBV monoclonal antibodies to protect the animals. Humanized mice had detectable viremia, but due to small sample size (associated with the expense of the animals), it was difficult to observe distinguishable results between different strains of humanized mice. SCID mice injected with PBMCs from EBV seronegative donors also were tested, but unlike the humanized mice, not all animals became infected. Thus, humanized mice were found to be the most reproducible model for EBV infection.

## 2.1 Introduction

EBV is the most common cause of infectious mononucleosis. 75% of infected individuals shows symptoms like sore throat and fatigue, but usually only last 3-4 weeks (Dunmire et al., 2015). Infectious mononucleosis is not a life-threatening disease in most cases, but still EBV is an oncogenic virus and other diseases associated with EBV can result in severe morbidity and death. EBV is associated with B cell lymphomas such as Hodgkin and Burkitt lymphomas, and epithelial cell malignancies such as nasopharyngeal and gastric carcinomas (Cohen et al, 2011). Each year, 200,000 cases of cancer are associated with EBV infections worldwide. EBV infection is also associated with PTLD. Patients undergoing solid organ transplant have higher chance of developing PTLD within 2-3 years of transplantation and within one year for bone marrow transplant (Cohen et al., 2015). There are no licensed vaccines or therapeutics for EBV and they are needed.

Although EBV is one of the most prevalent viruses, its natural host is only humans. EBV is a lymphocryptovirus and nonhuman primate lymphocryptoviruses have some similarity with EBV (Cho et al., 1999). While rhesus lymphocryptovirus infects rhesus monkeys, EBV cannot infect these animals (Herrman et al., 2016). To overcome the limitation on the lack of a small animal model for EBV research, severely immunodeficient mice engrafted with human PBMCs or $CD34^+$ cells (humanized mice) have been used and are currently the best small animal model for EBV infection research. There are three methods to engraft human immune systems in immunodeficient mice: injection of human PBMCs; injection of $CD34^+$ human hematopoietic stem cells from bone marrow, umbilical cord, fetal liver, or G-CSF-mobilized peripheral blood; and injection of human fetal thymus and liver under the kidney capsule along with human hematopoietic stem cells from the same fetal liver (Walsh et. al., 2017). All humanized mice express human lymphocytes such as B and T cells. Previous studies have shown humanized mice

infected with EBV had peak viral loads at week 4-6 after challenge which is similar to the kinetics seen in symptomatic humans with primary EBV infection (Dunmire et al., 2015). However, humanized mice still have mouse epithelial cells; thus, EBV lytic infection in which the virus replicates in oropharyngeal epithelial cells cannot be studied using this model and only latent infection in B cells can be evaluated (Munz 2017).

Various EBV strains have been isolated from different sources. The most widely used and studied strain is B95-8. B95-8 is a cotton-top marmoset cell line transformed by virus from a human LCL from a patient with transfusion-induced infectious mononucleosis (Skare et al., 1982). The B95-8 genome is similar to other EBV strains found in Western countries (Tsai et al., 2017). B95-8 virus has a high transforming efficiency and produces high yields of EBV. The EBV M81 strain was isolated from a Chinese patient with nasopharyngeal carcinoma (Tsai et al., 2017). This strain spontaneously replicates in B cells both in vivo and in vitro and therefore undergoes lytic infection more frequently than B95-8 virus (Tsai et al., 2013). EBV M81 also has a higher tendency to infect epithelial cells than B95-8. As B95-8 and M81 were isolated from different sources, different infection characteristics may be observed in humanized mice.

Here, SCID mice injected with human PBMCs and several commercially available humanized mice strains were evaluated for weight changes and the level of viremia after challenged with EBV. Also, different EBV strains and various titers of the viruses were examined to find optimal conditions to use EBV as a challenge virus to study the efficacy of monoclonal antibodies.

## 2.2 Result

### 2.2.1 Mice that received the highest dose of EBV had the lowest survival rate but no difference in viremia

SCID mice were injected with PBMCs isolated from healthy EBV-seronegative human donors and challenged on the next day with either of two different strains of EBV: M81 and B98-8 (**Figure 2.1A**). EBV B95-8 expresses GFP and EBV M81 expresses both GFP and luciferase. The titer of EBV was measured by infecting Raji cells and counting the number of GFP-positive cells (expressed as green Raji units, GRU [Sashihara et al., 2009]). Due to low level of EBV M81 produced, only 4 x $10^3$ GRU were tested in one group of mice. For EBV B95-8, 4 x $10^3$ GRU, 1 x $10^4$ GRU, and 1 x $10^5$ GRU titers were evaluated with 4 mice in each group (**Figure 2.1B**). Blood and weights were collected weekly starting one-week post infection. For mice that received M81 virus expressing luciferase, IVIS in vivo imaging was conducted weekly starting week 6 post infection and all mice were euthanized at week 19 post infection.

Mice that received the lowest titer of EBV B95-8 virus (4 x $10^3$ GRU) had the highest survival rate; the survival rate decreased as the titer of the virus increased (**Figure 2.1C**). All mice that received 1 x $10^5$ GRU of EBV B95-8 died by week 16 post infection. Mice that received EBV M81 had a 25% survival rate which was the same as mice that received 1 x $10^4$ GRU of EBV B95-8. One mouse from the EBV M81 group died at week 2 post infection and due to the short period of time after challenge, this was felt to be unlikely due to EBV infection. Viremia was measured from blood collected weekly by quantifying the copy number of EBV BamHI copies in the repeat sequence of the virus using qPCR. Mice that received M81 showed detectable EBV starting from week 3 post infection and continually increased in EBV copy numbers until end of the study (**Figure 2.1D**). Mice receiving 4 x $10^3$ GRU of EBV B95-8 started to show detectable EBV at week 7 post infection, but only 50% of mice showed viremia.

Mice receiving 1 x $10^4$ GRU of B95-8, all mice had viremia but fewer EBV copies were detected compared to animals receiving EBV M81 or 4 x $10^3$ GRU of B95-8 EBV. Only 75% of mice receiving 1 x $10^5$ GRU B95-8, showed viremia, but with higher EBV copy number than those receiving 1 x $10^4$ GRU. Based on survival rate and levels of viremia result, 4 x $10^3$ GRU B95-8 was not infectious enough to use for evaluation of EBV mAbs. Mice receiving 1 x $10^5$ GRU B95-8 virus had the lowest survival rate and high levels of viremia, but not all mice were infected at this titer.

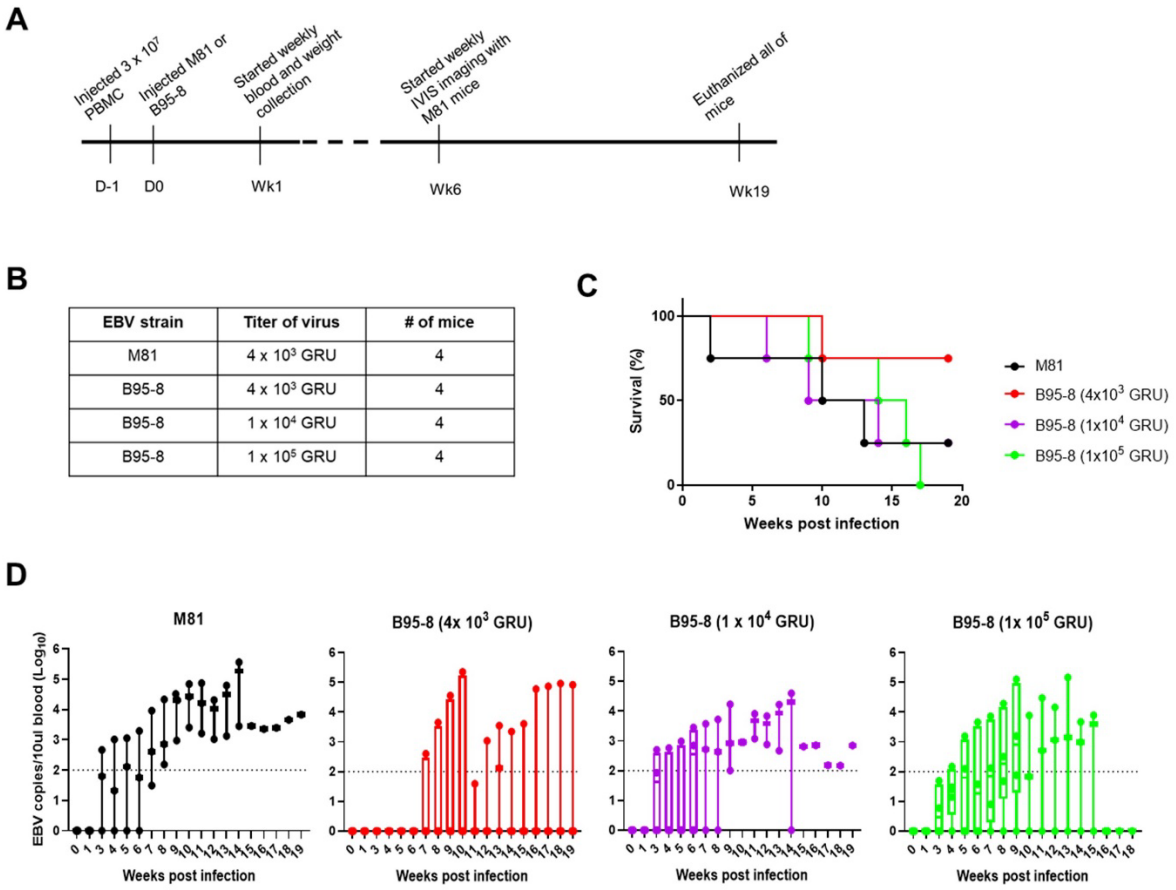


| EBV strain | Titer of virus | # of mice |
|---|---|---|
| M81 | 4 x $10^3$ GRU | 4 |
| B95-8 | 4 x $10^3$ GRU | 4 |
| B95-8 | 1 x $10^4$ GRU | 4 |
| B95-8 | 1 x $10^5$ GRU | 4 |

**Figure 2.1. Evaluation of EBV infection in SCID mice injected with human PBMCs.**
(A) experimental scheme of injections. (B) A summery table of EBV strains, virus titer, and number of mice in each group. (C) Survival rates for each group of mice after EBV challenge. (D) EBV DNA copies in the blood quantified by real-time qPCR. Each dot represents one mouse, and the dotted line indicates the limit of detection of the assay. Whiskers indicates minimum and maximum data points for EBV DNA copies in the blood, the box represents upper and lower quartiles, and the horizontal line in the box is the median.

### 2.2.2 Mice that received M81 expressing luciferase showed progressive increase in virus infected cells over time using an in vivo imaging system

The EBV M81 strain has a luciferase gene recombinantly incorporated into the genome so that EBV infection (increasing number of virus-infected cells) can be monitored in vivo by imaging for luminescence. Starting at week 6 post infection, luminescence was captured using an IVIS in vivo imaging system (**Figure 2.2**). Mouse #1 showed bright luminescence from both the abdomen and back at week 6 post infection and the intensity of the light increased over time. By week 10 post infection, mouse #1 had bright light luminescence over the entire body. Mouse #3 had very low luminescence on week 6 post infection, but the intensity grew starting at week 12 post infection. By week 18 post infection, mouse #3 had large areas on both the abdomen and back that were luminescent. For mouse #2, luminescence was never observed even though viremia was detected, and the mouse died at week 14 post infection.

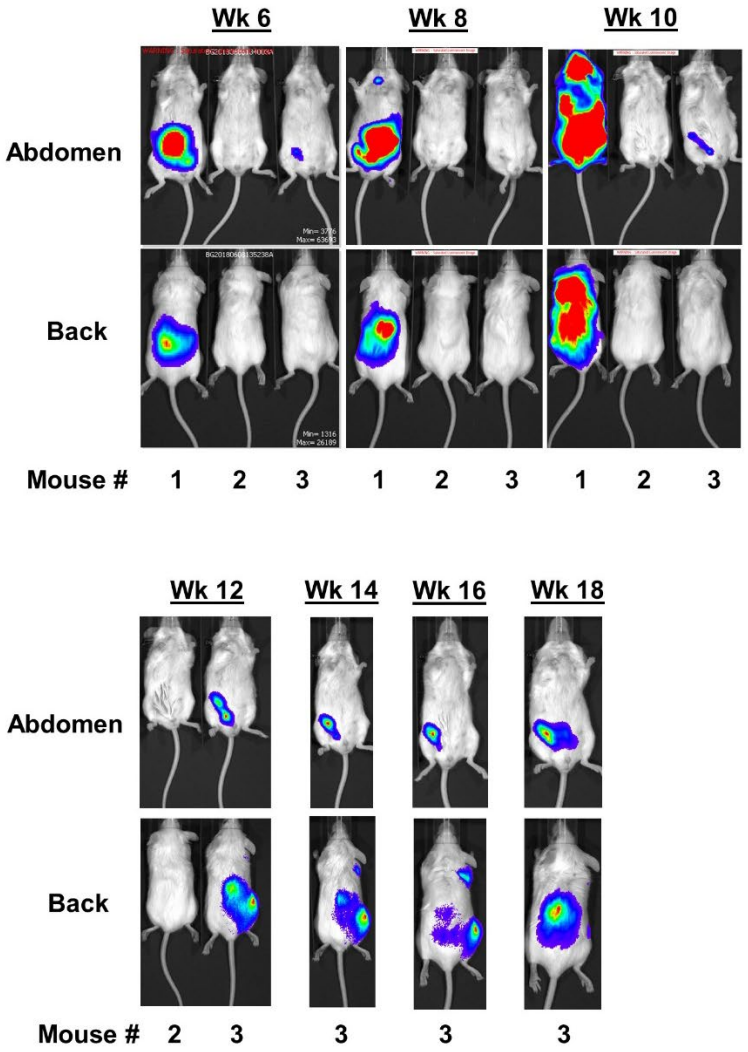


**Figure 2.2. In vivo images of mice challenged with EBV M81 expressing luciferase.**
Abdomen and back of mice were imaged for 1 min. Intensity of the light is depicted in colors with blue being lowest intensity and red being highest intensity.

### 2.2.3 EBV titration using different strains of humanized mice

Recently, humanized mice engrafted with human $CD34^+$ hematopoietic stem cells have been used to study EBV infection. To find the best EBV model of humanized mice, highly immunodeficient mice engrafted with human $CD34^+$ hematopoietic stem cells (huNSG), SCID mice engrafted with human $CD34^+$ hematopoietic stem cells and fetal liver and thymus (BLT mice), and NSG mice with cytokines that improve the level of engraftment better than huNSG mice (NSG-SGM3 mice) were evaluated for survival and viremia after EBV infection. A study using SCID mice with human PBMC injections showed that 1 x $10^5$ GRU can infect mice with detectable viremia, but not all animals were infected (**Figure 2.1**). Therefore, for the humanized mouse studies, both 1 x $10^5$ GRU and 1 x $10^6$ GRU were evaluated. All mice were challenged with EBV B95-8 on day 0 by IV injection and blood was collected and weights were measured weekly starting at week 1 post infection (**Figure 2.3A**). Evaluation of huNSG and BLT mice was conducted at the same time, while studies of NSG-SGM3 mice were conducted separately. huNSG and BLT mice were euthanized at week 16 post infection and NSG-SGM3 mice were euthanized at week 14 post infection. Due to the high cost of these animals, 2 huNSG and 2 BLT mice were used in each group; for NSG-SGM3 mice, 3 mice were injected with 1 x $10^5$ GRU and 4 mice were injected with 1 x $10^6$ GRU (**Figure 2.3B**). All huNSG mice that received 1 x $10^6$ GRU of EBV survived, all mice that received 1 x $10^5$ GRU died by week 11 post infection (**Figure 2.3C**). BLT mice receiving 1 x $10^5$ GRU or 1 x $10^6$ GRU of EBV had 50% survival. NSG-SGM3 mice that received 1 x $10^6$ GRU were all dead by week 7 post infection and mice that received 1 x $10^5$ GRU showed 33% survival at the end of the study. Due to low numbers of huNSG and BLT mice, it is difficult to conclude which titer of virus would be ideal to use in the future study of EBV mAbs.

A

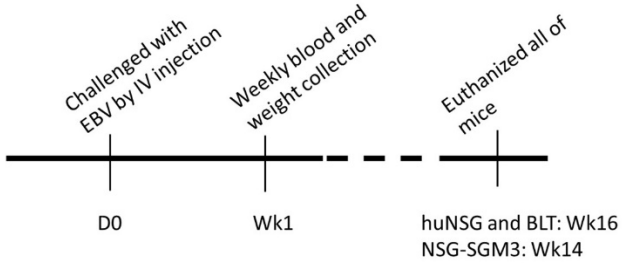


B

| Mouse strain | EBV strain | Titers of virus | # of mice |
|---|---|---|---|
| huNSG | B95-8 | 1 x $10^5$ GRU | 2 |
| | | 1 x $10^6$ GRU | 2 |
| BLT | B95-8 | 1 x $10^5$ GRU | 2 |
| | | 1 x $10^6$ GRU | 2 |
| NSG-SGM3 | B95-8 | 1 x $10^5$ GRU | 3 |
| | | 1 x $10^6$ GRU | 4 |

C

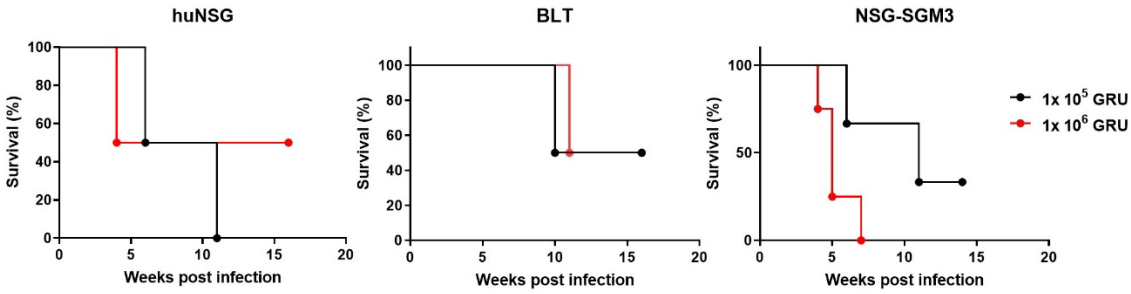


**Figure 2.3. Evaluation of EBV infection in different strains of humanized mice.**
(A) Experimental scheme of EBV challenge and sample collection. (B) A summery table of mouse strain, EBV strains, virus titer, and number of mice in each group. (C) Survival rates for each group of mice after EBV challenge.

### 2.2.4 All mice had viremia with a peak at week 4-7 post infection that declined over time

From weekly collected blood, the EBV repeat sequence, BamHI W, was quantified by qPCR. In huNSG mice, viremia was observed after inoculation with two different titers of virus starting week 1 post infection with a peak at week 5 post infection (**Figure 2.4**). Viral copy numbers with the two different titers of inoculum were similar. In BLT mice, viremia was detected at week 3 post infection for mice that received 1 x $10^5$ GRU and at week 2 post infection in mice that received 1 x $10^6$ GRU. A peak at week 7 post infection was noted; mice that received 1 x $10^5$ GRU had higher viral copy numbers in the early stages of infection. In NSG-SGM3 mice, both titers of inoculum resulted in viremia starting at week 1 post infection and mice that received 1 x $10^6$ GRU had higher numbers of viral copies. For all mice strains, viremia was detectable with both titers of EBV inoculum, but due to the small number of huNSG and BLT mice tested, it was difficult to observe a clear difference in the level of viremia between the two titers. For NSG-SGM3 mice, 1 x $10^6$ GRU resulted in a higher level of viremia so this titer was chosen for evaluation of mAb evaluation study.

Based on these studies, huNSG mice were selected for studies of EBV mAbs. Research with BLT mice was put on hold by the US government shortly after our studies were completed, since these mice contain human fetal tissues. huNSG and NSG-SGM3 gave similar results, although as noted above, the number of mice tested was not sufficient to detect significant differences in the two mouse strains. Since huNSG mice are less expensive than humanized NSG-SGM3 mice, the former was used for testing EBV mAbs.

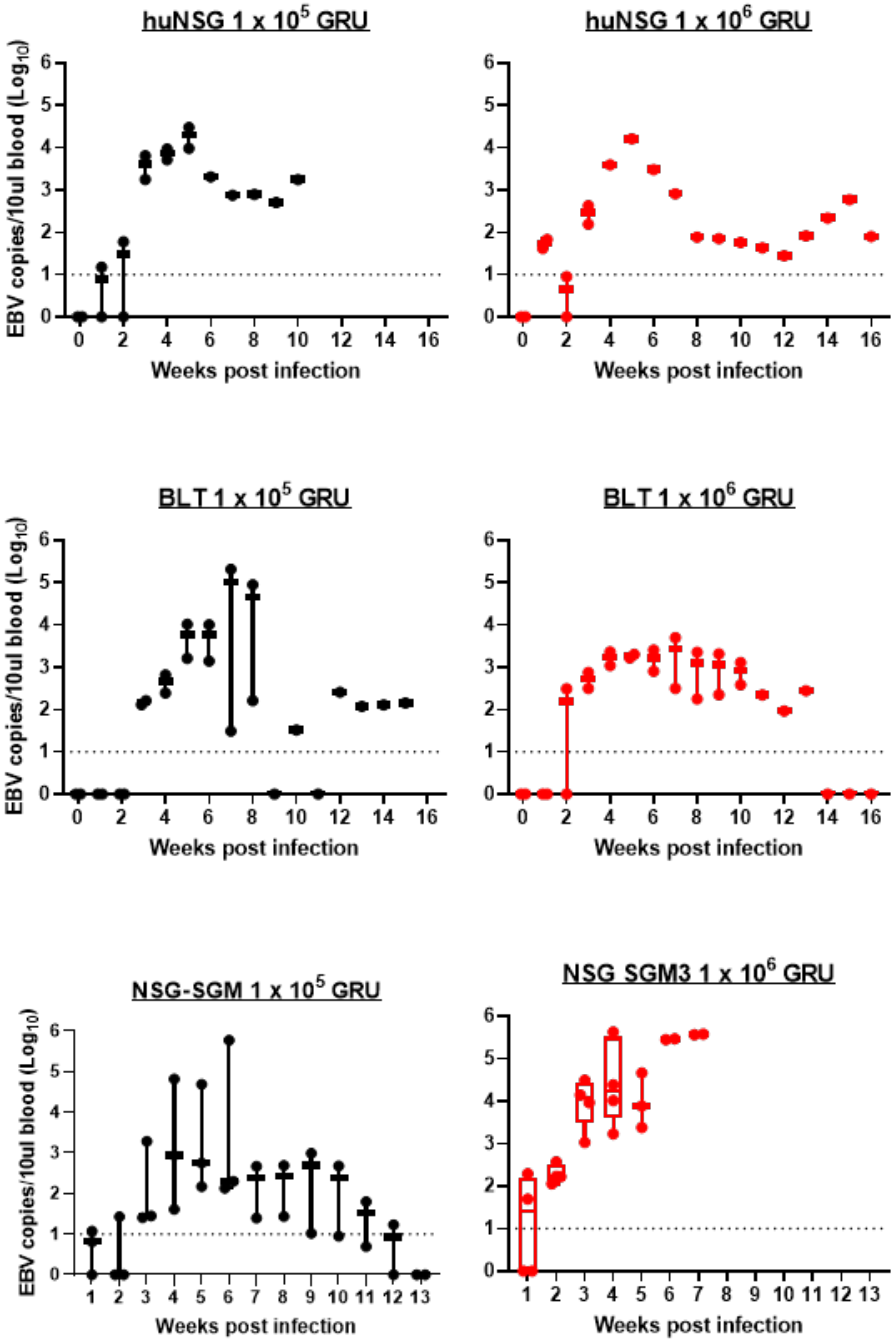


**Figure 2.4. Viremia in different strains of humanized mice inoculated with two different titers of EBV.**
EBV DNA copies in the blood quantified by real-time qPCR. Each dot represents one mouse, and the dotted line indicates the limit of detection of the assay. Whiskers indicates minimum and maximum data points for EBV DNA copies in the blood, the box represents upper and lower quartiles, and the horizontal line in the box is the median.

## 2.3 Discussion

In this chapter, SCID mice injected with human PBMCs and several commercially available humanized mice strains were evaluated for their ability to be infected with EBV. In addition, the effects of different EBV strains and titers of the viruses were examined for EBV infection. The B95-8 virus used expresses GFP, while the M81 strain expresses GFP and luciferase. In SCID mice with human PBMCs, the survival rate correlated with the titer of B95-8 virus used to infect the animals; mice that received the highest titer showed lowest survival rate. However, the level of viremia did not correlate with the titer of B95-8 in the inoculum. All mice that received M81 virus developed viremia and virus infection could be observed directly in mice via in vivo imaging of luciferase. In commercially available humanized mice, all mice showed viremia, but due to small number of huNSG mice and BLT mice, it was difficult to distinguish effects of two different titers of virus. Difference between the two titers were more easily distinguished in humanized NSG-SGM3 mice where higher virus titer in the inoculum resulted in lower survival rate and higher viremia.

In a study reported by Haque et al., SCID mice were injected with EBV seronegative human PBMCs from 4 different donors, then intraperitoneally injected with gp350 antibody 72A1(3 mice from each donor) or PBS (3 mice from each donor), and then infected with EBV (Haque et al., 2007). After 100 days, 8/12 mice (67%) from the PBS group developed EBV-positive PTLD-like lesions and 0/12 (0%) mice that received 72A1 antibody developed lesions. It is difficult to compare my results with their data as their study did not measure the level of viremia and I did not examine PTLD-like lesions at the end of the study, but at least 50% of mice in all 4 groups showed viremia in my study which may increase the likelihood of developing PTLD-like lesions.

M81, a virus isolated from a Chinese patient with nasopharyngeal carcinoma (NPC), can spontaneously replicate in B cells at an unusually high level (Tsai et al., 2013). This trait is similar to the enhanced viral replication seen in patients with NPC. However, in a study conducted by Tsai et al., when the same number of B95-8 or M81 recombinant EBV genomes were injected into mice, the number of B95-8-infected B cells in the spleen was higher than the number of M81-infected B cells. This showed that M81 has reduced B cell tropism than B95-8. The M81 virus used in our animal study has a luciferase gene recombinantly inserted into the genome so that infection can be monitored over time in mice by an in vivo imaging system. Unlike B95-8 virus where high titers of viruses can be obtained using a producer cell line, it was difficult to produce M81 in high concentrations; therefore, only 4 x $10^3$ GRUs of M81 was used for inoculations. All mice that were challenged with M81 virus showed viremia by qPCR, but luciferase activity was observed in 2/3 (66%) mice. The ability to follow EBV infection over time by monitoring luciferase activity in vivo is a very useful tool; however, due to the low level of M81 obtained from the producer cell line, M81 was not an ideal EBV strain to use for future studies. Since B95-8 can produce in high concentrations, I tried to insert a luciferase gene into the B95-8 producer cell line by BAC recombineering but was unable to generate a clone that expressed luciferase that produced useful amounts of virus.

In both huNSG and BLT mice, due to small animal numbers in each group, it was difficult to conclude what titer of the virus would be optimal to use in future humanized mice studies. Infection of humanized NSG-SGM3 mice with EBV showed that high titer virus, 1 x $10^6$ GRU, resulted in a lower survival rate and higher level of viremia. In work published by Yajima et al. in which mice received high titers of virus, inoculation with 1 x $10^3$ 50% transforming doses ($TD_{50}$) of virus resulted in high levels of EBV in the blood and severe illness with weight

loss, general inactivity, and piloerection from week 5-10 post infection; in contrast, mice that received low titers of EBV, 1 x $10^{1}$ to 1 x $10^{-1}$ $TD_{50}$, appeared to be healthy throughout the study (Yajima et al., 2008). Mice infected with lower titers of virus had EBV in the blood for several weeks after infection, but the level then fell to undetectable. In my study, similar results were observed; all three strains of humanized mice showed peak viremia at week 5-7 post infection and the level of virus declined as the study progressed. All mice that died during the study were between week 4-11 post infection which is a similar time frame as in Yajima's study.

None of the mouse models that I've evaluated are perfect models to study EBV infection since humanized mice can only be used to study B cell infection and there will always be variability due to mice engrafted with different donors. However, humanized mice are so far the best model that can recapitulate EBV infection similar to the high viral loads, kinetics of virus in the blood, and development of lymphoma which occurs in EBV-infected hematopoietic stem cell transplant recipients. As usage of BLT mice was highly restricted by the US government due to the use of human fetal tissue after my first study was completed, this model could no longer be used. Since results with huNSG and NSG-SGM3 mice were similar and NSG-SGM3 mice are more expensive, I determined that huNSG mice were the best model to use in future studies to evaluate the ability of EBV mAbs to protect animals from viremia and EBV LPD. The optimal titer for infecting these mice was found to be 1x $10^{6}$ GRU.

# Chapter 3. EBV hyperimmune globulin isolated from donors with high gp350 antibody titers protect humanized mice from challenge with EBV

This work was published in:

Kim JH, Bu W, Mine S, Tariq Z, Nguyen H, Wang Y, Tolman C, Mond J, and Cohen J.I. (2021) Epstein-Barr virus (EBV) hyperimmune globulin isolated from donors with high gp350 antibody titers protect humanized mice from challenge with EBV. Virology 561, 80-86. https://doi.org/10.1016/j.virol.2021.06.006

**Abstract**

Primary infection with EBV is associated with post-transplant lymphoproliferative disease and severe disease in patients with X-linked lymphoproliferative disease; no therapies are approved to prevent EBV infection in these patients. Hyperimmune globulin has been used to prevent some virus infections in immunocompromised persons. Here, we identified plasma donors with high titers of EBV gp350 and EBV B cell neutralizing antibodies. Pooled IgG isolated from these donors was compared to intravenous immunoglobulin (IVIG) for its ability to reduce viral load in the blood in humanized mice challenged with EBV. Mice that received EBV hyperimmune globulin had significantly reduced EBV DNA copy numbers compared to animals that received saline control; however, while animals that received EBV hyperimmune globulin had lower EBV DNA copies than those that received IVIG, the difference was not significant. Thus, while EBV hyperimmune globulin reduced viral load compared to IVIG, the effect was modest.

## 3.1 Introduction

EBV is one of the most prevalent human viruses with more than 90% of the world's adult population infected with EBV (Cohen et al., 2011). EBV is the primary cause of infectious mononucleosis and is also associated with certain B cell lymphomas and epithelial cell malignancies. In immunocompromised individuals who undergo solid organ or hematopoietic stem cell transplant, EBV is responsible for > 70% of cases of PTLD (San-Juan et al., 2014). PTLD usually develops within first year after transplant in hematopoietic stem cell transplant recipients and in the first 2 years in solid organ transplant recipients (Fujimoto and Suzuki, 2020; Wistinghausen, Gross, and Bollard, 2013). The frequency of PTLD is 24- to 33-fold higher in persons with primary EBV infection after transplant than in EBV seropositive persons (Preiksaitis and Cockfield, 1998). EBV infection can also result in fatal disease in boys with X-linked lymphoproliferative disease (XLPD) and in certain other primary immunodeficiencies (Cohen, 2015).

Intravenous immunoglobulin (IVIG) or antiviral therapy has been used to try to prevent infection in some patients at high risk of PTLD or XLPD; however, fatal breakthroughs have occurred. Neither IVIG nor antivirals affect latent EBV infection; thus, they have only been used to try to reduce infection or in the case of antivirals to inhibit EBV lytic replication. IVIG contains polyclonal antibodies prepared from pooled plasma of >15,000 donors (Orange et al., 2006). While plasma donors are not screened for antibodies to EBV, since 90% of adults are infected with the virus, IVIG contains EBV antibodies, although antibody levels to different EBV proteins can vary from batch to batch.

Hyperimmune globulin is available to prevent or attenuate virus infections (Slifka and Amanna, 2018). FDA licensed products include varicella, rabies, and hepatitis B hyperimmune globulins that are used to prevent disease after exposure (post-exposure prophylaxis) to the

corresponding virus infections. Cytomegalovirus and hepatitis B hyperimmune globulins are used to prevent disease before exposure, while vaccinia hyperimmune globulin is used to treat persons with progressive vaccinia. The FDA recently issued an emergency use authorization for convalescent plasma from persons with high titers of antibody to SARS-CoV-2 to treat hospitalized persons with COVID-19.

Currently there is no approved hyperimmune globulin for EBV. In view of the limited effectiveness associated with IVIG for prevention of EBV PTLD (Humar et al., 2006) and prevention of primary infection in patients with XLPD (Seemayer et al. 1995), EBV hyperimmune globulin may be more effective than IVIG due to the higher titer of neutralizing antibody. Here, we isolated EBV hyperimmune globulin from plasma of donors with high titers of EBV gp350 and EBV B cell neutralizing antibodies and evaluated its effect on protection against EBV infection using a humanized mouse model.

## 3.2 Results

### 3.2.1. Screening of plasma from EBV seropositive donors for EBV gp350 antibody and B cell neutralizing titers

Plasma from 200 EBV seropositive donors were evaluated for EBV gp350 antibody titers by LIPS assay. As a control, plasma previously obtained from NIH blood bank donors that had been categorized as having high, medium, or low levels of gp350 antibody were used as a control (**Fig. 3.1A**). Many of the plasma donors had similar or higher levels of gp350 antibody titers compared to the high titer gp350 antibody control group. Based on these results, a subset of plasma donors was evaluated for EBV B cell neutralizing titers to select donors for preparation of EBV hyperimmune globulin. Seven donors were selected that had high titers of both gp350 and EBV B cell neutralizing antibodies (**Fig. 3.1B**). All 7 donors had higher EBV neutralizing titers (1-2 log lower $IC_{50}$ values) than 4 different preparations of IVIG.

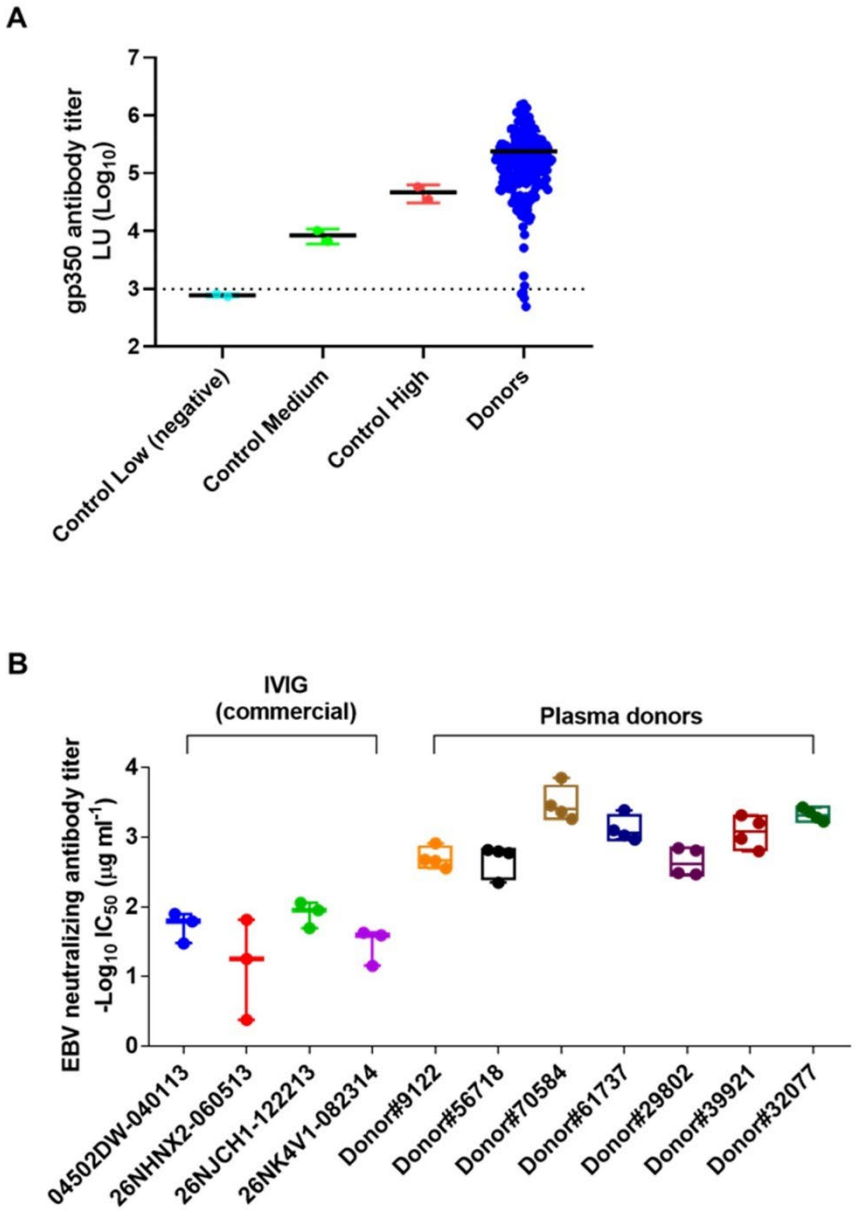


**Figure 3.1. EBV gp350 antibody levels in plasma from donors and EBV B cell neutralizing titers in IVIG and selected plasma donors with high EBV gp350 antibody titers.**
(A) gp350 antibody levels in human plasma donors were quantified using a gp350 LIPS assay. Plasma previously obtained from blood bank donors that had been categorized with high, medium, and low gp350 antibody titers were used as controls. Antibody titers are expressed in light units (LUs) based on the LIPS assay. Each dot indicates the mean titer of triplicate results for each donor and the solid black line indicates the mean. The dotted line represents the cutoff value defined as the mean plus 2 standard deviations of the antibody titer of EBV negative sera. (B) EBV B cell neutralizing antibody titers from separate lots of IVIG and 7 plasma donors with the highest EBV gp350 antibody titers based on LIPS assay. Each dot represents the $IC_{50}$ value of individual neutralization assay result.

### 3.2.2. Comparison of IVIG and EBV hyperimmune globulin by passive transfer in humanized mice and EBV challenge

Three plasma donors (donors #9122, 39921, 32077), available for further plasma donation after their initial screening, were chosen from the 7 donors with the highest gp350 and EBV B cell neutralizing titers, and IgG was purified from their plasma and pooled. This pooled IgG was termed EBV hyperimmune globulin and had comparable levels of EBV B cell neutralizing titers as IgG obtained from individual plasma donors (**Fig. 3.2A**). Differences in the individual donors' neutralizing titers in Fig 3.1B and 3.2A were due to the use of plasma from donors in the former and purified IgG from donors in the latter. EBV hyperimmune globulin was compared with IVIG for its ability to reduce the number of EBV DNA copies in the blood in humanized mice challenged with EBV. Groups of 6 mice received 0.5 mg of either IVIG or EBV hyperimmune globulin on days -1, 0, 1, 4, 7, and 10 of challenge (**Fig. 3.2B**). Another group of mice was given PBS at the same time points as a control. On the day of challenge, 1 x $10^6$ GRU of EBV B95-8 was given by intravenous injection. Mouse weights were recorded, and peripheral blood was collected weekly from week 1 to 15 after infection. The concentration of total human IgG in plasma and the level of EBV DNA in whole blood was measured.

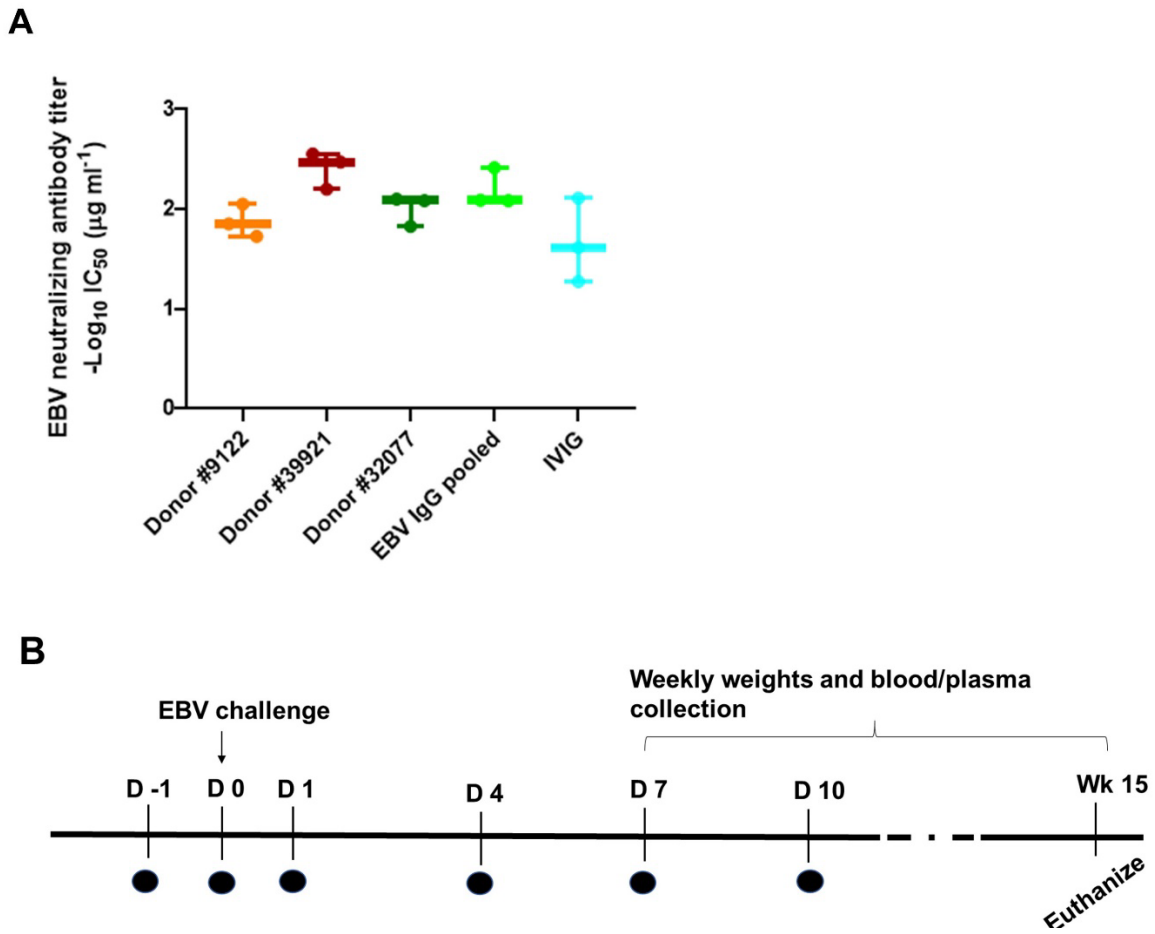


**Figure 3.2. Passive transfer protocol for humanized mice and EBV B cell neutralizing titers of IVIG or EBV hyperimmune globulin.**
(A) EBV B cell neutralization titers for IgG isolated from individual donors, hyperimmune globulin from pooled donors, and IVIG were plotted. (B) Six doses of either PBS, IVIG or EBV hyperimmune globulin, indicated by the black circles, were given by intraperitoneal injection and $1x10^6$ GRU of EBV was used to challenge mice by intravenous injection.

Mice in all three groups were monitored for weight changes. In the PBS group, one mouse reached the endpoint of 30% weight loss and was euthanized, while none of the mice in the other groups had significant weight loss (**Fig. 3.3A – 3.3C**). PBS control group showed 83% survival while all mice in the IVIG and hyperimmune EBV globulin groups survived (**Fig. 3.3D**).

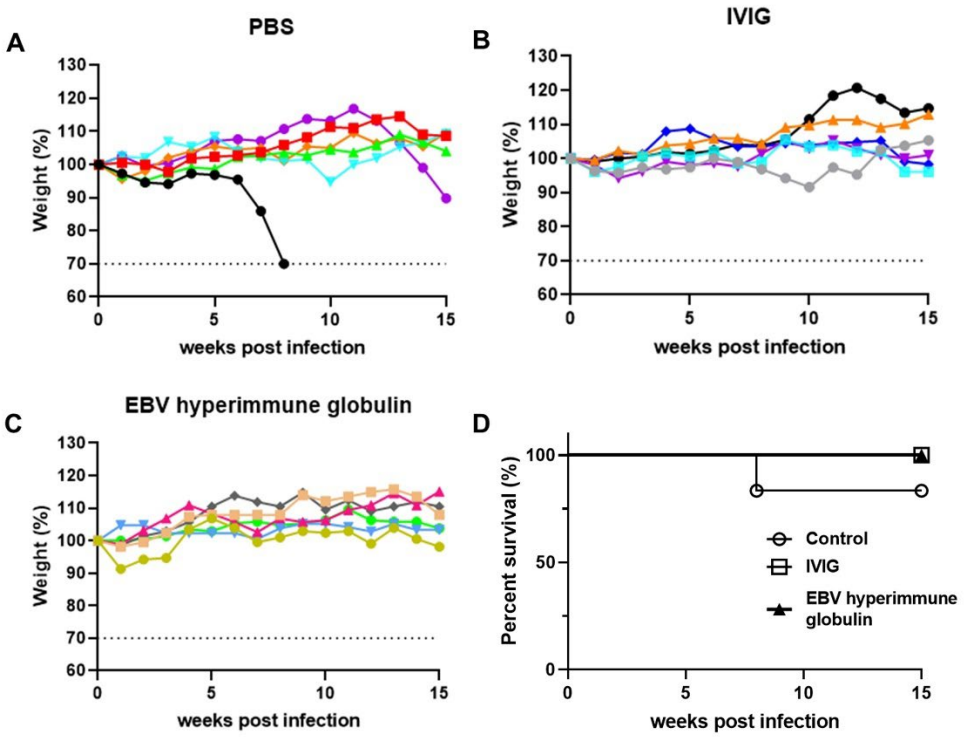


**Figure 3.3. Changes of weight and survival rate for mice receiving IVIG, EBV hyperimmune globulin, or PBS and challenged with EBV.**
Percentage weights relative to initial weights (set at 100%) are plotted for mice that received: (A) PBS control, (B) IVIG, or (C) EBV hyperimmune globulin. Each line represents one animal and dotted lines indicate study end point 30% weight loss. (D) Survival rates were plotted for each group of mice up to week 15 after infection.

### 3.2.3. Mice receiving hyperimmune EBV globulin had the lowest EBV viral load in the blood after virus challenge

DNA was extracted from the blood of mice after challenge with EBV and the level of viral DNA was measured by qPCR using a probe for the EBV BamHI W sequence. There are 11 copies of BamHI W, a repeat sequence, in the EBV B95-8 genome (Le et al., 2005); therefore, amplifying this repeat sequence increases the sensitivity of the assay. All three groups of mice had peak levels of EBV DNA in the blood 5 weeks after infection and thereafter the levels decreased (**Fig. 3.4A – 3.4C**). When the number of EBV DNA copies in the blood was compared over the full 15-week study period, an area under the curve analysis showed that mice that received EBV hyperimmune globulin had a significantly lower viral load in the blood compared to PBS group ($p = 0.004$, Welch two sample t test); however, animals that received IVIG did not have significantly lower viral load than those that received PBS ($p = 0.19$) (**Fig. 3.4D**). While mice that received EBV hyperimmune globulin had a lower viral load in the blood than those that received IVIG over the 15-week study period, the difference was not significant ($p = 0.13$). Since the majority of the adult population is infected with EBV, IVIG may contain high levels of EBV antibodies and therefore may had resulted in no significant difference between humanized mice that received IVIG versus EBV hyperimmune globulin.

Mice were euthanized at the end of the study, and sections of liver, spleen, lung, and kidney were examined for evidence of lymphoproliferative disease or lymphoma. Tissues from 33.3% of mice in the PBS group, 16.7% of mice in the IVIG group, and none of the mice in the EBV hyperimmune globulin group showed lymphoproliferative disease or lymphoma (**Table 3.1**).

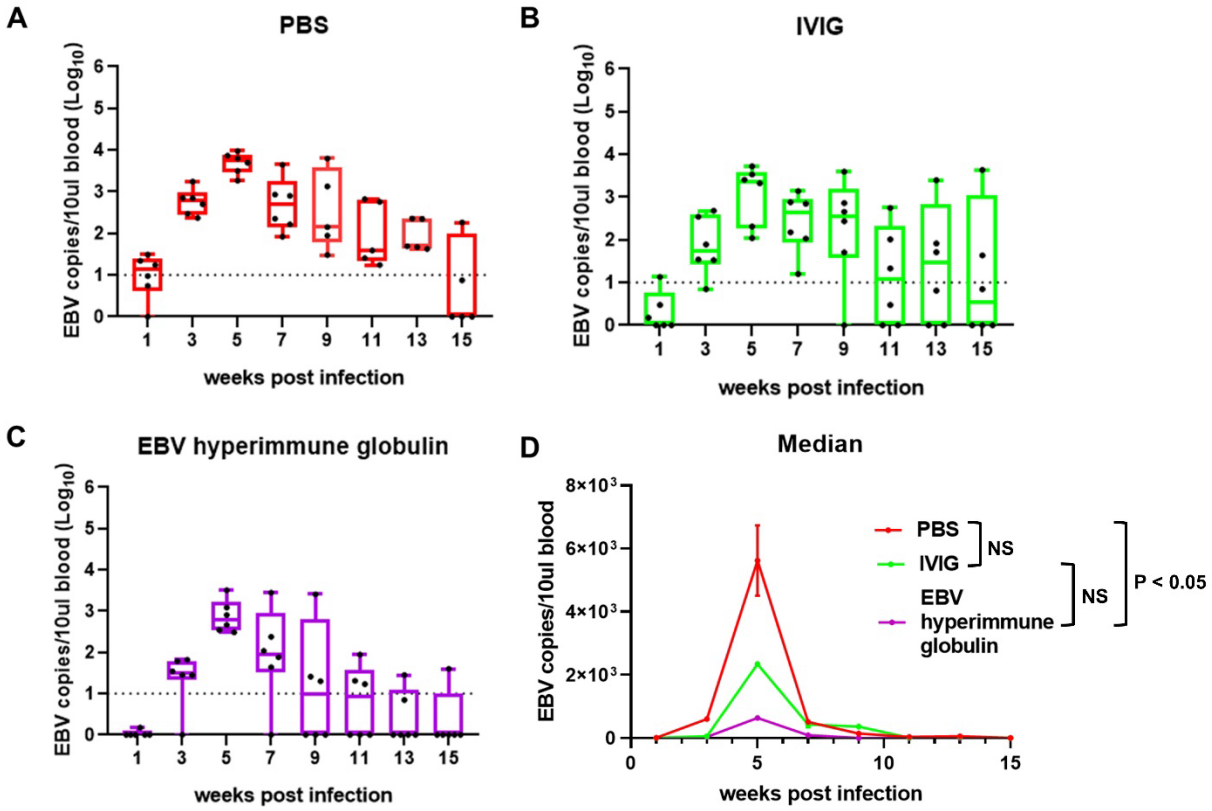


**Figure 3.4. Quantification of EBV viral load from weeks 1 to 15 after challenge.**
EBV viral load expressed as EBV copy numbers per 10 µl of blood was plotted for each mouse over time. Each dot represents one mouse. Whiskers are the minimum and maximum data points and box represents upper and lower quartiles with the horizontal line at the median. EBV DNA was quantified in mice in the (A) PBS control group, (B) IVIG group, and (C) EBV hyperimmune globulin group. (D) Median EBV DNA copies for each group at separate time points were calculated. NS indicates not significant.

| Treatment group | No LPD or lymphoma (%) | LPD or lymphoma (%) |
|---|---|---|
| PBS | 4/6 (66.7%) | 2/6 (33.3%) |
| IVIG | 5/6 (83.3%) | 1/6 (16.7%) |
| EBV hyperimmune globulin | 6/6 (100%) | 0/6 (0%) |

**Table 3.1. Number of animals with LPD or lymphoma after challenge with EBV**

### 3.2.4 Mice that received IVIG or EBV hyperimmune globulin had similar levels of total human IgG in the plasma

To be certain that differences in EBV DNA copy number in the blood between mice receiving EBV hyperimmune globulin and IVIG was not due to differences in plasma levels of the two immune globulin products, plasma from mice was tested for total human IgG concentration by ELISA. Mice that received IVIG or EBV hyperimmune globulin showed an increase in the level of human IgG that peaked at 1 to 3 weeks after infection (**Fig. 3.5A -3.5C**), while animals that received PBS showed no increase in IgG levels. Mice that received IVIG or EBV hyperimmune globulin had a decline in human IgG from weeks 3 to 11 after infection and then remained stable. Similar levels of IgG were present in plasma of mice receiving IVIG or EBV hyperimmune globulin each week with the exception of week 3 when IgG was significantly higher in animals receiving IVIG than those receiving EBV hyperimmune globulin ($p = 0.04$) **(Fig. 3.5D)**. Therefore, the lower number of EBV DNA copies in the blood of mice that received EBV hyperimmune globulin compared to those that received IVIG was not due to a difference in the plasma level of total human IgG.

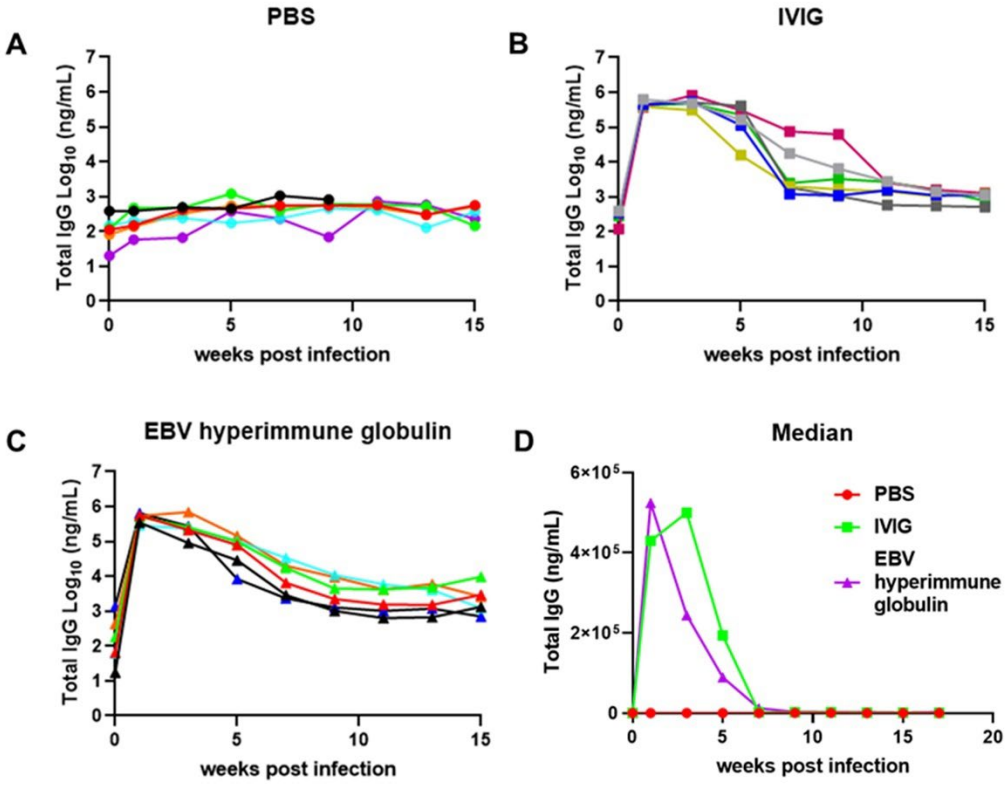


**Figure 3.5. Quantification of total human IgG in mouse plasma.**
The total human IgG concentration was measured by ELISA in the plasma of mice that received (A) PBS, (B) IVIG, or (C) EBV hyperimmune globulin. Each line represents one mouse and plasma samples collected bi-weekly were used in the assay. (D) Median total IgG level of each group at different time points was calculated.

### 3.3 Discussion

We have shown that humanized mice that received EBV hyperimmune globulin isolated from the plasma of donors with high levels of gp350 and B cell neutralizing antibodies had significantly reduced EBV DNA copies in the blood compared with mice that received PBS after challenge with EBV. However, EBV hyperimmune globulin was not significantly better than IVIG to reduce EBV DNA copies in the blood of mice after challenge.

We screened plasma donors for those with high gp350 titers since EBV gp350 is the major target of B cell neutralizing antibodies in human plasma (Bu et al., 2019) and gp350 antibody titers correlate strongly with EBV neutralizing antibodies in human plasma (Sashihara et al, 2009). While EBV gp350 has been the major target for an EBV vaccine (Sokal et al., 2007) and EBV monoclonal antibodies have been developed as potential therapeutics (Herrman et al., 2016; Tanner, Hu, and Alfieri, 2018; Mutsvunguma et al., 2019), recent studies have focused on other EBV glycoproteins including gH/gL as vaccine candidates or therapeutics. gp350 is important for virus attachment to B cells through CR2 (Nemerow et al., 1987) or CD35 (Ogembo et al., 2013), but is not essential for infection in vitro (Janz et al., 2000). In contrast, EBV gH/gL is essential for virus fusion to B cells and epithelial cells (Wu and Hutt-Fletcher, 2007). In addition, a vaccine containing gH/gL nanoparticles induced higher titers of antibody to neutralize virus infection of B cells and epithelial cells than a similar gp350 nanoparticle vaccine (Bu et al., 2019). Monoclonals to EBV gH/gL have been isolated that block fusion of the virus to both B cells and epithelial cells and potently neutralize infection of both cell types (Bu et al., 2019; Snijder et al. 2018). Thus, isolation of EBV hyperimmune globulin from donors with high titers of antibodies to EBV gH/gL may have provided more effective reduction in the number of EBV DNA copies in the blood than EBV hyperimmune globulin selected for antibody to gp350.

We found that EBV hyperimmune globulin did not completely eliminate detection of EBV DNA in the blood of humanized mice challenged with EBV intravenously. EBV does not naturally infect small animals. Lymphocryptoviruses that are closely related to EBV can infect rhesus monkeys (Cho et al., 1999), but the sequence of EBV and rhesus lymphocryptovirus gp350 share only 49% amino acid similarity and EBV cannot infect rhesus macaques (Herrman et al., 2016). Humanized mice engrafted with $CD34^+$ hematopoietic stem cells are currently the best small animal model to study EBV infection. Infection of these mice with high doses of EBV results in viremia and B cell lymphoproliferative disease or lymphoma with similar histopathology and latent EBV gene expression as EBV infected immunocompromised patients; infection with low doses of EBV cause persistent infection without lymphoproliferative disease (Yajima et al., 2008). Humanized mice reach their peak viral load 4-to-6 weeks after primary infection which is similar to the course in symptomatic infections in humans (Munz, 2017). Despite the similarities between EBV infection in humans and humanized mice, there are several limitations in the mice model. Humanized mice have engraftment of human lymphocytes, but not human epithelial cells. Since mouse epithelial cells cannot be infected with EBV in the absence of expression of human CR2 (Ahearn et al., 1988), only B cells in humanized mice can be infected. Thus, these animals require intravenous inoculation with EBV for efficient infection and therefore the natural route of EBV infection, the oropharynx, cannot be studied in humanized mice. This difference in the route of infection may affect the evaluation of the efficacy of EBV hyperimmune globulin. Thus, administration of EBV hyperimmune globulin to humans, may or may not reach sufficient levels in the mucosa of the oropharynx to protect them from the natural route of infection, despite protection observed in the humanized mice model.

While hyperimmune globulin may be more effective than IVIG due to its higher EBV antibody and neutralizing titers, mAbs to EBV glycoproteins may be even more effective. In fact, a gp350 monoclonal antibody, 72A1, prevented EBV tumor development in severe combined immunodeficient mice injected with EBV seronegative donor peripheral blood mononuclear cells and challenged intravenously with EBV (Haque et al., 2006). More recent studies with a gH/gL mAb showed protection of humanized mice from challenge with EBV (Singh et al, 2020). Future studies might use a combination of EBV mAbs to reduce the chance of immune escape by the virus.

# Chapter 4. Characterization of EBV mAbs and nanoparticle vaccines and testing their efficacy in a humanized mouse model

Portions of the works in this chapter is published in:

Wei C.J, Bu W, Nguyen L.A, Batchelor J, Kim JH, Pittaluga S, Fuller J, Nguyen H, Chou TH, Cohen J.I, Nabel G.J. (2022) A bivalent Epstein-Barr virus vaccine induces neutralizing antibodies that block infection and confer immunity in humanized mice. Science Translational Medicine 14 (643): eabf3685. doi: 10.1126/scitranslmed.abf3685

Additional authors contributed on the works in this chapter: Wang Y, Pittaluga S, Dowdell K, and Pegu A

**Abstract**

EBV is the leading cause of infectious mononucleosis and is associated with ~200,000 cases of cancer annually worldwide. There is no available vaccine but even with a vaccine, highly immunocompromised persons may not produce a potent immune response. B cell entry during EBV infection is an orchestrated process between viral glycoproteins gp350, gH/gL, gp42, and gB. gp350 is most abundant glycoprotein on the surface of the virus and on infected cells and important for the virus to attach to B cells. gp350 is not required during B cell entry but it is a major target of neutralizing antibodies in human plasma. Previous EBV vaccine and therapeutic research were focused on gp350. gH/gL and gp42 are glycoproteins involved in the initiation of virus fusion in B cells and gB allows the virus and host membranes to fuse together. gH/gL, gp42, and gB are required during B cell entry but it is unknown whether these glycoproteins are ideal antigens for therapeutics since these proteins are not the major target of neutralizing antibodies in B cells.

Here, we have developed monoclonal antibodies (mAbs) against EBV glycoproteins gp350, gH/gL and gp42 and evaluated the efficacy of these mAbs in humanized mice. When animals were injected with gp350, gH/gL, gp42 mAbs, or a combination of all three mAbs and challenged with EBV, one gH/gL mAb one gp42 mAb, and a combination of mAbs resulted in greater reduction in the level of viremia and a higher survival rate of the mice compared to all of the other gH/gL or gp42 mAbs. Surprisingly, mice that received gp350 mAb showed similar level of viremia to PBS control group.

We have also developed nanoparticle (NP)-based vaccines against gH/gL and gH/gL/gp42 and passively transferred IgG isolated from mice immunized with these vaccines to humanized mice. Our previously published gp350-NP vaccine was used as a vaccine in

combination with gH/gL-NP or gH/gL/gp42-NP to provide more robust protection. Humanized mice that received IgG from naïve BALB/c mice and were challenged with EBV showed viremia and developed EBV B cell lymphomas, while mice that received IgG from gH/gL-NP+gp350-NP or gH/gL/gp42-NP+gp350-NP immunized mice had very low levels of viremia and did not develop lymphomas. These findings demonstrate that gH/gL and gp42 may be important targets for EBV therapeutics and vaccines.

## 4.1 Introduction

90% of adults in the world are infected with EBV and can transmit the virus from their infected saliva (Cohen et al., 2011). EBV is responsible for most cases of infectious mononucleosis and is associated with various cancers such as Burkitt lymphoma, Hodgkin lymphoma, and nasopharyngeal carcinoma (Cohen et al., 2011). In addition to the association of EBV with cancer, patients with congenital, acquired, or post-transplant immunodeficiencies may develop EBV lymphoproliferative disease. These patients have impaired T cell immunity that leads to uncontrolled EBV driven B cell proliferation (Cohen 2015). Some immunodeficient patients are given IVIG to provide antibodies to reduce EBV infection, but breakthrough infections occur and IVIG is not an effective EBV disease preventive measure.

EBV B cell infection is initiated by attachment of viral glycoprotein gp350 to complement receptor 2 (CR2/CD21) on the surface of B cells (Fingeroth et al., 1984). The next step for virus entry requires the viral glycoprotein complex, gH, gL, and gp42 (Spriggs et al., 1996). EBV gp42 in the complex binds to HLA class II molecules on B cells and along with gH/gL initiates fusion of viral and B cell membranes by activating gB (Spriggs et al., 1996; McShane and Longnecker, 2004). For epithelial cells, EBV attaches to the cell through EBV BMRF2 binding to integrins (Tugizov et al., 2003). This leads to binding of gH/gL both to integrins and ephrin receptor A2 and activates gB to allow fusion of viral and cellular membranes (Chen et al., 2018; Chesnokova et al., 2009; Zhang et al., 2018). Antibodies against gH/gL or gp42 can prevent or reduce viral infection both by neutralizing virus infection and by blocking fusion of virus and host cell membranes (Bu et al., 2019).

Our lab previously has developed a gp350-ferritin nanoparticle vaccine in which self-assembling nanoparticles were generated that present the EBV gp350 CR2 receptor-binding sites

on the surface in an ordered, high-density array (Kanekiyo et al., 2015). When mice or non-human primates were vaccinated with the gp350-ferritin nanoparticle vaccine, the vaccine elicited > 100-fold higher B cell neutralizing antibody titers than soluble gp350. Nevertheless, gp350 vaccine may only protect infection of B cells and not epithelial cells.

The natural host of EBV is humans, and mice cannot be infected with this virus; therefore, mice are not a suitable animal model to study EBV infection. In contrast, humanized mice transplanted with human $CD34^+$ hematopoietic stem cells that reconstitute human immune components including B cells, T cells, NK cells, and macrophages is the best small animal model to study B cell EBV infection (Fujiwara et al., 2015). Infection of these humanized mice with EBV results in similar diseases as seen in immunocompromised humans including EBV-associated B cell lymphoproliferative disease and EBV-associated hemophagocytic lymphohistiocytosis (Fujiwara et al., 2015). When mice are inoculated with low doses of virus, low grade EBV viremia is present in the peripheral blood, and the persistent, latent infection does not result in lymphoproliferative disease or hemophagocytic lymphohistiocytosis similar to healthy EBV seropositive humans (Yajima, 2008).

Here, we test the ability of individual gp350, gH/gL and gp42 mAbs or a combination of these mAbs in humanized mice to identify which mAb(s) best protects the mice from EBV infection. We also test the efficacy of gH/gL and gH/gL/gp42 nanoparticle vaccines in humanized mice by passive transfer of IgG isolated from immunized mice. Most EBV vaccine development has focused on gp350 since it is the major glycoprotein targeted by serum-neutralizing antibodies for B cell infection (Thorley-Lawson and Poodry, 1982) and our study shows the importance of targeting other EBV glycoproteins for development of future vaccines or therapeutics.

## 4.2 Results

### 4.2.1 mAbs 769C2 and 769B10 have longer half-lives than 770F7 in human FcRn transgenic mice

EBV gH/gL-specific mAbs have been isolated using fluorescent labeled gH/gL probes and B cells from healthy human donors with high B cell and epithelial cell EBV neutralization titers. Three gH/gL neutralizing mAbs, 769C2, 770F7, and 769B10, that target different epitopes on gH were evaluated for their half-life in mice and their efficacy to protect humanized mice from EBV infection.

The variable regions of each gH/gL mAb were cloned in a vector resulting in a human Fc backbone for each antibody. Since human IgG binds to FcRn resulting in endocytosis and recycling of the antibody, the half-life of mAbs 769C2, 770F7, and 769B10 were determined by injecting a single dose of each mAb in human FcRn transgenic mice. The concentration of the mAb in the serum were measured by ELISA. The half-life was calculated using a non-compartmental model (**Table 4.1**). mAbs 769C2 and 769B10 had similar half-lives of 19.7 and 17.3 days, respectively, and similar clearance rates of 5.2 mL/day/kg and 6.6 mL/day/kg in the mice. mAb 770F7 had a shorter half-life of 10.7 days and a faster clearance rate of 10.5 mL/day/kg. Since the variable region of each mAb had been cloned into same IgG1 constant region backbone plasmid, the pharmacokinetic differences depended on the variable region of the antibody.

| mAbs | Half-life (days) | AUC (day*ug/mL) | Clearance (mL/day/kg) |
|---|---|---|---|
| mAb 769C2 | 19.7 | 1020.9 | 5.2 |
| mAb 770F7 | 10.7 | 492.5 | 10.5 |
| mAb 769B10 | 17.3 | 787.3 | 6.6 |

**Table 4.1. Pharmacokinetics of gH/gL mAbs in human transgenic FcRn mice.**
Averaged half-life, area under the curve (AUC), and clearance rate of each mAb in each group of human FcRn transgenic mice was calculated using WinNonLin software. There were 5 mice in each group.

### 4.2.2 mAb 769B10 is the most effective mAb to protect humanized mice from death after EBV challenge

Since EBV infects human, but not mouse B cells, humanized mice with human lymphocytes were used to determine the efficacy of gH/gL mAbs in vivo. Groups of 5 humanized mice were inoculated intraperitoneally with 0.5 mg of mAb 769C2, 769B10, or 770F7 on days -1, 0, 1, 4, 7, and 10 of infection and challenged with 1 x $10^6$ GRU of EBV B95-8 intravenously on day 0 (**Figure 4.1A**). Due to the limited number of animals that can be engrafted with cells from a single human donor, mice from two different donors were equally distributed among the different groups. Mice were weighed and blood was collected for 15 weeks after infection and animals were euthanized when they lost $\geq$ 30% of their weight or were unresponsive to external stimuli. Mice in the PBS control group all died or were euthanized by 11 weeks after EBV challenge (**Figure 4.1B**). 80% of mice receiving mAb 770F7 died or were euthanized before week 5 post infection. From previous studies with humanized mice, the peak viremia level was often seen at week 5 post infection, so deaths that occurred earlier than 5 weeks post infection were considered unlikely to be due to EBV infection. Mice that received mAb 769B10 had the highest survival rate (60%), followed by animals that received mAb 769C2 group (20% survival) at the end of the study.

### 4.2.3 mAb 769B10 is the most effective mAb to protect mice from viremia after EBV challenge

To increase sensitivity to detect EBV in the blood of the mice, qPCR was performed using primers and probes for the EBV repeat sequence, BamHI W, which is present in 11 copies in the EBV B95-8 strain used in the experiments. DNA was extracted from mouse blood collected weekly and EBV DNA was amplified and quantified by qPCR. All mice in the PBS control group developed viremia after challenge with EBV with peak levels 5 weeks after infection (**Figure 4.1C**). All mice that received mAbs 769C2 and 770F7 also became viremic after EBV challenge with the peak level of viremia at 5 weeks. When area under the curve analysis was performed, a p value of $< 0.001$ was considered significant. Mice receiving mAb 769C2 or 770F7 did not have significantly reduced viremia compared to the PBS control group ($p = 0.006$ for 769C2 vs. PBS and $p=0.018$ for 770F7 vs. PBS). In contrast, only 20% of mice that received mAb 769B10 became viremic after challenge and the number of EBV DNA copies in the blood was significantly reduced compared to the PBS, mAb 769C2, or mAb 770F7 groups ($p <0.001$ for 769B10 vs. each of the other three groups).

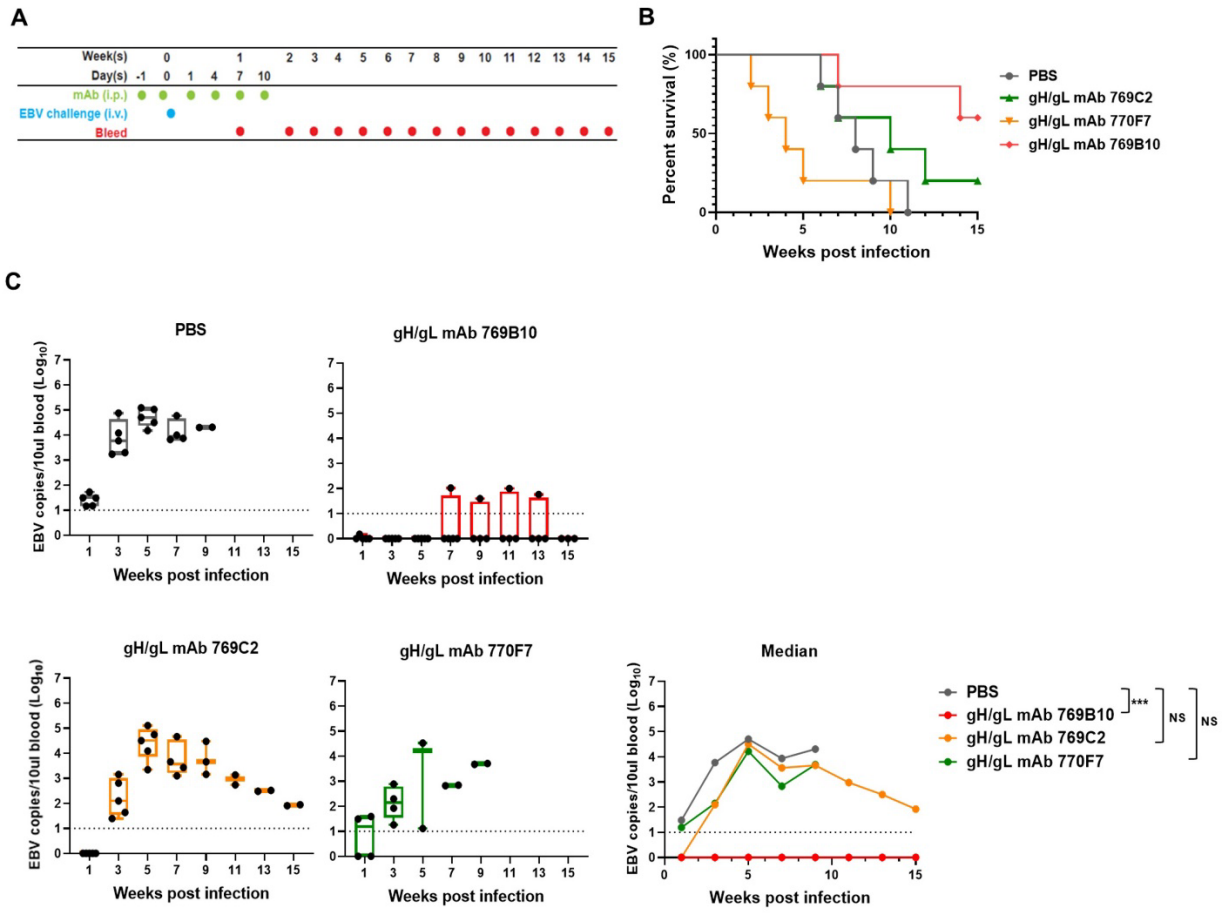


**Figure 4.1. Evaluation of efficacy of gH/gL mAbs.**
(A) Experimental scheme of injections. Mice were given six doses of gH/gL mAbs 769C2, 770F7, 769B10, or PBS intraperitoneally and challenged intravenously with EBV after the second dose of mAb. (B) Survival rates for each group of mice after EBV challenge. Five humanized mice were in each group. (C) EBV DNA copies in the blood quantified by real-time qPCR. Each dot represents one mouse, and the dotted line indicates the limit of detection of the assay. Whiskers indicates minimum and maximum data points for EBV DNA copies in the blood, the box represents upper and lower quartiles, and the horizontal line in the box is the median. ***$p \leq 0.001$

To quantify mAb concentrations in plasma collected weekly, ELISA assays were performed. gH/gL mAbs were present in the plasma until week 9 and 11 post infection in mice that received mAb 770F7 and mAb 769C2, respectively (**Figure 4.2**). Mice that received mAb 769B10 had the longest duration of mAb detected in the plasma with a gradual reduction until week 13 post infection.

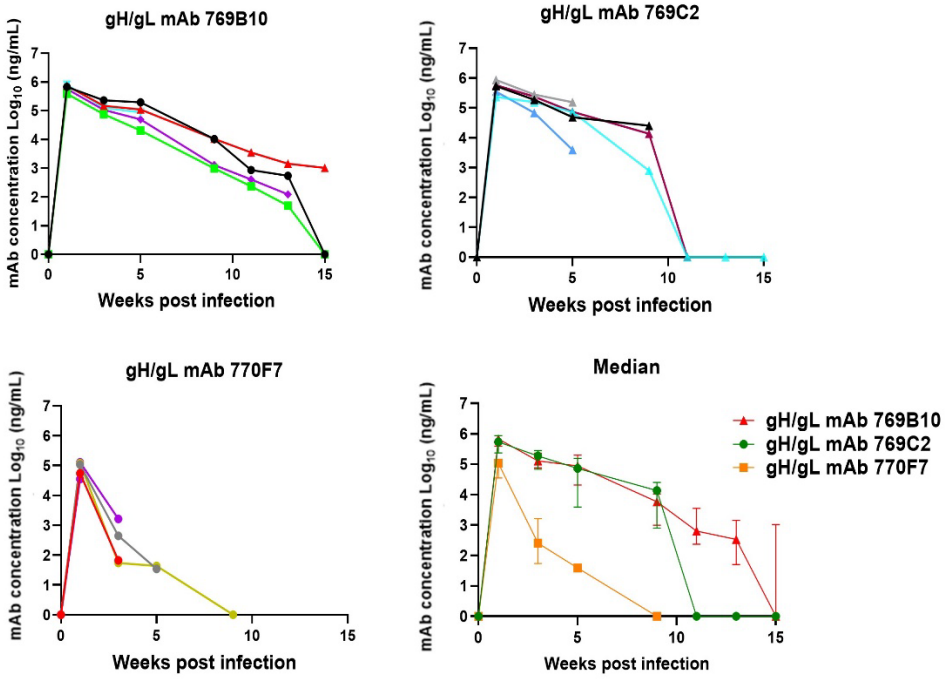


**Figure 4.2. Quantification of gH/gL mAbs in the plasma.**
Concentration of gH/gL mAbs in the plasma of individual humanized mice at various times after EBV challenge measured in duplicate by ELISA. The median and standard errors of gH/gL mAb concentrations for each group of 5 humanized mice are also shown.

### 4.2.4 Mice that received mAb 769B10 have no macroscopic lesions in organs or signs of lymphoproliferative disease or lymphoma

At the end of the study, liver, lung, kidney, and spleen were collected and evaluated for any macroscopic lesions on the surface of the organs. 60% of mice that received PBS or mAb 769C2 had macroscopic lesions on the surface of at least one of the organs (**Figure 4.3A and B**). Only one of five mice (20%) that received mAb 770F7 had a macroscopic lesion. In contrast, mice that received mAb 769B10 had no observable lesions on the surface of any of the organs. Next, tissue sections from each organ were evaluated for signs of atypical infiltrates, lymphoproliferative disease, or lymphoma by staining with hematoxylin and eosin (H&E) and an antibody to human CD20 (a B cell marker) and by in situ hybridization using an EBV-encoded RNA (EBER1) probe. The tissues were evaluated by a pathologist who was unaware of the treatments that the animals had received. None of the mice receiving mAb 769B10 showed disease in any of the organs (**Figure 4.3A**). However, all mice that received PBS or mAb 769C2 had disease in at least one organ and one mouse receiving mAb 770F7 had disease in an organ. Three mice in the PBS group, and one mouse each receiving mAb 769C2 or 770F7 developed EBV-positive B cells lymphomas (based on staining for CD20 and EBER1) (**Figure 4.3A, 4.3C**).

EBER1-stained tissues were scored based on the number of EBER-positive cells (0 for no EBER-positive cells, up to 3+ for many EBER-positive cells) (**Figure 4.3D**). 80% of mice in the PBS group and 60% of mice receiving mAb 769C2 had scores of 2-to-3 in at least one organ, while only 20% of mice receiving mAb 770F7 or 769B10 had a score of 1 in at least one organ (**Figure 4.3E**). Therefore, mAb 769B10 was the best gH/gL mAb to protect mice from lymphoma and lesions on the surface of organs.

A

| | Number of mice with diease (%) | | | | |
|---|---|---|---|---|---|
| | Macroscopic lesions | Atypical infiltrates | LPD | Lymphoma | Lymphoma, atypical infiltrates, or LPD |
| PBS | 3/5 (60%) | 3 (60%) | 0 (0%) | 3 (60%) | 5 (100%) |
| 769B10 | 0/5 (0%) | 0 (0%) | 0 (0%) | 0 (0%) | 0 (0%) |
| 769C2 | 3/5 (60%) | 4 (80%) | 0 (0%) | 1 (20%) | 5 (100%) |
| 770F7 | 1/5 (20%) | 0 (0%) | 0 (0%) | 1 (20%) | 1 (20%) |

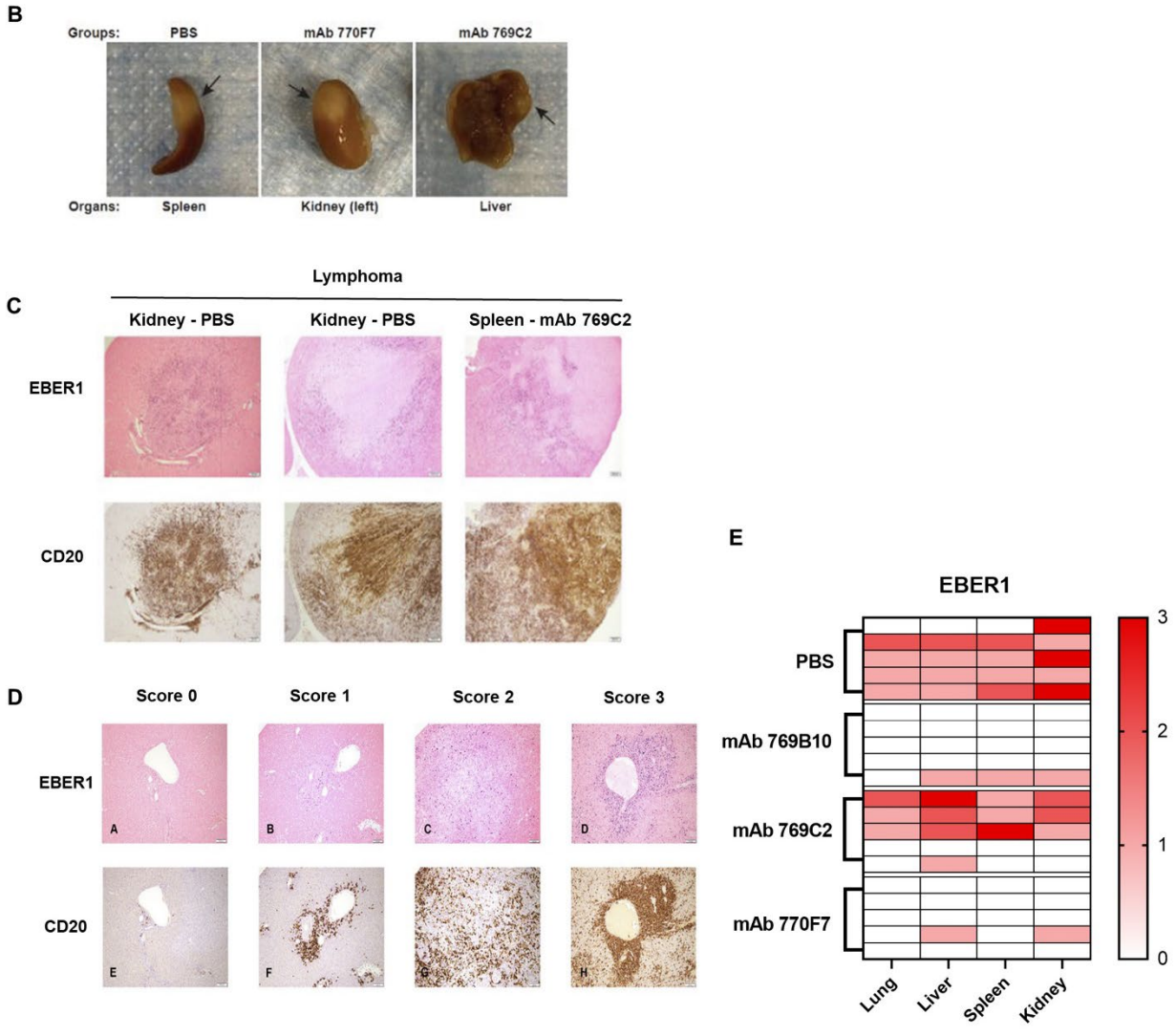


**Figure 4.3. Pathology evaluation of organs.**
(A) Summary table of mice with macroscopic lesions, atypical infiltrates, lymphoproliferative disease, and lymphoma. (B) Images of organs with macroscopic lesions. (C) EBER1 and CD20 stained tissues with lymphoma. (D) Representative images of EBER1 scoring. (E) A heatmap of organs with EBER1 scores in each group of mice with score 0 indicating no EBER1 positive cells and scores 1-3 indicating EBER1 positive cells with increased numbers of positive cells as the score increases.

### 4.2.5 Mice that received gp42 mAb A10 have the highest survival rate and no viremia after EBV challenge compared with other gp42 mAbs

EBV infection of B cells requires gp42 for fusion of the viral membrane to the host cell plasma membrane; in addition, gp42 binds to human leukocyte antigen (HLA) class II molecules on host cells (Bu et al, 2019). gp42 mAb A10 was isolated from a cynomolgus monkey vaccinated with an EBV gH/gL/gp42 vaccine. B cell neutralization demonstrated that gp42 mAb A10 was more potent than the previously published gp42 mAb F2-1 (Strnad et al., 1982) (**Figure 4.4A**). Similar to evaluation of the gH/gL mAbs, gp42 mAb A10 and gp42 mAb F2-1 were evaluated for efficacy in humanized mice. As controls, PBS and gH/gL mAb 769C2, a mAb that did not protect against viremia in humanized mice, were used in the study. Humanized mice received 6 doses of PBS or mAbs and challenged with EBV on day 0 using the same protocol as for mAb gH/gL (**Figure 4.4B**). Animals were weighed weekly and blood samples were collected weekly for 15 weeks post infection (**Figure 4.4B**). Mice in the PBS group had a 40% survival rate, while 80% of mice that received gp42 mAb F2-1 or gH/gL mAb C2 survived (**Figure 4.4C**). In contrast, all of the mice that received gp42 mAb A10 survived until the end of the study. Thus, gp42 mAb A10 protected humanized mice from death better than the other mAbs.

### 4.2.6 gp42 mAb A10 is the best gp42 mAb to protect mice from viremia after EBV challenge

DNA was extracted from blood collected weekly and EBV DNA was quantified by qPCR as reported above for the EBV gH/gL mAb experiments. All mice in the PBS group and all animals that received gH/gL mAb 769C2 were viremic with a peak at week 5 post infection (**Figure 4.4D**). 80% of mice that received gp42 mAb F2-1 were viremic. However, none of the mice that received gp42 mAb A10 had detectable EBV DNA in blood. Next, the concentration of

mAb in plasma collected weekly was measured by ELISA to evaluate whether the difference in the percentage of mice that were viremic was due to different levels of mAbs present in the plasma. mAb concentrations in mice that received gH/gL mAb 769C2 had more rapid decreases between week 5 and 9 post infection compared to mice that received gp42 mAb 10 or gp42 mAb F2-1; however, overall patterns of antibody levels were similar in all three mAb groups (**Figure 4.4E**). In summary, gp42 mAb A10 protected mice from viremia better than mAb F2-1 or gH/gL mAb 769C2.

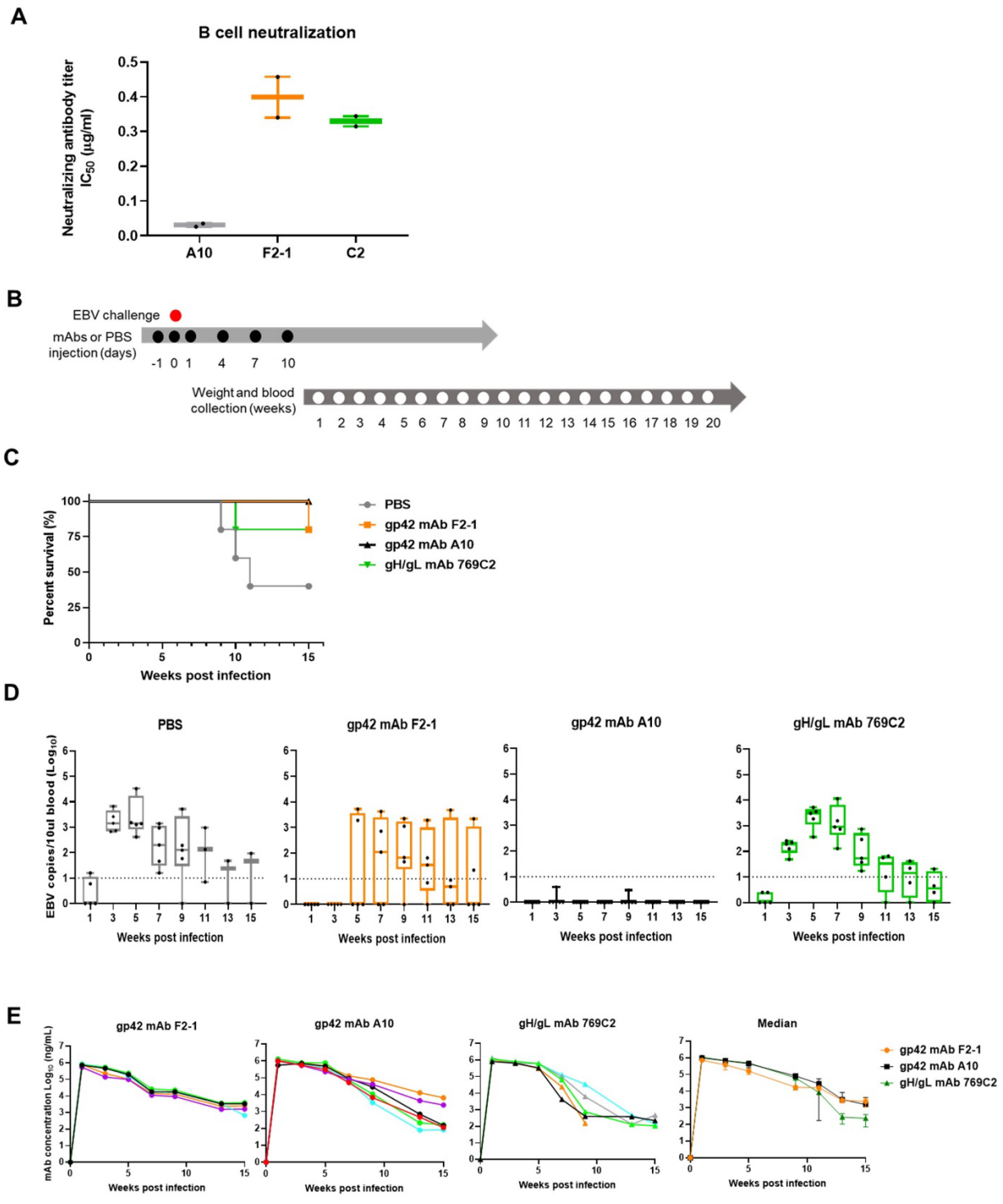


**Figure 4.4. Evaluation of efficacy of gp42 mAbs in humanized mice.**
(A) B cell neutralization of gp42 mAb A10, gp42 mAb F2-1, and gH/gL mAb 769C2. (B) Schedule of injections and sample collections. (C) Survival rates of mice that received PBS, gp42 mAb A10, gp42 mAb F2-1, or gH/gL mAb 769C2 and challenged with EBV. Five humanized mice were in each group except for gp42 mAb A10 with 6 humanized mice in the group. (D) Graphs for viremia of each mouse from week 1 to week 15 post infection. Each dot represents one mouse, and the dotted line indicates the

detection limit of the assay. Whiskers indicates minimum and maximum data points, boxes represent upper and lower quartiles, and horizontal lines in boxes are medians. (E) Concentration of gp42 or gH/gL mAbs in the plasma of individual humanized mice at various times after EBV challenge measured in duplicate by ELISA. The median and standard errors of gp42 or gH/gL mAb concentrations for each group of 5 humanized mice are also shown.

### 4.2.7 Mice that received gp42 mAb A10 have no macroscopic organ lesions or signs of lymphoproliferative disease or lymphoma

At 15 weeks post infection, all mice were euthanized, and lungs, liver, spleen, and kidneys were collected from each animal. 80% of mice in the PBS group had macroscopic lesions in one of the organs and 20% of mice receiving gp42 mAb F2-1 had lesions in the organs (**Figure 4.5A and B**). Mice that received gp42 mAb A10 or gH/gL mAb 769C2 were free from any observable lesions in the organs. Organs were sectioned and stained with H&E and antibody to CD20, and in situ hybridization was performed with a probe to EBER1. All tissues with lymphoma had EBER1 positive and CD20 positive cells (**Figure 4.5C**). Tissues stained with EBER1 were scored from 0 to 4 based on the number of EBER1-positive cells with 0 indicating no EBER1-positive cells and 4 indicating the most EBER1-positive cells. 80% of mice in the PBS group and 60% of mice receiving gH/gL mAb 769C2 had at least one organ with an EBER1 score of 1 or higher (**Figure 4.5D**). Only 20% of mice that received gp42 mAb F2-1 had an EBER1 score of 1 or higher. In contrast, none of the mice that received gp42 mAb A10 had EBER1-positive cells. Thus, gp42 mAb A10 best protected all mice from EBV infection and lymphoma.

A

| | Number of mice with diseases | | |
|---|---|---|---|
| | Macroscopic lesions | LPD | Lymphoma |
| PBS | 4/5 (80%) | 1/5 (20%) | 3/5 (60%) |
| gp42 mAb A10 | 0/6 (0%) | 0/6 (0%) | 0/6 (0%) |
| gp42 mAb F2-1 | 1/5 (20%) | 0/5 (0%) | 1/5 (20%) |
| gH/gL mAb 769C2 | 0/5 (0%) | 1/5 (20%) | 0/5 (0%) |

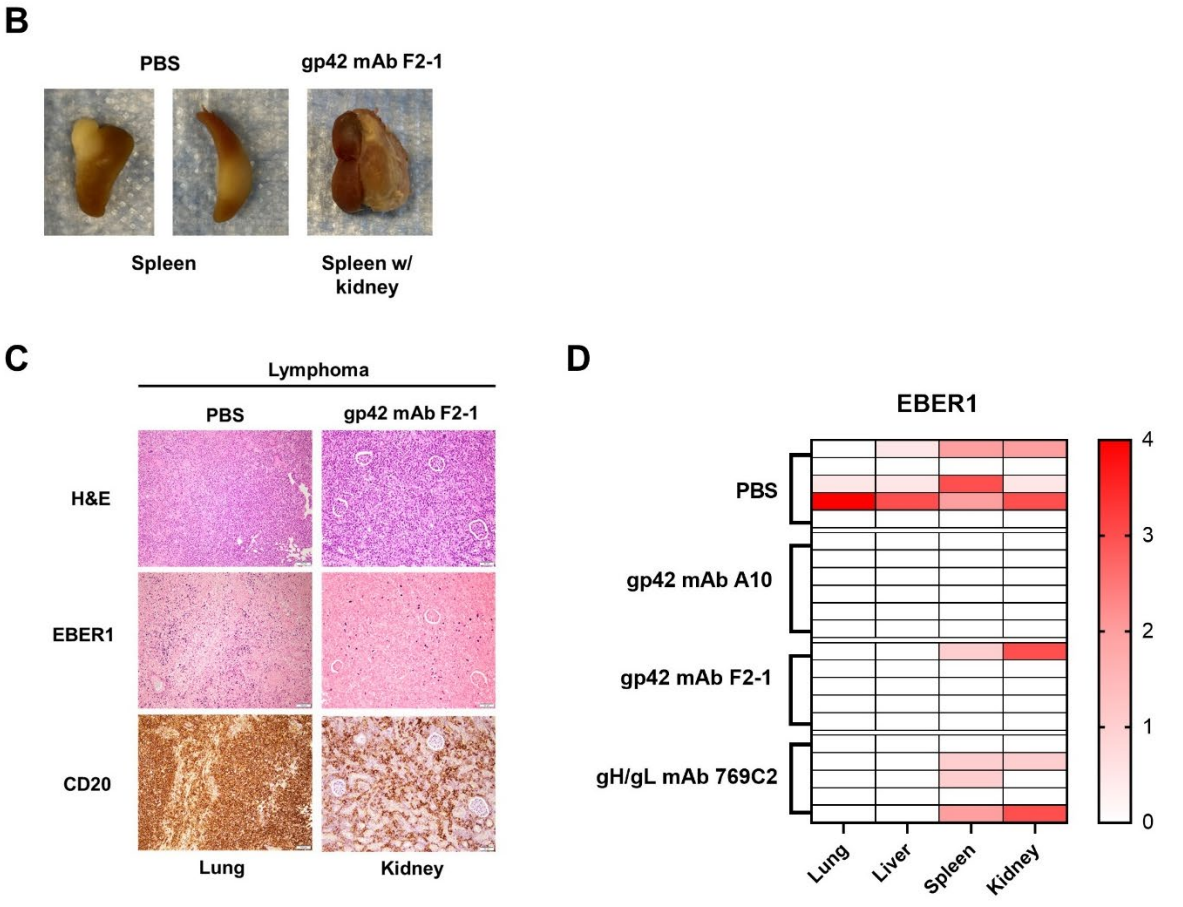


**Figure 4.5. Pathology of organs from mice that received gp42 or gH/gL mAbs.**
(A) Summary table of organs with macroscopic lesions, signs of atypical infiltrates, lymphoproliferative disease, or lymphoma. (B) Representative images of organs with macroscopic lesions. (C) H&E, EBER1, and CD20 stained images of organs with lymphoma. (D) Heatmap of organs with EBER1 scores in each group of mice with 0 indicating EBER1 negative cells and scores 1-4 indicating EBER1 positive cells with increased numbers of positive cells as the score increases.

### 4.2.8 gp350 mAb H02 did not protect humanized mice from death or viremia

gp350 mAb H02 was isolated from a cynomolgus macaque vaccinated with an EBV gp350-ferritin vaccine using a fluorophore-labeled gp350 probe. gp350 is the most abundant glycoprotein on the virus and on virus-infected cells and antibodies against gp350 are responsible for 50-60% of the EBV B cell neutralizing activity in human plasma (Bu et al., 2019). gp350 mAb H02 was much more potent to neutralize EBV infection of B cells than a panel of gH/gL mAbs (data not shown). Thus, I hypothesized that gp350 mAb H02 would show excellent protection against EBV infection in humanized mice. Also, since B cell infection is a highly orchestrated process involving gp350, gH/gL, and gp42, I hypothesized that mAbs targeting multiple glycoproteins would provide stronger protection compared to a single mAb. To compare the efficacy of a gp350 mAb with gH/gL mAbs and a gp42 mAb, mice were injected with gp350 mAb H02 only, gH/gL mAbs + gp42 mAb A10, or gp350 mAb H02 + gH/gL mAbs + gp42 mAb A10. For the gH/gL mAbs, 769C2, 769B10, and 770F7 mAbs were mixed in a 1:1:1 ratio and used. The total amount of mAb was the same whether animals received a single mAb or a combination of mAbs. The same injection scheme was followed as for the gH/gL mAb or gp42 mAb studies reported above, with a total of 6 doses of mAb and the EBV challenge given shortly after the second dose of mAb. Mice that received PBS or gp350 mAb H02 died by week 15 post infection; in contrast, all of the mice that received gH/gL mAbs + gp42 mAb A10 or that were given gp350 mAb H02 + gH/gL mAbs + gp42 mAb A10 survived at week 15 post infection (**Figure 4.6A**). When viremia was measured by qPCR, all mice in both the PBS group and the gp350 mAb H02 group were viremic with a peak level of EBV DNA at week 5 post infection (**Figure 4.6B**). In contrast, only ~40% of mice that received gH/gL mAbs + gp42 mAb A10 had EBV DNA detected in the blood with a peak level at 5 weeks post infection. About

15% of mice that received gp350 mAb + gH/gL mAbs + gp42 mAb A10 had EBV DNA detected in their blood. Thus, despite gp350 being the predominant glycoprotein on the virus and a potent target for neutralizing antibody in B cells, gp350 mAb H02 alone did not protect humanized mice from death or viremia. The combination of gp350, gH/gL, and gp42 mAbs provided the best protection for humanized mice challenged with EBV.

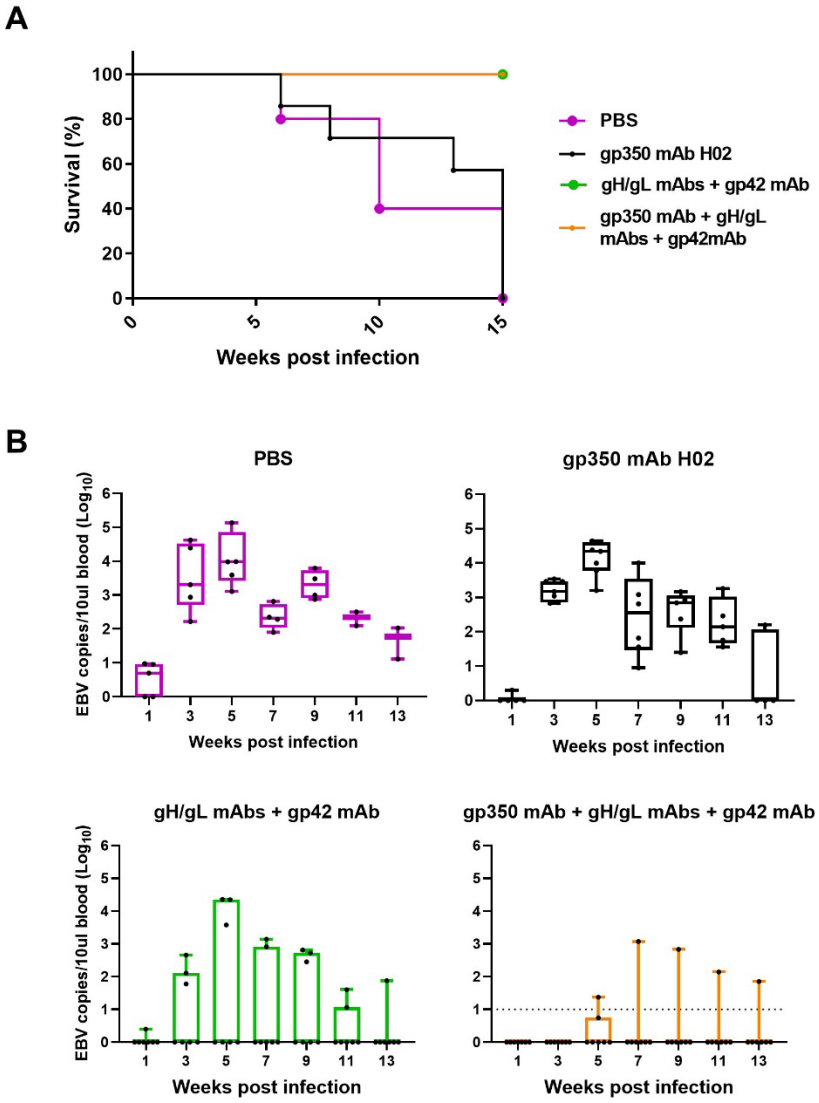


**Figure 4.6. Evaluation of gp350 mAb and combinations of gH/gL and gp42 mAbs with gp350 mAb in humanized mice.**

(A) Survival rate of mice that received PBS, gp350 mAb H02, gH/gL mAbs (769C2, 769B10, and 770F7) + gp42 mAb A10, or gp350 mAb H02 + gH/gL mAbs (769C2, 769B10, and 770F7) + gp42 mAb A10 and challenged with EBV. Seven humanized mice were in each group except for the PBS control group with 5 humanized mice. (B) Viremia of each mouse from week 3 post infection to week 13 post infection. Each dot represents one mouse. Whiskers indicates minimum and maximum data points and boxes represents upper and lower quartiles; the horizontal line in the box is the median.

### 4.2.9 Level of surface expression of CR2 on different B cells correlate with levels of EBV B cell neutralizing activity by mAbs in vitro

To understand why humanized mice that received gp350 mAb H02 showed no protection from viremia after EBV challenge, while gp350 mAb H02 was more potent than gH/gL mAbs in the in vitro B cell neutralization assay, the level of CR2 in the cell line used in the neutralization assays was examined. EBV enters B cells first by attachment of viral gp350 to CR2 (also known as CD21) to the cells (Fingeroth et al., 1984). Thus, the level of CR2 on the surface of the cells used for the in vitro neutralization may affect the neutralization results of the gp350 mAbs. To determine if this is the case, various B cells were evaluated for their level of CR2. Raji cells, used for most in vitro neutralization assays, had highest CR2 levels, followed by BL41 and BL30 Burkitt lymphoma cells (**Figure 4.7A**). In contrast, DG75 Burkitt lymphoma cells showed no detectable surface expression of CR2 by flow cytometry. In vitro neutralization assays of gp350 and gH/gL mAbs were performed using these cell lines. To confirm that results in various B cell neutralization assays were generalizable and not specific to gp350 mAb H02, another gp350 mAb, A9, was also included in the assays. Both of the gp350 mAbs were more potent than the gH/gL mAbs in neutralization assays that were performed using Raji cells (**Figure 4.7B**). However, in BL41 or BL30 cells which have less surface expression of CR2 than Raji cells, the neutralizing titer of gp350 mAbs was reduced. In DG75 cells which have no detectable surface expression of CR2, both of the gp350 mAbs showed no neutralization. In neutralization assays performed in various B cell lines using gH/gL mAbs, the level of surface expression of CR2 in the cell line did not affect the neutralizing titer of the gH/gL mAbs. These results demonstrate that there is a correlation between neutralization of gp350 mAbs, but not gH/gL mAbs, with the level of CR2 expression on the surface of the cell lines.

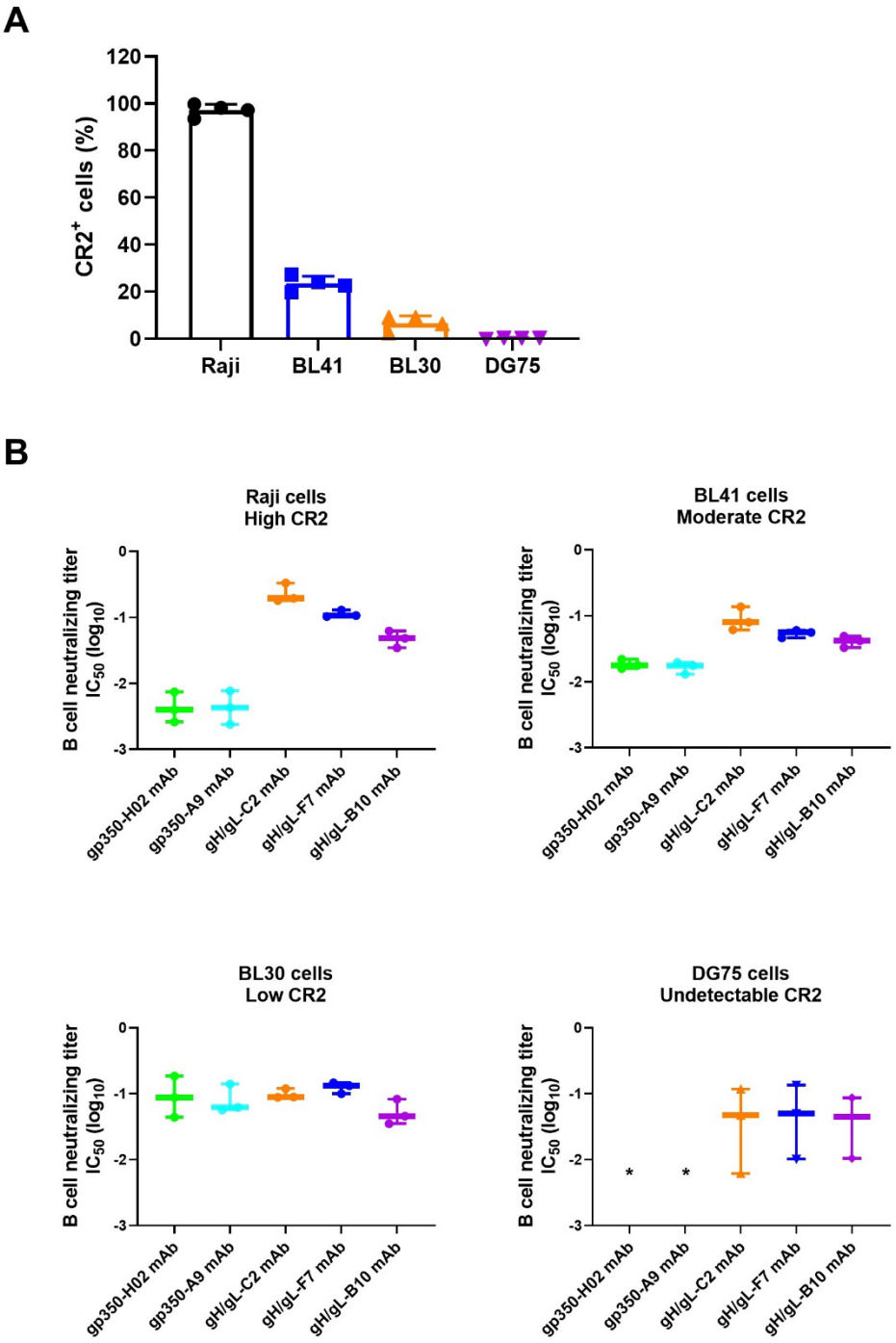


**Figure 4.7. In vitro neutralization using B cell lines with various level of CR2 expression.**
(A) Surface expression of CR2 on Raji, BL41, BL30, and DG75 cells measured by flow cytometry using a mAb to CR2. Each dot represents one independent assay. The long horizontal lines indicate the mean of 4 independent assays and the short horizontal lines are the standard errors. (B) In vitro neutralization of gp350 mAbs and gH/gL mAbs in Raji, BL41, BL30, and DG75 B cells. Each dot represents one experiment. Whiskers indicates minimum and maximum data points, and the horizontal lines are the medians. *Neutralization was not observed.

### 4.2.10 Humanized mice passively transferred with immune sera from vaccinated mice showed protection from EBV infection and lymphoma after challenge with virus

Apart from our own development of EBV mAbs, we have developed additional EBV nanoparticle vaccines in collaboration with Sanofi. Our lab previously showed that a gp350-nanoparticle (NP) vaccine elicited antibodies in mice and monkeys that protect B cells from EBV infection and that gH/gL and gH/gL/gp42 NP vaccines induce antibodies in animals that protect both B cell and epithelial cells from infection (Kanekiyo et al., 2015; Bu et al., 2019). Based on structural data of gH/gL and gp42, self-assembling nanoparticles from a single polypeptide chain containing gH/gL or gH/gL/gp42 fused with bacterial ferritin were designed. gH and gL or gH, gL, and gp42 were constructed as a single chain so that it was certain that the ratio of gH:gL:ferritin or gH:gL:gp42:ferritin would be 1:1:1 or 1:1:1:1, respectively (Wei et al., 2022). Efficacy of these vaccines were evaluated by passive transfer of immune sera from vaccinated mice to humanized mice following by challenge with EBV. First, BALB/c mice were immunized on week 0, 3, and 7 with gH/gL-NP + gp350-NP or gH/gL/gp42-NP + gp350-NP along with AF03 adjuvant. Next, sera collected at various time points post-immunization were pooled and IgG was isolated. As a control, IgG from unimmunized BALB/c mice were isolated. Purified IgG from each of the two vaccine groups and from the PBS group was injected into humanized mice on days -1, 0 (day of EBV challenge), and 1. Then 1 x $10^5$ GRU of EBV was injected intravenously on day 0. Mice that received IgG from gH/gL/gp42-NP + gp350-NP had highest survival rate followed by mice that received gH/gL-NP + gp350 (**Figure 4.8A**). Next, viremia at week 5, 7, and 9 post infection was quantified. All animals in the control group had viremia while only one animal each from the gH/gL-NP + gp350-NP or the gH/gL/gp42-NP + gp350-NP group had very low EBV DNA copies in the blood at week 7 post infection (**Figure 4.8B**). Week 5 and 9 viremia levels were significantly reduced in animals in the gH/gL-NP + gp350-NP and

gH/gL/gp42-NP + gp350-NP groups compared to the PBS control group ($p<0.05$ at week 5 and 9).

In addition, the levels of anti-gH/gL, anti-gp42, and anti-gp350 antibody were determined in plasma of animals 1 week after challenge by LIPS assay (**Figure 4.8C**). The gH/gL-NP + gp350-NP and gH/gL/gp42-NP + gp350-NP groups had similar levels of gp350, gH/gL, and gp42 antibody ranging from $10^5$ to $10^6$ relative light units which were comparable to animals that were immunized with 2 doses of EBV vaccines in previous studies (Kanekiyo et al., 2015; Bu et al., 2019).

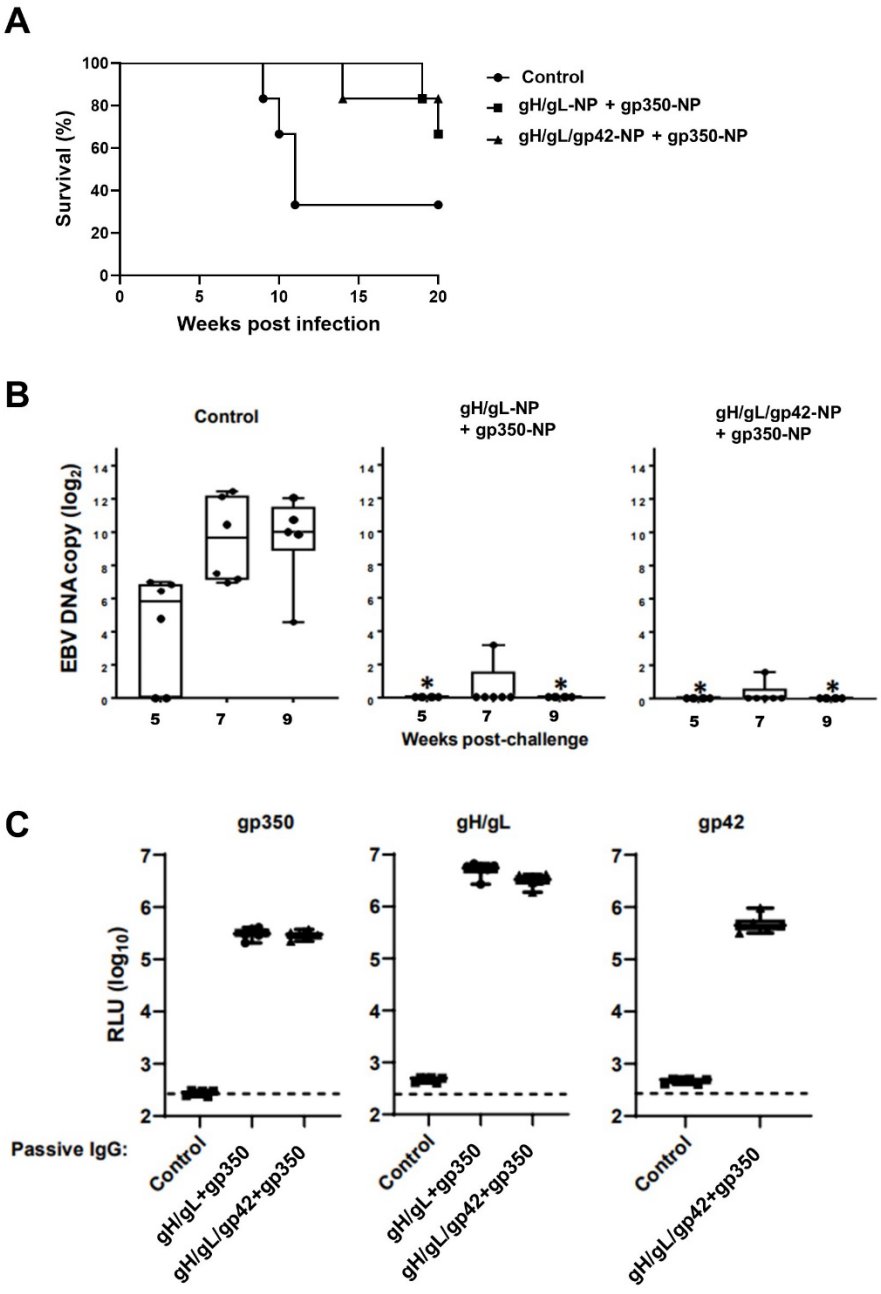


**Figure 4.8. Passive transfer of IgG from gH/gL-NP+gp350-NP or gH/gL/gp42-NP+gp350-NP immunized mice.**

(A) Survival rate of mice that received IgG from control, gH/gL-NP + gp350-NP or gH/gL/gp42-NP + gp350-NP immunized animals and challenged with EBV. Six humanized mice were in each group. (B) Viremia from each group measured at week 5, 7, and 9 post infection. Medians with 25% and 75% percentiles are shown. (C) Antibody titers in the plasma samples at week 1 post infection for gp350, gH/gL, and gp42 measured by LIPS assay. Results are shown in relative light units (RLU). Each dot represents one mouse and whiskers represent minimum and maximum data points, the box represents upper and lower quartiles, and the horizontal line is the median. * $p < 0.05$

At the end of the study, liver, spleen, and kidneys were collected and stained with H&E and CD20, and in situ hybridization for EBER1 was performed. In the kidneys of mice that received PBS control, EBV-positive B cell lymphomas were observed based on CD20 and EBER1, while no lymphomas were seen in mice that received gH/gL-NP + gp350-NP and gH/gL/gp42-NP + gp350-NP (**Figure 4.9A**). The same results were seen in the spleens of mice that received IgG from control, gH/gL-NP + gp350D-NP, and gH/gL/gp42-NP + gp350-NP (**Figure 4.9B**). Three of the six animals that received control IgG had EBV B cell lymphomas while none of the animals that received gH/gL-NP + gp350-NP or gH/gL/gp42 + gp350-NP developed lymphoma. In each tissue, an EBER1 score was assigned based on the number of EBER1-positive cells where 0 was no EBER1-positive cells and 3 was the maximal EBER1-positive cells. In the control group, 4 of 6 animals showed an EBER1 score of 1 or greater while the other two groups were negative for EBER1 (**Figure 4.9C**). Thus, passive transfer of IgG from mice immunized with gH/gL-NP + gp350-NP or gH/gL/gp42-NP + gp350-NP can provide protective immunity in humanized mice by reducing viremia and preventing development of lymphomas.

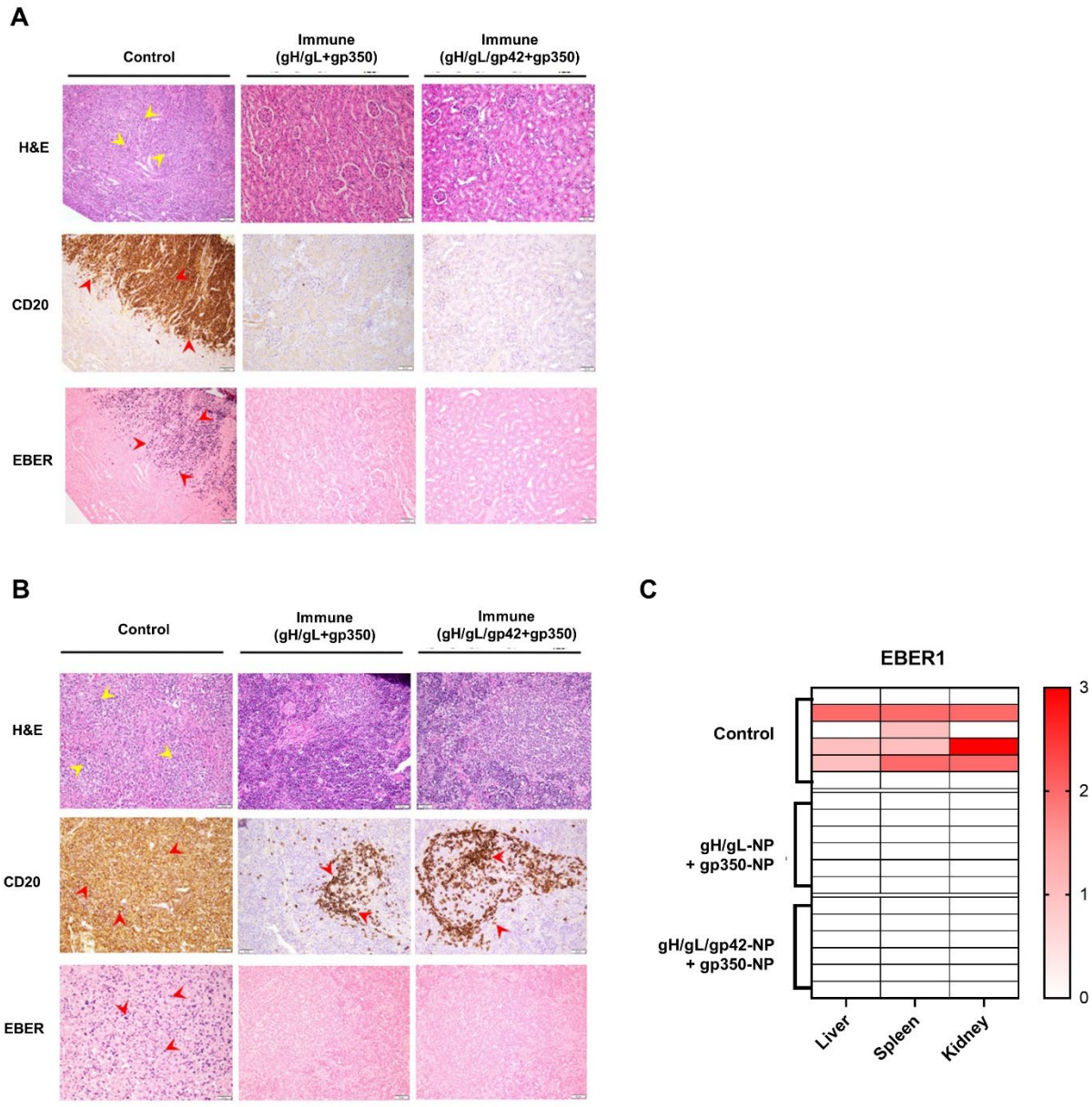


**Figure 4.9. Protection against EBV lymphoma in humanized mice.**
(A) H&E, CD20, and EBER1 stained images of kidney tissues in control, gH/gL-NP + gp350-NP, or gH/gL/gp42-NP + gp350-NP group. (B) H&E, CD20, and EBER1 stained images of spleen tissues in control, gH/gL-NP + gp350-NP, or gH/gL/gp42-NP + gp350-NP group. (C) Heatmap of organs with EBER1 scores in each group of mice with 0 indicating EBER1 negative cells and scores of 1-3 indicating EBER1 positive cells with increased numbers of positive cells as the score increases. Yellow arrows indicate lymphoma, and red arrows indicate cells staining positive for CD20 or EBER1.

### 4.3 Discussion

Here, we evaluated gp350, gH/gL, and gp42 mAbs isolated from human and cynomolgus monkeys as well as the combination of these mAbs. Of the three gH/gL mAbs that were tested, mice that received gH/gL mAb 769B10 that were challenged with EBV showed the highest survival rate, lowest level of viremia, and no evidence of EBV lymphoma or lymphoproliferative disease. gp42 mAb A10 also showed similar results as mAb 769B10 in humanized mice with high survival rates, no viremia, and no lymphoma after EBV challenge. However, humanized mice that received gp350 mAb H02 showed no protection in survival or from viremia and had similar results as mice given PBS and challenged with EBV. The combination of gp350, gH/gL, and gp42 mAbs resulted in the best protection of the humanized mice with low level viremia and a high survival compared to mice that received gp350 mAb H02 only. Also, in evaluation of gH/gL-NP + gp350-NP and gH/gL/gp42-NP+gp350-NP vaccines for their efficacy to protect humanized mice from EBV infection and lymphoma, both groups of humanized mice that received IgG from gH/gL-NP + gp350-NP and gH/gL/gp42-NP + gp350-NP immunized mice showed very low viremia and no development of lymphoma after challenge with EBV. In contrast, mice that received IgG from naïve mice showed high level of viremia with EBV B cell lymphomas after EBV challenge.

In a previous paper (Singh et al., 2020) using gH/gL mAb AMMO1, humanized mice were injected with one dose of mAb before being challenged with a low dose of EBV and 15% (2/13) of mice had viremia. In our study, humanized mice were injected with 6 doses of gH/gL mAbs and challenged with a higher dose of virus. Interestingly, only one mouse receiving gH/gL mAb 769B10 had low copy numbers of EBV DNA in the blood, and the rest of the animals had undetectable levels of EBV. gH/gL mAb 769B10 shares ~50% of gH/gL contact residues with AMMO1. Mice that received mAb 769B10 also showed better protection from mortality and

development of lymphoma compared to our other gH/gL mAbs. This demonstrates that areas of gH where gH/gL mAb 769B10 and AMMO1 bind may be sites that have an important role in EBV infection.

Our humanized mice study evaluating the efficacy of gp42 mAbs showed that gp42 mAb A10 was more potent than gp42 mAb F2-1 in neutralizing infection in B cells in vitro. Also, gp42 mAb A10 protected humanized mice from death, viremia, and development of lymphoma or lymphoproliferative disease better than mAb F2-1 (Strnad et al., 1982) when animals were infected with EBV. Since mAb F2-1 was isolated from a mouse hybridoma and gp42 mAb A10 was isolated from a cynomolgus monkey vaccinated with an EBV gH/gL/gp42 vaccine, both mAbs would need to be humanized in order to conduct clinical trials. Thus, our lab has humanized gp42 mAb A10 and the same results were observed as seen with the cynomolgus mAb when given to humanized mice. gH/gL mAb 769B10 and gp42 mAb A10 individually demonstrated potent protection in humanized mice, but the combination of these two mAbs may elicit even stronger protection as both mAbs target glycoproteins responsible for fusion.

gp350 mAb H02 showed greater potency than gH/gL mAbs in in vitro B cell neutralization assays. Since gp350 is the most abundant glycoprotein on the virus and EBV-infected cells and is responsible for 50-60% of EBV neutralization of B cell infection by antibodies in human plasma, I hypothesized that gp350 mAb H02 would show potent protection against EBV infection in humanized mice. Surprisingly, mice that received gp350 mAb H02 showed the lowest survival rate and highest level of viremia, compared to mice given gH/gL mAbs. Based on in vitro neutralization assays using B cell lines with various levels of CR2 on their surface, I found that the level of CR2 on the target cell affects the measurement of neutralizing activity of gp350 mAbs in vitro. When EBV infects B lymphocytes, virus particles

enter the cells by EBV gp350 binding to its receptor, CR2, on host cells (Fingeroth et al., 1984; Frade et al., 1985). Thus, ability of B cell lines to be infected with EBV is known to correlate with expression of CR2 on the cells (Speck and Longnecker 1999). However, the mechanism for the correlation we observed between CR2 on the cell lines and high neutralizing activity of gp350 mAbs is known. Higher levels of CR2 should allow EBV to bind to cells more effectively and therefore should require higher concentrations of gp350 antibodies to neutralize infection. It is possible that other differences in the cell lines such as the level of CD35, another complement receptor that gp350 bind to during B cell entry, may have a major influence on neutralization of EBV in vitro (Ogembo et al., 2013). The level of CD35 on the surface of the B cell lines was not evaluated; therefore, the mechanism behind the correlation of the EBV infectivity and the neutralizing activity of gp350 mAb is unclear and further studies are needed. In the humanized mice study in which gp350 mAb H02 resulted in no protection against EBV infection, it is possible that the use of a very high titer of challenge virus ($10^6$ GRU) was sufficient such that virus was in close contact with cells and did not need the help of gp350 which enhances attachment of the virus to cells. In this circumstance, gp350 which is important, but not essential, for attachment of virus to the cells can be bypassed and becomes less important for virus entry.

Since gH/gL-NP and gH/gL/gp42-NP vaccines have not yet been tested in humans to evaluate their efficacy, we performed passive transfer of isolated IgG from immunized BALB/c mice with these vaccines. Passive transfer of IgG has been used in prior studies and has been shown to induce vaccine-induced immune protection for other viruses. Espinosa and colleagues passively transferred immune sera from mice immunized with a virus-like particle (VLP) ZIKA to naive mice and showed that the immune sera could protect the animals from weight loss, morbidity, and mortality after virus challenge (Espinosa et al., 2018). Howard et al., also

demonstrated that passive transfer of immune sera from mice vaccinated with an inactivated whole-virus H5N1 vaccine provided dose-dependent protection from challenge with lethal doses of wild-types H5N1 virus (Howard et al., 2011). Our passive transfer study with EBV nanoparticle vaccines also demonstrated protection with increased survival rates, reduction in viremia, and no development of B cell lymphomas.

Humanized mice are currently the best small animal model to study EBV infection since the virus only infects and replicates in human cells. Mice engrafted with human $CD34^+$ hematopoietic stem cells develop a transient high-level viremia similar to that seen in EBV-infected humans, and like hematopoietic stem cell transplant recipients, the mice with transplanted $CD34^+$ cells can develop EBV lymphoproliferative disease and lymphoma (Yajima et al., 2008). Nonetheless, there are limitations with this model. Humanized mice still have mouse epithelial cells. Since B cells and epithelial cells are two major cell types infected with EBV, and gH/gL is required for infection of both cell types, the efficacy of gH/gL mAbs in these mice can only be evaluated in B cell infection (Spriggs et al., 1996; Chen et al., 2018). The presence of mouse epithelial cells in this model also limits the route of infection. Normally, EBV infects oropharyngeal epithelial cells, but in humanized mice, EBV cannot infect mouse epithelial cells through this route. For the purposes of my study, virus was given by intravenous inoculation, and it is possible that a different route of infection (e.g. saliva via the oropharynx or transplanted tissue containing EBV-infected cells) may result in different outcomes for the ability of mAbs to protect humans. Another downside of using humanized mice is that there is a limitation on number of animals that can be engrafted from a single donor. Humanized mice engrafted with different donors must be used when several mAbs are evaluated and conducting a study with mice engrafted from several donors can lead to variability in the results. For the

gH/gL or gp42 mAb studies, I tried to combine mice from different donors in each group to reduce variability in results so that one group of mice are not from a single donor. Commercially available humanized mice have >25% human $CD45^+$ cells (a marker on white blood cells); therefore, the percentage of $CD45^+$ cells can vary between mice. Variability in the percentage of $CD45^+$ cells in each mouse may affect the rate of B cell infection which explains why not all animals in the PBS group have similar levels of viremia, even when they were challenged with same amount of EBV.

In conclusion, I have found two mAbs, gH/gL mAb 769B10 and gp42 mAb A10, that potently protect humanized mice from death, viremia, and development of lymphoma. In my model, mice receiving gp350 mAb H02, which has strong neutralizing activity in vitro, were not protected from EBV infection. However, the combination of mAbs against gp350, gH/gL, and gp42 provided potent protection against EBV infection. Also, passive transfer of IgG from gH/gL-NP + gp350-NP or gH/gL/gp42-NP + gp350-NP immunized mice to humanized mice showed excellent protection from viremia with no lymphoma development after challenge with EBV. Previous EBV vaccines (Sokal at al., 2007; Kanekiyo et al., 2015) or therapeutic studies with mAbs (Haque et al., 2006) have been focused on gp350, but the humanized mouse study results in this chapter demonstrate that vaccines or therapeutics targeting EBV gH/gL and/or gp42 may be more effective than those targeting gp350.

# Chapter 5. Development of an EBV bispecific antibody that might provide better efficacy than conventional mAbs

Additional authors contributed on the works in this chapter: Wang Y, Bu W, and Mine S

**Abstract**

Development of bispecific antibodies as therapeutics has been increasing with more than a hundred bispecific antibodies in various stages of clinical trials. Bispecific antibodies can target two different antigens or two different epitopes of one antigen allowing higher activity by acting cooperatively. Since two different antigens or epitopes are recognized, it may make neutralization escape mutants more difficult to evolve. In chapter 4, EBV mAbs against gH/gL and gp42 demonstrated markedly reduced viremia and prevented EBV lymphomas in humanized mice challenged with EBV. Here, I developed a bispecific mAb targeting both EBV gH/gL and gp42 and evaluated its efficacy in humanized mice. I found that the bispecific mAb bound to both gH/gL and gp42 and prevented viremia in humanized mice challenged with EBV. Targeting two different glycoproteins with a bispecific mAb gave robust protection and might reduce the risk of development of an antibody escape mutant. Although humanized mice that received bispecific mAb were protected from viremia and lymphoma, in vitro neutralization and fusion inhibition in both B cells and epithelial cells showed similar potency as one of the parental mAbs, 769B10.

## 5.1 Introduction

EBV is one of most prevalent human viruses infecting more than 90% of adults (Cohen et al., 2011). EBV is associated with Hodgkin and Burkitt lymphoma, nasopharyngeal and gastric carcinoma, and post-transplant lymphoproliferative disease (San-Juan et al, 2014). In boys with X-linked lymphoproliferative disease or individuals with certain other primary immunodeficiencies, EBV infection can be fatal (Cohen, 2015). EBV has also been shown to be an important risk factor for development of multiple sclerosis (Bjornevik et al., 2022). There is no licensed therapeutic or prophylactic vaccine to treat or prevent EBV diseases.

Previously, other investigators as well as ourselves (chapter 4) showed that humanized mice receiving EBV gH/gL mAbs are protected from viremia and lymphoma after challenge with EBV (Zhu et al., 2021; Singh et al., 2020; chapter 4). In addition, we showed that an EBV gp42 mAb also protected humanized mice from viremia and disease after infection with EBV (Chapter 4). gH/gL is essential for EBV fusion to B cells and epithelial cells (Wu and Hutt-Fletcher, 2007) and EBV gp42 is required for fusion of the virus to B cells (Kirschner et al., 2007). Thus, antibodies against these glycoproteins may be useful to reduce EBV infection and/or disease.

Bispecific mAbs have advantages over conventional mAbs by targeting two different epitopes and thereby potentially reduce the cost of manufacturing. In addition, by binding to two different epitopes, the mAb may bind more effectively to the target and there may be less risk of development of antibody escape mutants. Bispecific mAbs can be developed in various formats with differences in valency, in vivo half-life, manufacturability, and/or Fc-effector functions (Labrijn et. al., 2019). Bispecific mAbs have been developed to use as therapeutics in several viral infections such as hepatitis B, HIV, and SARS-Cov-2 (Tan et al., 2013; Sung et al, 2015; De Gasparo et al., 2021; Cho et. al., 2021).

Here, we developed an EBV bispecific mAb using the variable regions of a gH/gL and a gp42 mAb in the CrossMab$^{CH1\text{-}CL}$ format (Klein, Schaefer, and Regula, 2016) and evaluated the mAb for virus neutralization, cell-to-cell fusion blocking activity, and protection of humanized mice from challenge with EBV.

## 5.2 Results

### 5.2.1 Construction and structural characterization of a bispecific mAb containing Fabs from EBV gH/gL mAb B10 and gp42 mAb A10

Previously we found that EBV gH/gL mAb B10 and gp42 mAb A10 were the most potent of the EBV mAbs we isolated to neutralize EBV infection in vitro and to prevent development of EBV lymphomas in humanized mice. Before constructing a bispecific mAb containing the Fab regions of EBV gH/gL mAb B10 and gp42 mAb A10, we first evaluated the ability of Fab fragments from each of the two mAbs to neutralize EBV in vitro. Full-length gp42 mAb A10 was significantly more effective to neutralize EBV infection of B cells than the gp42 mAb A10 Fab fragment (p-value = 0.007); in contrast the gH/gL mAb B10 Fab fragment neutralized EBV infection of B cells more potently at a ~10-fold lower $IC_{50}$ than the corresponding full-length mAb (p-value = 0.153) (**Figure 5.1A**). An equimolar mixture of the two mAb Fab fragments neutralized virus infection at a ~ 3-fold lower $IC_{50}$ than an equimolar mixture of the two full-length mAbs (p-value = 0.168).

Based on the neutralizing antibody results, we constructed a bispecific mAb containing Fab fragments of both EBV gH/gL mAb B10 and gp42 mAb A10 using a $CrossMAb^{CH1\text{-}CL}$ construct (**Figure 5.1B**). $CrossMAb^{CH1\text{-}CL}$ was constructed to have the gH/gL mAb B10 arm in the format of a conventional mAb, while the gp42 mAb A10 arm had the constant region of light chain and CH1 domain of heavy chain exchanged. To increase likelihood of the assembling of two heavy chains correctly, knobs-into-holes mutations (T366S, L368A, Y407V, and T366W) were introduced in the CH3 region of the Fc portion of the antibody. A bispecific mAb with an equimolar amount of IgG heavy and light chains was confirmed by SDS-PAGE (**Figure 5.1C**) and an absence of excess heavy or light chains was verified by size-exclusion chromatography (**Figure 5.1D**).

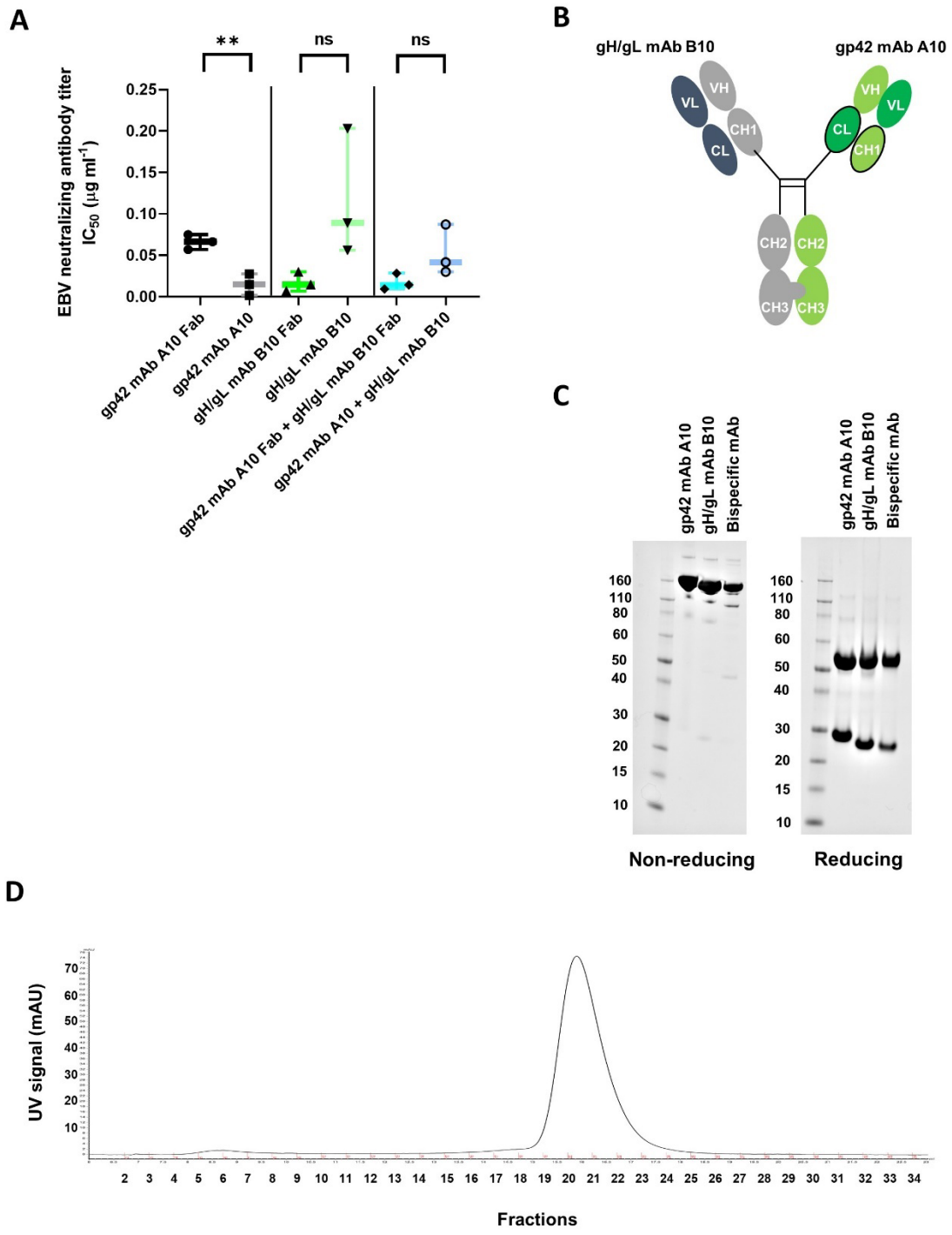


**Figure 5.1**. **Neutralization of full-length and Fab fragment of gH/gL mAb B10 and gp42 mAb A10 and the characterization of bispecific antibody.**
(A) B cell EBV neutralizing antibody titers of full-length and Fab fragments of gp42 mAb A10, gH/gL mAb B10, or combination of two mAbs. (B) A representative image of the constructed bispecific mAb. Domains that are swapped in gp42 mAb Al0 arm is outlined in black. (C) Purified gH/gL mAb B10, gp42 mAb A10, and bispecific mAb in reducing and non-reducing SDS-PAGE gel. (D) Size-exclusion chromatography of bispecific mAb. ** p≤0.01

### 5.2.2 The bispecific mAb binds to both gH/gL and gp42

To verify that the bispecific mAb binds to both gH/gL and gp42, we performed LIPS assays with the viral glycoproteins. The bispecific mAb bound to gH/gL at a similar titer as gH/gL mAb B10 (**Figure 5.2A**) and the bispecific mAb bound to gp42 at a concentration similar to gp42 mAb A10 (**Figure 5.2B**). The bispecific mAb bound to gH/gL and to gp42 at a similar titer as the combination of gH/gL mAb B10 with gp42 mAb A10.

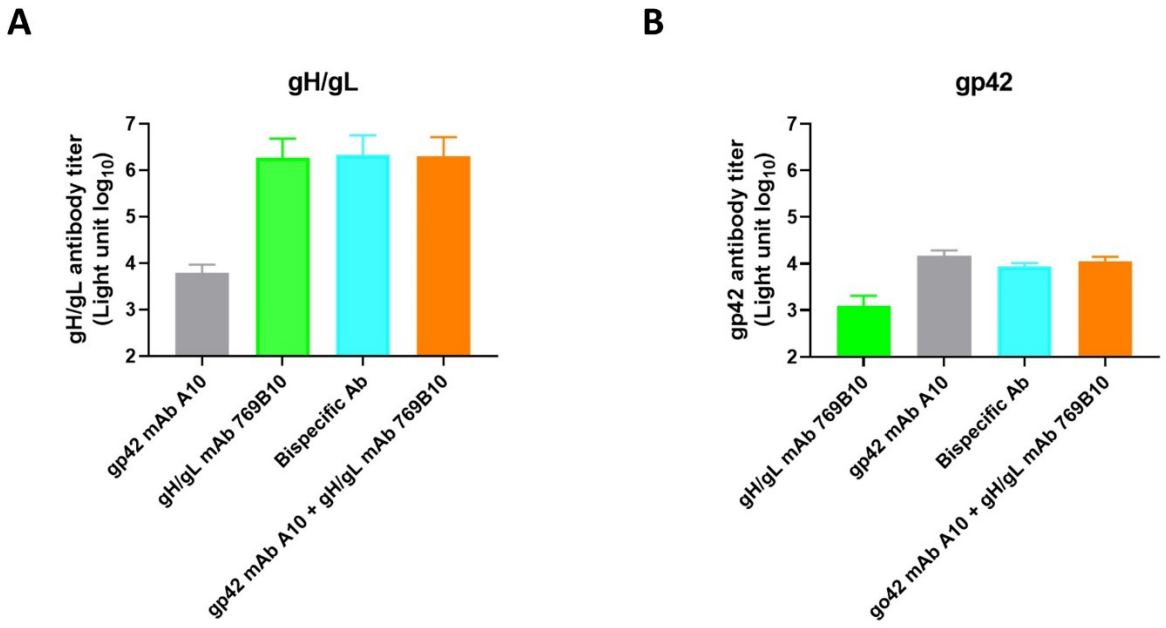


**Figure 5.2. The bispecific mAb binds to both gH/gL and gp42 by LIPS assay.**
(A) Binding of gp42 mAb A10, gH/gL mAb B10, bispecific mAb, and combination of parental mAbs to gH/gL. (B) Binding of gp42 mAb A10, gH/gL mAb B10, bispecific mAb, and combination of parental mAbs to gp42. The top of the bars indicates the means of three independent assays and the short horizontal bars represent the standard errors.

Next, we evaluated sequential binding of the mAbs to the glycoproteins using biolayer interferometry (BLI). Since the assay involves gH/gL binding to the bispecific mAb after it has bound to gp42, and gH/gL can also bind gp42, we constructed gp42 with deletion of the gH/gL binding domain. The gp42 deletion mutant (gp42-del) that we used lacks amino acids 36-86 which includes the N-terminal gH/gL binding domain (Liu et al., 2010). Using a streptavidin biosensor, biotinylated gp42-del was bound first, followed by the $F(ab)_2$ fragment of the bispecific mAb, and then gH/gL was added (**Figure 5.3A**). The $F(ab)_2$ fragment of the bispecific mAb rather than a full-length bispecific mAb was used as only the binding domains are present on the Fab fragments of the bispecific mAb. Also, gp42 mAb A10 was tested in place of the bispecific mAb to confirm that gp42 mAb A10 can only bind to gp42-del but not to gH/gL. As a negative control for non-specific binding, EBV gp350 mAb was used in place of the bispecific mAb. BLI showed that the mAb $F(ab)_2$ fragment of the bispecific mAb bound to gp42-del and gH/gL subsequently bound to this complex; in contrast, gp42 mAb A10 bound to gp42-del, but gH/gL could not bind to the complex (**Figure 5.3B**). As expected, the gp350 mAb did not bind to either gp42-del or gH/gL. Thus, the bispecific antibody could bind to both gp42 and gH/gL sequentially. When the order of binding to gp42-del and gH/gL were reversed, mAb $F(ab)_2$ fragment of the bispecific mAb successfully bound to gH/gL but failed to bind to gp42-del subsequently (**Figure 5.3C**). This observation points out possible steric hinderance between gp42-del and gH/gL when bispecific mAb is bound.

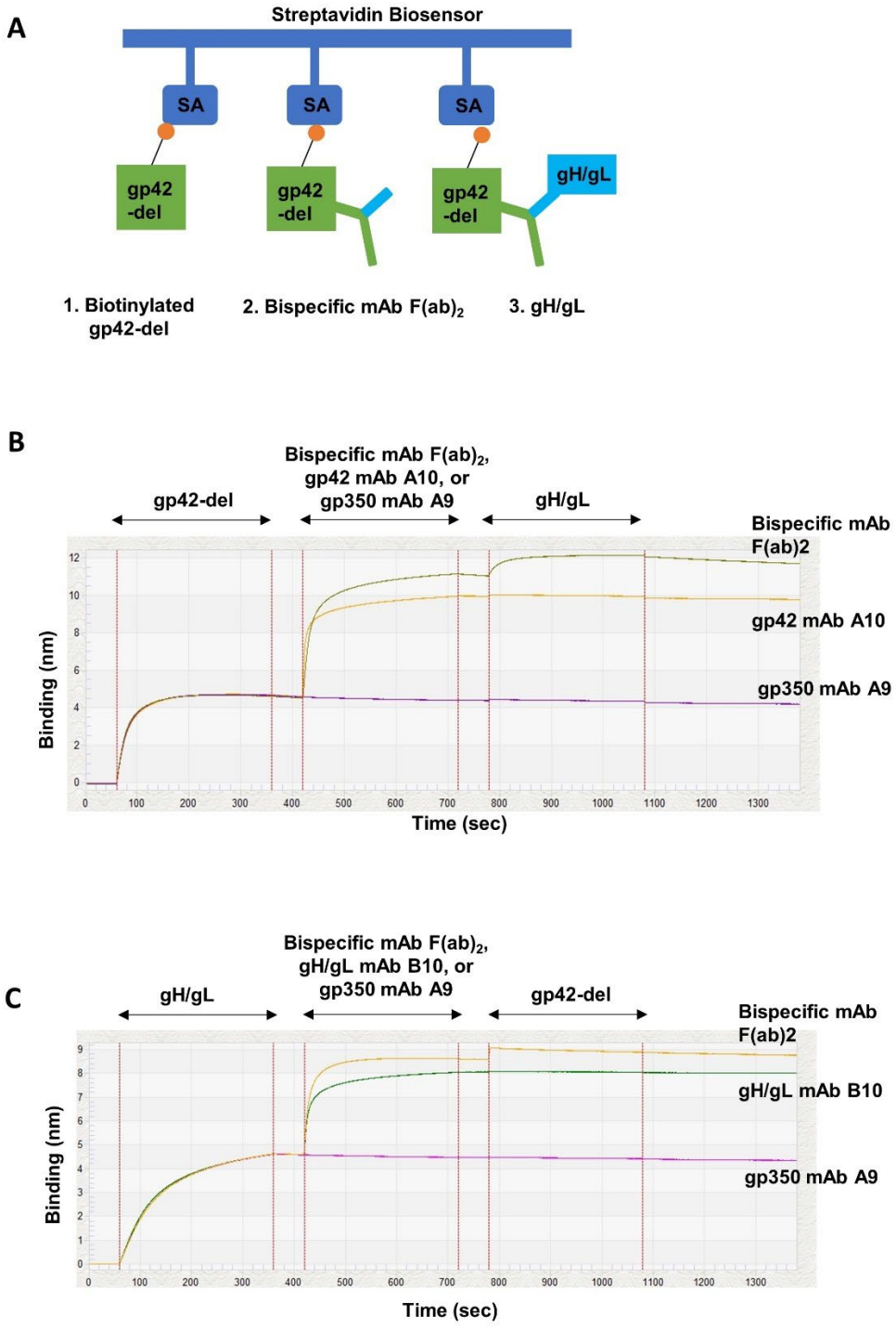


**Figure 5.3. Sequential binding of bispecific mAb by BLI.**
(A) Overview steps of binding assay by biolayer interferometry. (B) Sequential binding of bispecific mAb $F(ab)_2$, gp42 mAb A10, or gp350 mAb A9 to gp42-del followed by gH/gL. (C) Sequential binding of bispecific mAb $F(ab)_2$, gH/gL mAb B10, or gp350 mAb A9 to gH/gL followed by gp42-del.

### 5.2.3 The bispecific mAb has similar EBV B cell neutralizing titer and EBV-mediated glycoprotein fusion inhibition as gH/gL mAb B10

B cell neutralizing antibody titers were measured for the bispecific mAb and the two mAbs from which it was derived to determine if the bispecific mAb could neutralize EBV infection similar to or better than its parental mAbs. The potency of the bispecific mAb to neutralize EBV infection in B cells was similar to gH/gL mAb B10, but less than gp42 mAb A10 (**Figure 5.4A**). Combining gH/gL mAb B10 and gp42 mAb A10 in the EBV B cell neutralization assay resulted in a similar level of virus neutralization as the bispecific mAb. In epithelial cells, gH/gL mAb B10 was most potent to neutralize EBV infection followed by combination of gH/gL mAb B10 with gp42 mAb A10, and then the bispecific mAb (**Figure 5.4B**).

The gH/gL/gp42 complex is required for EBV fusion to B cells, while the gH/gL complex is necessary for virus fusion to epithelial cells. Therefore, we measured the ability of the mAbs to inhibit virus glycoprotein-mediated fusion using a luciferase-based cell-to-cell fusion assay (Bu et al., 2019). In B cells, the concentrations of gH/gL mAb B10, the bispecific mAb, and the combination of gH/gL mAb B10 with gp42 mAb A10 needed to block fusion were similar and were ~5-fold lower than gp42 mAb A10 (**Figure 5.4C**). In epithelial cells, gH/gL mAb B10 was the most potent mAb for inhibiting fusion, followed by the combination of gH/gL mAb B10 with gp42 mAb A10, and the bispecific mAb (**Figure 5.4D**). Inhibition of glycoprotein-mediated fusion was not detected with gp42 mAb A10 in epithelial cells even when used at 300 μg/ml. Thus, the bispecific mAb had a similar B cell neutralizing and fusion inhibition titer in B cells as gH/gL mAb B10.

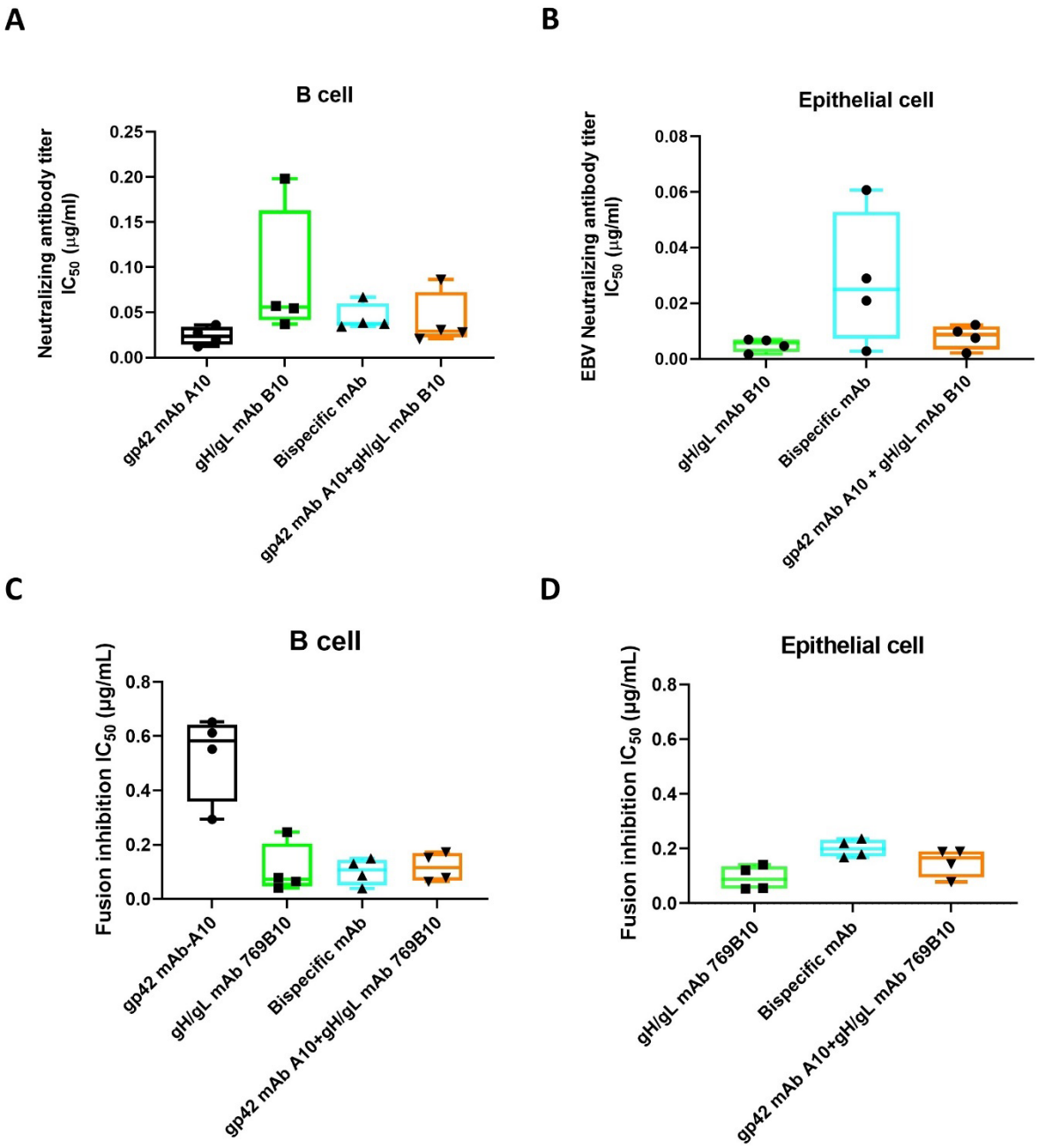


**Figure 5.4. EBV neutralizing and fusion blocking activity of the bispecific mAb in B cells and epithelial cells.**
(A) Raji B cell neutralization of two parental mAbs, bispecific mAb, and combination of parental mAbs. (B) SVKCR2 epithelial cell neutralization of gH/gL mAb B10, bispecific mAb, and combination of parental mAbs. (C) B cell fusion inhibition of two parental mAbs, bispecific mAb, and combination of parental mAbs using Daudi-T7 and CHO-K1 cells. (D) Epithelial cell fusion inhibition of gH/gL mAb B10, bispecific mAb, and combination of parental mAbs using HEK 293T14 and CHO-K1 cells. Each dot represents one independent assay, the whiskers represent minimum and maximum data points, the box represents upper and lower quartiles, and the horizontal line is the median of 4 independent assays.

### 5.2.4 The bispecific mAb protected humanized mice from death and viremia after EBV challenge

EBV infection of mice engrafted with human hematopoietic cells results in viremia and EBV lymphomas (Kim et al., 2021). We injected humanized mice intraperitoneally with 6 doses of the bispecific mAb, PBS, or combined gp42 mAb A10 with gH/gL mAb B10; 2 doses of mAb were given before intravenous challenge with EBV and 4 doses of mAb were given after challenge (**Figure 5.5A**). Blood was collected and animals were weighed each week for 15 weeks post challenge. Mice that received the bispecific mAb or combined parental mAbs had 80% and 75% survival rates respectively, whereas mice that received PBS showed 20% survival rate (**Figure 5.5B**). Mice that received the bispecific mAb generally maintained their weight throughout the study whereas mice that received combined parental mAbs had a slight decrease in weight at the end of the study; one mouse in each of these groups had severe weight loss and had to be euthanized between 5 and 6 weeks after virus challenge (**Figure 5.5C**). Quantification of the number of EBV DNA copies in the blood by qPCR showed that all mice in the PBS group had detectable viral DNA with peak DNA copy numbers on week 7 post infection; 3 mice were euthanized due to severe weight loss at that time (**Figure 5.5D**). The two mice in the PBS group that survived past week 7 subsequently had DNA copy numbers below the detection limit of the assay. All mice that received the bispecific mAb had no detectable EBV DNA in the blood throughout the study except for one mouse that had EBV DNA measured just at the detection limit at week 15. Most of mice that received combined gp42 mAb A10 with gH/gL mAb B10 also had undetectable EBV DNA in the blood except for one mouse with a low number of EBV DNA copies at week 13.

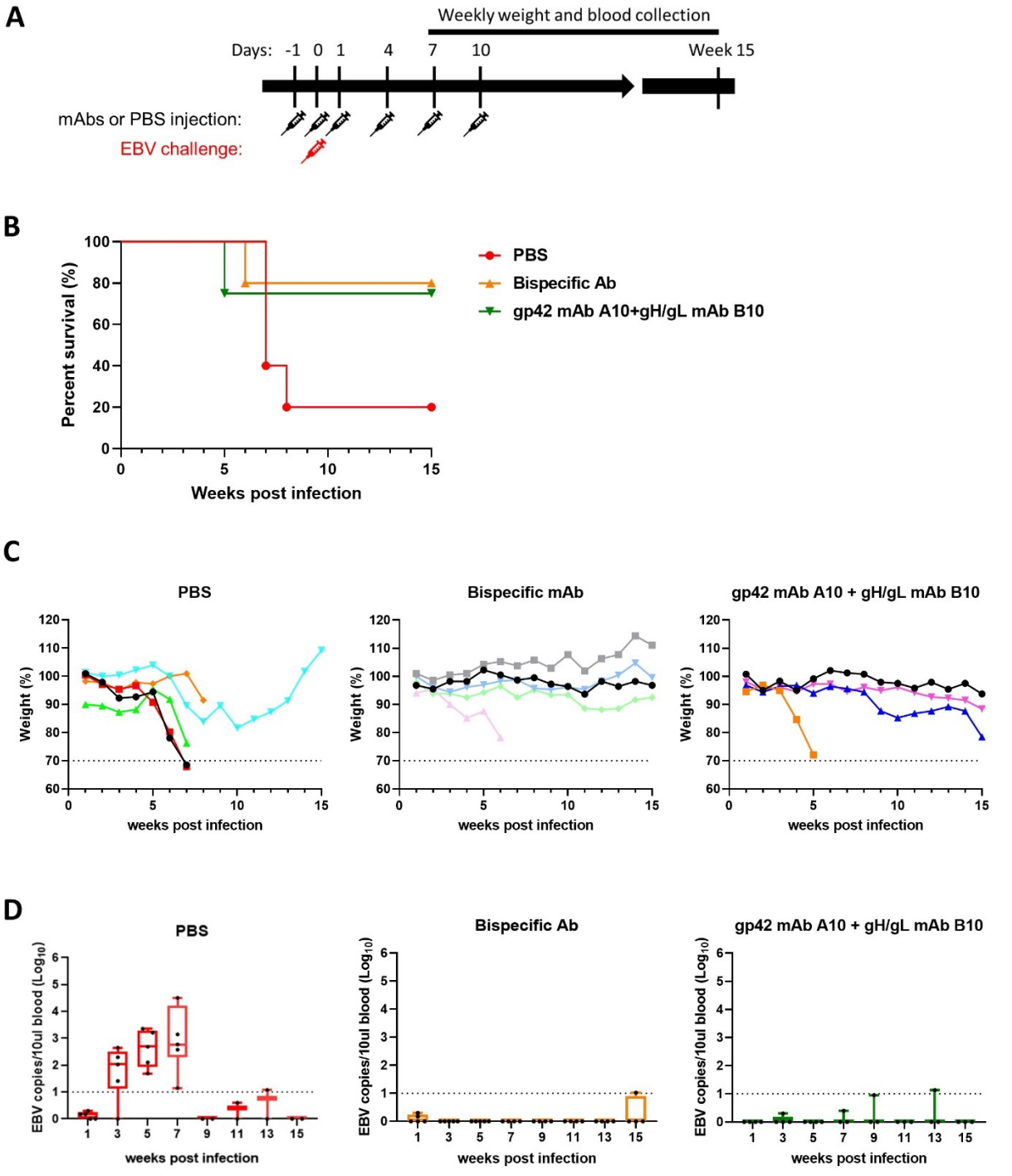


**Figure 5.5. The bispecific mAb improves survival and prevents viremia in humanized mice after EBV challenge.**

(A) Experimental scheme of injections. Mice were given six doses of bispecific mAbs, a combination of parental mAbs, or PBS intraperitoneally and challenged intravenously with $10^6$ green Raji units of EBV after the second dose of mAb. (B) Survival rates for each group of mice after EBV challenge. Five humanized mice were in the PBS group, 5 were in the bispecific Ab group, and 4 were in the combination

of parental mAbs group. (C) Weight changes throughout the study. A dotted line represents end point weight loss. (D) EBV DNA copies in the blood quantified by real-time qPCR. Each dot represents one mouse, and the dotted line indicates the limit of detection of the assay. Whiskers indicates minimum and maximum data points for EBV DNA copies in the blood, the box represents upper and lower quartiles, and the horizontal line in the box is the median.

### 5.2.5 The bispecific mAb reduced infiltration of organs with virus-infected B cells and prevented EBV lymphoma in humanized mice challenged with EBV

At the end of the study, lungs, liver, kidneys, and spleen were collected from each mouse and evaluated for macroscopic lesions and histology. Two of five (40%) mice from the PBS group had splenic lesions present at the time of necropsy in at least one of the organs; in contrast, none of the mice that received the bispecific mAb or combined parental mAbs showed visible lesions in the organs (**Figure 5.6A and B**). Tissues were stained with H&E and CD20 and in situ hybridized with an EBER1 probe to look for signs of atypical B cell infiltrates, B cell lymphoproliferative disease, or EBV B cell lymphoma. 40% of mice that received PBS showed signs of lymphoproliferative disease while none of the mice that received bispecific mAb or combination of parental mAbs developed any disease (**Figure 5.6A**).

The level of mAbs in the plasma of the mice during the study were evaluated by quantifying gH/gL and gp42 antibody levels by ELISA (**Figure 5.6C**). Antibodies against gp42 or gH/gL showed similar trends in mice that received the bispecific mAb or combined gp42 mAb A10 with the gH/gL mAb B10 having the highest level at week 1 post infection and a gradual decrease throughout the study. At the end of the study at week 15 post infection, mAb levels in the plasma were reduced ~3-logs lower than the peak level at week 1 post infection.

A

| Diseases | PBS | Bispecific Ab | gp42 mAb A10 + gH/gL mAb B10 |
|---|---|---|---|
| Macroscopic lesions | 2/5 (40%) | 0/5 (0%) | 0/4 (0%) |
| Atypical infiltrate | 0/5 (0%) | 0/5 (0%) | 0/4 (0%) |
| Lymphoproliferative disease | 2/5 (40%) | 0/5 (0%) | 0/4 (0%) |
| Lymphoma | 0/5 (0%) | 0/5 (0%) | 0/4 (0%) |

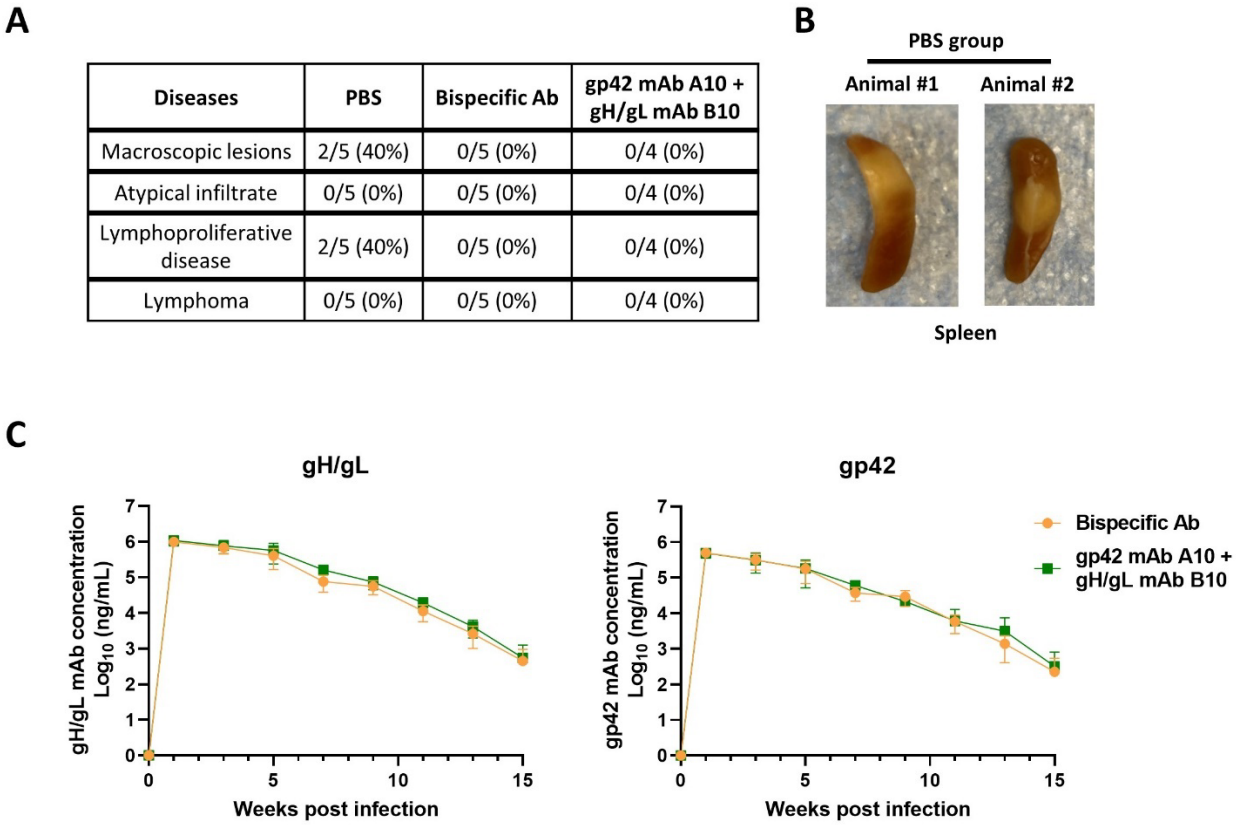


**Figure 5.6. pathology evaluation of organ tissues and gH/gL and gp42 mAb concentration in the plasma.**
(A) Summary table of mice with macroscopic lesions, atypical B cell infiltrates, B cell lymphoproliferative disease, and/or EBV B cell lymphoma. (B) Images of spleens with macroscopic lesions. (C) Concentration of gH/gL and gp42 mAbs in the plasma of individual humanized mice at various times after EBV challenge measured in duplicate by ELISA. Each dot represents the mean of gH/gL mAb or gp42 mAb concentrations in 5 humanized mice in the bispecific Ab group and 4 humanized mice in the combination of parental mAb group. The short horizontal lines represent the standard errors.

## 5.3 Discussion

We developed a bispecific mAb containing the antibody binding domains of two potent gH/gL and gp42 mAbs and found that it neutralized EBV infection in B cells and epithelial cells at a similar titer as gH/gL mAb B10. The bispecific mAb also inhibited fusion at a similar concentration as gH/gL mAb B10 in B cells and was slightly less effective than gH/gL mAb B10 in epithelial cells. The bispecific mAb completely protected humanized mice from both viremia and EBV-positive lymphoma after challenge with EBV.

Although, the bispecific mAb was confirmed to bind to both gH/gL and gp42 by LIPS and BLI, it did not show a clear advantage over its two parental mAbs. Since the bispecific mAb does not target two different epitopes on one glycoprotein but rather epitopes on two different glycoproteins, it is not certain whether each arm of the bispecific mAb is binding to both glycoproteins (gH/gL and gp42) within one gH/gL/gp42 molecule or two glycoproteins on two different molecules. Using BLI, we confirmed that the bispecific can bind sequentially to gp42 first and gH/gL later, but not vice versa. Since gH/gL is larger than gp42, it is possible that binding of the bispecific mAb to gH/gL first results in steric hinderance such that the other arm of the antibody cannot bind to gp42. It is possible that if a linker was inserted proximal to the gp42 mAb binding domain of the arm or the gH/gL binding domain on the other arm, it would allow each arm to be more flexible and might increase the chance of a single bispecific antibody to bind to gH/gL and gp42 on a single gH/gL/gp42 trimer.

The bispecific mAb we developed might be likely to be effective in neutralizing the activity of an EBV escape mutant in either gH/gL or gp42. mAb escape mutants are more commonly seen in RNA viruses, but escape mutants are reported in DNA viruses (Ray et. al., 2018; Wu et. al., 2021). While EBV does not have a high mutation rate compared with RNA viruses, a T cell escape mutant in a patient who underwent hematopoietic stem cell

transplantation resulted in fatal EBV lymphoproliferative disease (Gottschalk et. al., 2001). By targeting two different glycoproteins, the bispecific mAb has the potential for higher activity by acting cooperatively. Another advantage of the bispecific mAb is reduced cost of manufacturing. Since both gH/gL mAb B10 and gp42 mAb A10 showed excellent protection in humanized mice, combining both mAbs may provide better efficacy. Manufacturing of a single bispecific mAb instead of two separate gH/gL and gp42 mAbs should reduce the cost. One caveat is that purity of a homogenous preparation of a bispecific mAb can be challenging since there are two different heavy chains and light chains each that can assemble in different proportions.

Bispecific mAbs have been developed as therapeutics for various viral infections such as Ebola, Zika, human immunodeficiency virus (HIV), dengue virus, and SARS-CoV-2 (Frei, et, al., 2016; Wang et. al., 2017; Sung et. al., 2015; Shi et. al., 2016; De Gasparo et al., 2021; Cho et. al., 2021) although none has been licensed. Another herpesvirus bispecific mAb with antibody binding sites obtained from a mAb to the cytomegalovirus (CMV) pentamer (gH/gL/UL28/UL29/UL31) and a mAb to CMV gB has been published (Su et. al., 2021). In vitro studies with this CMV bispecific antibody showed that it had activity similar to the gB mAb to neutralize fibroblasts and neuronal cells, as well to the pentamer mAb to neutralize infection of epithelial and endothelial cells. In our in vitro neutralization assays, our bispecific mAb showed a similar neutralizing titer as parental gH/gL mAb B10 in both B cells and epithelial cells but did not neutralize infection better than gp42 mAb A10 in B cells. While the CMV bispecific mAb was evaluated for pharmacokinetics in rhesus monkeys, the mAb was not tested for protection against CMV infection in vivo. To our knowledge, our mAb is the only herpesvirus glycoprotein bispecific mAb that has been tested in a challenge model in an animal.

In summary, we have developed a bispecific mAb that binds sequentially to EBV gp42 and gH/gL with comparable neutralizing titer and fusion inhibition to one of its parental mAb, gH/gL mAb B10, and completely protects humanized mice from EBV viremia and lymphomas. Although our bispecific mAb did not show higher potency in neutralization and fusion inhibition than its parental mAbs, targeting epitopes on two different antigens may reduce the risk of development of EBV escape mutants when high concentrations of virus are present. The EBV bispecific mAb might be especially useful for preventing EBV infection or disease in EBV seronegative immunocompromised patients, especially when exposed to high titers of virus as can occur in transplant recipients receiving an EBV-infected lymphocyte-rich lung or small intestine (Dharnidharka et al., 2002).

# Chapter 6. Conclusions and future directions

## 6.1 Conclusions

EBV vaccine and therapeutic research had been moving at a slow-pace as development of vaccines and therapeutics were not considered a high priority as symptoms of infectious mononucleosis, the most well-known disease caused by EBV, are rarely life-threatening and the perceived market for such a vaccine has been considered as relatively small. Nonetheless, there are immunocompromised patients who have a real risk of developing post-transplant lymphoproliferative disease/lymphoma or fatal X-linked lymphoproliferative disease after EBV infection and for these patients, there is a need for therapeutics (Panchal et al., 2018; Al-Mansour et al., 2013). Recently, EBV has been reported to have a major role in the development of multiple sclerosis (Bjornevik et al., 2022) and interest in developing vaccines and therapeutic has increased. In my dissertation research, I wanted to seek an answer to a question: what is the most efficient EBV mAb that can protect humanized mice from EBV infection and development of lymphoma? To address this question, I've evaluated various formats of therapeutics from hyperimmune globulins to monoclonal antibodies and a bispecific antibody using a humanized mouse model.

There are no small animals that can be infected with EBV which makes EBV vaccine and therapeutic research difficult. Recently, immunodeficient mice engrafted with human $CD34^+$ cells that have circulating human lymphocytes have been used in EBV research (Singh S et al., 2020; Zhu et al., 2021). In **chapter 2**, to address an answer to the question of what is the most appropriate humanized mouse model to assess efficacy of EBV therapeutics, different strains of humanized mice were evaluated. Four different types of humanized mice were evaluated: SCID mice injected with human PBMCs from EBV-seronegative donors, NSG mice engrafted with human $CD34^+$ cells (huNSG), SCID mice engrafted with human fetal thymus, liver, and $CD34^+$ cells (BLT), and NSG mice engrafted with human $CD34^+$ cells and expressing cytokines that

improve engraftment (NSG-SGM3). In SCID mice injected with human PBMCs, not all mice showed viremia despite inoculation with a high titer of EBV which makes this animal model not suitable for evaluation of EBV mAbs. For BLT mice, usage was severely restricted by the US government immediately after our first study was completed due to the use of human fetal tissues. All huNSG mice and NSG-SGM3 mice showed viremia after challenge. Because humanized mice are costly, we decided to use huNSG mice to evaluate EBV mAbs as these mice are less expensive than NSG-SGM3 mice.

Some patients with X-linked lymphoproliferative disease or severe combined immunodeficiency are given IVIG to prevent infection with EBV. However, IVIG is not always effective and breakthrough infections may occur which can be fatal. In **chapter 3**, I evaluated EBV hyperimmune globulin as a replacement for IVIG treatment. When IgG isolated from donors who have high titers of EBV gp350 binding and EBV B cell neutralizing antibody was given to humanized mice, viremia level was significantly reduced. Nonetheless, when the level of viremia in mice given hyperimmune globulin and animals given IVIG was compared, hyperimmune globulin did not show significant superiority to IVIG. This may be due to high concentrations of EBV antibodies in IVIG since EBV is one of the most prevalent viruses in adults. Also, we selected donors with high gp350 binding antibody titers because gp350 is responsible for most (50-60%) of the EBV B cell neutralizing activity in human plasma (Bu et al., 2019). However, in a study where efficacy of a gp350 mAb 72A1 and a gH/gL mAb AMMO1, both of which potently neutralize EBV infection in B cells, were evaluated in humanized mice challenged with EBV, the authors found that mice that received the gp350 mAb had much higher viremia compared to the gH/gL mAb (Singh et al., 2020). This observation demonstrates that gp350 is not an ideal target for a prophylactic mAb; instead, an antibody

against gH/gL provides better protection in this model. If we had selected donors with high gH/gL antibody titers for our IgG transfer experiment, we likely may have seen better protection compared to IgG from donors with high gp350 antibody titers.

gp350 has been a major target for EBV vaccine development for the last few decades. A clinical trial with a recombinant gp350 vaccine in 2007 was the only phase 2 trial that has been conducted for an EBV vaccine. While there was a 78% reduction in the incidence of infectious mononucleosis, there was no reduction of EBV infection (Sokal et al., 2007). Recently, EBV vaccine and therapeutic research are shifting towards other glycoproteins such as gH/gL and/or gp42. Our lab has isolated several EBV gH/gL and gp42 mAbs and I evaluated their efficacy in humanized mice in **chapter 4**. Evaluation of three gH/gL mAbs that target different epitopes showed that one mAb, 769B10 resulted in higher survival rates and reduced viremia when given to humanized mice challenged with EBV compared to the other two gH/gL mAbs. Also, unlike the other gH/gL mAbs, mAb 769B10 completely prevented development of EBV B cell lymphoma in the mice. Of the gp42 mAbs tested, mAb A10 showed higher survival rates, and prevented viremia and EBV B cell lymphoma in humanized mice challenged with EBV compared to the previously published gp42 mAb, F2-1 (Strnad et al., 1982). Based on these results, we decided to move forward towards clinical development of gH/gL mAb 769B10 and gp42 mAb A10.

We also developed nanoparticle (NP) vaccines, gH/gL-NP and gH/gL/gp42-NP and evaluated their efficacy in humanized mice by passively transferring immune sera from BALB/c mice that were vaccinated with gH/gL-NP+gp350-NP or gH/gL/gp42-NP+gp350-NP into humanized mice. Mice that received IgG isolated from gH/gL-NP+gp350-NP or gH/gL/gp42-NP+gp350-NP immunized BALB/c mice showed protection from EBV infection by an increase

in survival rate, reduction in viremia, and prevention of development of lymphoma. In contrast, humanized mice that received IgG isolated from naïve BALB/c mice showed a low survival rate, high level viremia, and development of lymphoma.

EBV entry into B cells is a highly orchestrated process that require several glycoproteins (Fingeroth et al., 1984; Spriggs et al., 1996; McShane and Longnecker, 2004). Although gp350 is important for attachment to B cells, it is not strictly required for B cell infection especially when high titers of EBV are used to infect cells (Janz et al., 2000). In contrast, gH/gL and gp42 are required for infection and have important roles during fusion of the virus membrane with the host cell membrane (Wu and Hutt-Fletcher 2007; Kirschner et al., 2007). Therefore, mAbs targeting multiple glycoproteins may provide more robust protection than targeting a single glycoprotein. To examine if combination mAb therapy can provide better protection than single mAbs, I evaluated the efficacy of gp350 mAb, combined gH/gL + gp42 mAbs, and combined gp350+gH/gL+gp42 mAbs in humanized mice challenged with EBV. From this study, we learned that gp350 mAb alone did not protect humanized mice from viremia whereas mice that received combinations of mAbs showed lower viremia. The failure of gp350 mAb to protect mice may have been related to the high dose of EBV ($10^6$ GRU) used to infect mice. Since gp350 is important for attachment, artificially providing a high concentration of virus may result in attachment to B cells even if gp350 is occluded by mAb. More mice receiving combined gH/gL+gp42 mAb were viremic compared to those receiving combined gp350+gH/gL+gp42. This observation supports the hypothesis that targeting multiple glycoproteins important for B cell entry provides better protection and may be necessary to develop an effective therapeutic using a mixture of mAbs targeting different glycoproteins.

In general, neutralizing antibody is thought to be the major correlate of protection against most virus infections. Therefore, EBV neutralizing activity was used to select mAbs for further characterization among the many mAbs that we isolated. Based on in vitro B cell neutralization, gp350 mAbs showed greater potency than gH/gL mAbs. However, when humanized mice were injected with gp350 mAbs and challenged with EBV, these mice showed similar viremia as the PBS control group. This was surprising as gp350 mAbs were especially potent to neutralize EBV infection of B cells. EBV attaches to B cells by binding of gp350 to the CR2 receptor and Raji cells, a cell line most commonly used for in vitro neutralization, express high levels of CR2 (Speck and Longnecker 1999). We evaluated neutralization of gp350 and gH/gL mAbs in cell lines with various levels of CR2 and demonstrated that the neutralizing activity of gp350 mAbs correlate in a dose-dependent manner with expression of CR2 on target cells. gp350 mAbs showed higher potency in B cell lines expressing high levels of CR2 and no neutralization in B cell lines that express very low or no CR2. Neutralization of gH/gL mAbs were not affected by the level of CR2 expression on the B cells. The observation that gp350 mAbs were more potent in B cells expressing higher levels of CR2 contradicts with our knowledge of the infection process where higher levels of CR2, increase the likelihood of EBV to infect B cells, and one would expect higher levels of gp350 antibodies to be required to neutralize infection. It is possible that another gp350 receptor, CD35, may function as a dominant receptor for gp350 to bind during in vitro neutralization. However, the level of CD35 on different B cell lines were not evaluated in this study.

Based on the observation of increased protection from viremia and absence of development of lymphoma in humanized mice using the combination of gH/gL mAb and gp42 mAb, in **chapter 5**, I developed a bispecific mAb using gH/gL mAb 769B10 and gp42 mAb

A10. An effective bispecific mAb may have many advantages including a reduction in manufacturing costs, higher activity in protection than a single mAb by working cooperatively, and possibly inhibition of evolving escape mutants. I successfully produced a bispecific mAb that binds to both gH/gL and gp42 confirmed by LIPS assay and BLI. Humanized mice that received the bispecific mAb had no detectable viremia. However, the bispecific mAb showed similar in vitro B cell and epithelial cell neutralizing titers and fusion-inhibition activity as one of the parental gH/gL mAbs, 769B10. Since the neutralization and fusion-inhibition activity of the bispecific mAb had a level comparable to that of the gH/gL mAb 769B10, it is possible that the gp42 mAb A10 arm of the bispecific antibody could not bind after the gH/gL mAb 769B10 arm bound to gp42 first . More investigation will be needed to confirm binding of each arm at the same time and if there are potential benefits of the bispecific mAb compared to a single mAb.

### 6.2 Future Plans

gH/gL mAb 769B10 and gp42 mAb A10 were shown to protect humanized mice from viremia and development of B cell lymphoma. Nonetheless, the injection scheme that I used where each mouse was injected with total of 6 doses of mAbs in a 10-day period may be unnecessary and not practical when these mAbs are given to patients. Therefore, one future in vivo study is to reduce the number of doses to 1-3 injections and see if a similar protection can be observed. Singh et al. (2020) demonstrated that their gH/gL mAb, AMMO1, showed reduction in viremia in humanized mice after a single dose of gH/gL mAb 48 hours prior to challenge with EBV. Also, Zhu et al. (2021) conducted a similar animal study with their gH mAb, 1D8, and with a single injection a day before infection, showed that humanized mice that received 1D8 all survived with lower viremia than the controls. Fewer injection of mAbs would

be a more stringent test of the mAbs and may help to distinguish more potent mAbs among all the ones that showed protection using 6 doses of antibody.

Developing a mAb that can be used prophylactically, when given before infection, is likely to be beneficial to patients undergoing transplant to reduce the risk PTLD; however, a therapeutic mAb, when given after infection, is also needed. An effective therapeutic mAb might reduce severe EBV infection associated with continued lytic viral replication in immunocompromised persons or in those with chronic active EBV infection. There have been multiple studies showing that EBV mAbs are effective for prophylactic use in animal models, but none showing that mAbs could be effective for therapy. Thus, it would be interesting to evaluate our gH/gL and/or gp42 mAbs therapeutically in humanized mice by injecting mAbs only after infection with EBV.

With the bispecific mAb I produced, I confirmed that it can bind to both antigens by performing LIPS assays separately for gH/gL or gp42; however, in the BLI assay, the bispecific mAb only showed binding to both gp42 and gH/gL when gp42 was bound first followed by gH/gL. Binding of gH/gL prior to gp42 somehow prevented the bispecific mAb from binding to gp42. This observation may be due to steric hinderance as the bispecific mAb is targeting two different glycoproteins and binding to an epitope on gH/gL first might interfere with accessing an epitope on gp42 where the other arm of bispecific mAb needs to bind. Performing cryo-EM would help to understand the spatial orientation of how the bispecific mAb is binding to both gH/gL and gp42. Another possibility is that each arm of the bispecific mAb is not long or flexible enough to bind to two different epitopes at the same time. Thus, adding a linker within one arm or in both arms of the bispecific mAb to make it longer and more flexible may allow

both arms to bind to their epitopes simultaneously. This might result in a more potent mAb compared to its parental mAbs.

### 6.3 Concluding Remarks

EBV is one of the most common viruses found in humans; however, since most people are asymptomatic when infected or experience only mild symptoms, the need for a vaccine or a therapeutic has not been considered a high priority. Nonetheless, 200,000 new cases of cancer are associated with EBV worldwide each year and with increasing numbers of immunocompromised persons, EBV infection is causing more diseases in these patients, including transplant recipients who may develop of the post-transplant lymphoproliferative disease. Recent findings of a strong association of EBV with multiple sclerosis also bolsters the need for effective vaccines and therapeutics for EBV. Because EBV has two phases of replication, including latent virus replication when B cells divide, it is difficult to clear the virus from the body once infected. After optimizing our humanized mouse model and evaluating multiple different EBV mAbs, we found two potent EBV mAbs 769B10 and A10 targeting gH/gL and gp42, respectively, that demonstrated strong protection from viremia and development of lymphomas in humanized mice as discussed in chapter 4. These findings suggest that we may not be far from having an effective EBV therapeutic to those who are in need.

# Chapter 7. Materials and methods

### 7.1 Cells

293/2089 cells containing the B95-8 EBV genome or M81 EBV genome, which express green fluorescent protein (GFP), were cultured in DMEM with 10% fetal bovine serum, penicillin (100U/mL), streptomycin (100U/mL) and hygromycin (100 μg/mL) (Delecluse et al., 1998). The following human B cells were cultured in RPMI 1640 medium with 10% fetal bovine serum (FBS), penicillin, and streptomycin: Raji (an EBV-positive Burkitt lymphoma cell line), BL41 (an EBV-negative Burkitt lymphoma cell line), BL30 (an EBV-negative Burkitt lymphoma cell line), DG75 (an EBV-negative Burkitt lymphoma cell line), and Daudi (an EBV-positive peripheral blood cell line from a patient with Burkitt lymphoma). HEK 293 (a human embryonic kidney cell line), HEK 293T14 (a human embryonic kidney cell line expressing T7 RNA polymerase [Omerović, Lev, and Longnecker, 2005]), and CHO-K1 (a Chinese hamster ovary cell line) cells were cultured in DMEM medium with 10% FBS, penicillin, and streptomycin. SVKCR2 epithelial cells (SV40-transformed human keratinocyte cells expressing CR2 [Li et al., 1992]) were cultured in 1:1 mixture of DMEM and F12 medium with 10% FBS, penicillin, and streptomycin (Bu et al., 2019). 293F cells were cultured in Expi293 expression medium (Thermo Fisher Scientific).

### 7.2 Viruses

EBV B95-8 and M81 were prepared by transfecting 293/2089 cells with plasmids expressing EBV BZLF1 and BALF4 (Neuhierl et al., 2002) using PEI Max (Polysciences). After 7 days, medium was collected and filtered through a 0.80 μm MCE membrane filter (Millipore). Filtered supernatant was concentrated by ultracentrifugation at 21,000 rpm for 1 hr at 4°C. The

virus pellet was resuspended in DMEM with 10% FBS and EBV B95-8 or M81 was stored at -80°C.

### 7.3 Virus titration

EBV B95-8 or M81 were serially 2-fold diluted in a 96 well plate and incubated with 75 µl of 1 x $10^5$ Raji cells. After 72 hr, cells were fixed with 2% paraformaldehyde in PBS. GFP-positive Raji cells were counted using a BD FACS Canto II flow cytometer (BD Bioscience) and analyzed by FlowJo software (Tree Star Inc.). The EBV titer was measured in Green Raji units (GRU) as previously described (Sashihara et al., 2009).

### 7.4 Plasma collection and EBV IgG purification

Plasma donors were consented using FDA approved informed consents for plasmapheresis. Plasma was separated from red blood cells during plasmapheresis and the red blood cells were returned to the donors. Prior to donation, donors were screened in accordance with FDA regulations to protect the donor and ensure the safety, purity, and potency of the collected plasma. All plasma units were tested for presence of antigens and antibodies to human immunodeficiency viruses I and II, hepatitis A, B, and C, and parvovirus.

IgG was purified from plasma using Protein G Sepharose Fast Flow (Cytiva Life Sciences) using the manufacturer's protocol. Briefly, plasma was diluted with the binding buffer, centrifuged for 15 min to clarify the supernatant which was loaded onto a Protein G column, and the IgG was eluted with low pH buffer. The pH of the purified IgG was neutralized, extensively dialyzed with PBS, and sterile filtered. The concentration was determined by OD280 using 1 mg/ml = 1.4 AU.

### 7.5 Production and purification of EBV mAbs

Use of recombinant DNA was approved by University of Maryland Biosafety Committee. Antibodies to gH/gL were isolated using a fluorescent-conjugated gH/gL probe by single cell sorting from cryopreserved PBMCs of healthy blood bank donors selected for high serum EBV neutralization titers. gp42 mAb A10 was isolated from plasmablasts of a cynomolgus monkey vaccinated with a gH/gL/gp42 vaccine by single cell sorting. Reverse transcription was performed on sorted cells and Ig heavy and light chain genes were amplified by PCR. For gH/gL mAbs, amplified fragments of heavy and light chain sequences were synthesized and cloned into IgG1 and kappa chain expression vectors, respectively, by GenScript (Bu et al., 2019). For gp42 mAb A10, overlapping PCR was performed to assemble amplified fragments into an expression cassette that contains the CMV promoter, IgG variable and constant regions, and poly A tail. The expression cassettes were first cloned into pUC19 plasmid, and then variable regions of A10 heavy and lights chains were cloned into pFUSEss-CHIg-hG1 and pFUSEss-CLIg-hL2 plasmids (InvivoGen), respectively to produce A10 that contains human constant regions.

Heavy and lights chain plasmids of each EBV mAb were transfected in Expi293F cells with an ExpiFectamine transfection kit (Thermo Fisher Scientific). Transfected cells were incubated for 5 days at 37°C in a shaking incubator and supernatant was centrifuged at 4000 rpm for 30 min. Supernatant was filtered through a 0.2 μm PES membrane filter and purified by loading onto a 5 ml HiTrap rProtein A FF column (Cytiva). Antibody was eluted from the column with 0.05% trifluoroacetic acid and immediately neutralized to pH 7 with 1M Tris-HCl pH 8. The purified mAbs were dialyzed to 1X PBS using Slide-A-Lyzer dialysis cassette G2

(Thermo Fisher Scientific) and concentrated using Amicon Ultra-15 centrifugal filters (Millipore). Concentrated mAbs were filtered through 0.22 μm PES filter and stored at -80°C.

### 7.6 Production and purification of gH/gL and gp42 proteins

Expi293F cells were co-transfected with gH-AviHis and gL plasmids or a gp42-AviHis plasmid and incubated for 5 days. gH/gL or gp42 proteins were purified by batch purification. In brief, the supernatant from transfected cells was supplemented with 1M Tris pH 7.5 and 5M NaCl to make a final concentration of 200 mM Tris pH 7.5 and 150 mM NaCl, respectively. Ni-NTA agarose (Thermo Fisher Scientific) was added to supernatant and stirred in the cold room for 3 hours. Supernatant with Ni-NTA beads was loaded onto a disposable chromatography column and eluted in buffer containing 20 mM Tris pH 7.5, 150 mM NaCl, and various concentrations of imidazole ranging from no imidazole to 300 mM imidazole. Eluate fractions were collected and loaded on SDS-PAGE gels. Fractions with appropriate protein sizes were combined and evaluated for purity using size exclusion chromatography.

### 7.7 Luciferase immunoprecipitation system assay

EBV gp350, gH/gL, and gp42 antibody titers were determined by LIPS assay (Sashihara et al., 2009). Briefly, 293T cells were transfected with plasmids expressing EBV gp350, gH/gL, or gp42 fused with Renilla luciferase. Cell supernatants were collected and incubated with either human or mouse plasma, IVIG, gH/gL mAb B10, gp42 mAb A10, or bispecific mAb and immunoprecipitated with protein A/G beads for 1 hr. Coelenterazine substrate was added and luciferase activity was measured in light units (LU) by a luminometer. Each sample was tested in triplicate.

### 7.8 EBV B cell and epithelial cell neutralization

For B cell neutralization assays, 100 μg/mL of IVIG (Bivigam, ADMA Biologics), EBV hyperimmune globulin, EBV gp350 mAbs, EBV gH/gL mAbs, EBV gp42 mAbs, or bispecific mAb was serially diluted 23 times using 2-fold dilutions in a U-bottom 96-well plate. 25 μL of B95-8/F virus was added to each of the wells and incubated for 2 hr at 37°C. After incubation, 50 μL of 1 x $10^5$ Raji cells were added and incubated for 3 days at 37°C. Cells were fixed in 2% paraformaldehyde in DPBS.

For epithelial cell neutralization, mouse plasma, 100 μg/mL of EBV gH/gL mAbs or bispecific mAb was serially diluted 23 times using 3-fold dilutions in a flat-bottom 96-well plate. 25 μL of B95-8/F virus was added to each of the wells and incubated for 2 hr at 37°C. After incubation, 50 μL of 2 x $10^4$ SVKCR2 cells were added and incubated for 3 days at 37°C. Cells were washed with Dulbecco's PBS, trypsinized, and fixed in 2% paraformaldehyde in PBS.

GFP-positive cells were quantified using a FACSCanto II flow cytometer (BD Biosciences) and BD FlowJo software (BD Biosciences). The dilution of IVIG, EBV hyperimmune globulin, EBV mAbs, or bispecific mAb that inhibited infectivity by 50% ($IC_{50}$) based on reduction of the number of GFP-positive cells was calculated by non-linear regression analysis using GraphPad PRISM software. Neutralizing activity was considered absent when the software program failed to fit the results to an appropriate regression curve.

### 7.9 B cell and epithelial cell fusion inhibition

B cell and epithelial cell fusion was measured as previously reported in Bu et al., 2019. Briefly, for the B cell fusion assay, CHO-K1 cells were transfected with plasmids encoding gH, gL, gp42, gB, and luciferase. gH, gL, gp42, and gB are under the control of a CMV IE promoter

and the luciferase gene is under the control of the T7 polymerase promoter. Transfected CHO-K1 cells were incubated with gH/gL mAb B10, gp42 mAb A10, bispecific mAb, or a combination of two parental mAbs for 2 hours. Daudi-T7 B lymphocytes that stably express T7 RNA polymerase were added to the CHO-K1/mAb mixture and incubated overnight. The next day, cells were lysed and luciferase activity was measured using a luminometer.

To measure fusion activity in epithelial cells, CHO-K1 cells were transfected with plasmids encoding gH/ gL, gB, and luciferase. The promoter for each gene is same as that used in B cell fusion assay. Transfected CHO-K1 cells were incubated with gH/gL mAb B10, gp42 mAb A10, bispecific mAb, or combination of two parental mAbs for 2 hours and HEK 293T14 cells that express the T7 RNA polymerase were added. After overnight incubation, cells were lysed and luciferase activity was quantified using a luminometer.

### 7.10 SCID mice injections

All experiments were carried out in accordance with federal regulations and NIH guidelines and were approved by the Animal Care and Use Committee of the National Institute of Allergy and Infectious Diseases and University of Maryland. SCID mice (4 mice/group) were injected intraperitoneally with 3 x $10^7$ PBMCs the day before they were infected with EBV. Each group of mice was challenged with either of the two EBV strains by intravenous injections: EBV M81 (4 x $10^3$ GRU/100 µl), B95-8 (4 x $10^3$ GRU/100 µl, 1 x $10^4$ GRU/100 µl, or 1 x $10^5$ GRU/100 µl). One group of mice were injected with 100 µl of RPMI medium as a control.

### 7.11 Humanized mice injections

All animal experiments were performed in accordance with federal regulations and NIH guidelines and approved by the Animal Care and Use Committee of the National Institute of Allergy and Infectious Diseases and University of Maryland. Female HSCCB-NOG-F (NOD.Cg-*Prkdc*$^{scid}$ *Il2rg*$^{tm1Sug}$/ JicTac) mice that were 19 to 20 weeks post-engraftment were purchased from Taconic. IVIG, EBV hyperimmune globulin, EBV gp350 mAbs, gH/gL mAbs, gp42 mAbs, bispecific mAb, or 300 µl of PBS was injected intraperitoneally into each mouse on days -1, 0, 1, 4, 7, and 10 relative to the day of EBV challenge. For each injection, 0.5 mg of inoculum was given. On day 0, at least 4 hours after receiving mAbs or PBS, all animals were challenged with 1 x $10^6$ GRU of EBV B95-8/F virus given intravenously. Mouse weights and blood were collected weekly for 15 weeks after EBV infection. Mice were euthanized when they lost 30% of their original weight, were unable to obtain food or water, or were non-responsive to stimuli.

### 7.12 Pharmacokinetics of gH/gL mAbs in human FcRn transgenic mouse

Female and male B6. mFcRn−/− hFCRN Tg32 mice, purchased from Jackson Laboratory, were used to measure gH/gL mAb levels to determine the half-life of the antibodies. Mice were injected with 5 mg/kg of gH/gL mAb 769C2, 769B10, or 770F7 intravenously by tail injection on day 0. Serum was collected before injection and on days 1, 2, 5, 7, 9, 14, 21, 28, and 35 after injection. The concentration of each mAb was quantified by ELISA assay. Half-life, area under the curve, and clearance rate were calculated using WinNonLin software (Certara).

### 7.13 Passive transfer of IgG from immunized mice

On week 0, 3, and 7, BALB/c mice (n=80/group) were immunized with 5 μg gH/gL nanoparticle vaccine or 5 μg gH/gL/gp42 nanoparticle + 5 μg gp350 nanoparticle vaccine in the presence of AF03 adjuvant. Sera at weeks 4, 5, 8, 9, and 10 were pooled and mouse IgG was isolated. Purified mIgG (20 μg per gram of mouse) from each group was passively transferred by intraperitoneal injection to humanized mice on day -1, 0, and 1 post infection. On day 0, mice were challenged with 1 x $10^5$ GRU of EBV and weights were recorded and blood was collected weekly.

### 7.14 In vivo luciferase imaging

150 μl of D-Luciferin (15 mg/ml) was administered intraperitoneally 5 min before anesthesia. D-luciferin-injected mice were anesthetized with isoflurane. Once mice were anesthetized, mice were transferred to the maintenance cones inside the imaging box with their noses in the nose cones. Photographs were taken with exposure time of 1 min using an IVIS Lumina series III (Perkin Elmer). Images were taken on both the dorsal and ventral side of mice.

### 7.15 Quantifying the number of EBV DNA copies in the blood by qPCR

EBV DNA was quantified in blood as previously reported (Strowig et al., 2009) with minor modifications. DNA was isolated from mouse blood using a DNeasy Blood and Tissue kit (Qiagen, Germantown, MD). Forward primer 5'-GGACCACTGCCCCTGGTATAA-3'and reverse primer 5'-TTTGTGTGGACTCCTGGCG-3'were used to amply the EBV BamHI W repeat fragment and probe 5'-FAM-TCCTGCAGCTATTTCTGGTCGCATCA-3' was used to detect the PCR product. Human GAPDH was amplified using primers 5'-AGGGTGGTGGACCTCAT-3' and 5'-TGAGTGTGGCAGGGACT-3' and the PCR product

was detected with probe 5'-HEX-CAGCAAGAGCACAAGAGGAAGAGAGA-3'. EBV viral DNA was quantified using a TaqMan Universal PCR Master Mix kit and CFX96 Touch Real-Time PCR Detection System (BioRad, Hercules, CA). Genomic DNA isolated from Raji cells was used as a standard. p-values were calculated using the Welch two sample t-test.

### 7.16 Pathology of tissues in humanized mice

Humanized mice were euthanized at the end of the study and the liver, spleen, lung, and kidney were fixed in 10% neutral-buffered formalin, embedded in paraffin, and sectioned. Tissue slides were stained with hematoxylin and eosin and anti-CD20 monoclonal antibody, and in situ hybridization was performed with an EBER1 probe. Quantitation of EBER positivity (0 to 3+ or 0 to 4+ in some cases), and diagnosis of lymphoproliferative disease or lymphoma were performed by a pathologist who was blinded to the treatment arms.

### 7.17 Total human IgG quantification by ELISA

Plasma was separated from mouse blood by centrifuging at 800 x g for 10 min. Total human IgG concentration in plasma was measured using an IgG (Total) Human Uncoated ELISA kit (Invitrogen). Plasma was diluted to fall within the standard range of the kit. Briefly, 96 well plates were coated with purified anti-human IgG monoclonal antibody and incubated overnight at 4°C. Plates were washed with wash buffer and blocked with blocking buffer for 2 hr at room temperature. Plates were washed again, and plasma samples and standards were added to wells and incubated for 2 hr at room temperature. After incubation, plates were washed, and HRP-conjugated anti-human IgG monoclonal antibody was added. After incubation for 1 hr at

room temperature, tetramethylbenzidine substrate solution was added and incubated for 15 min. 1M $H_3PO_4$ was added as a stop solution and wells were read at 450 nm.

### 7.18 Quantification of gH/gL or gp42 mAb concentration by ELISA

96-well ELISA plates were coated with 200 ng/well of EBV gH/gL or gp42 in ELISA coating buffer (BioLegend) and incubated overnight at 4°C. Plates were washed 6 times with PBS with 0.05% Tween-20 (washing buffer) and blocked with PBS containing 0.05% Tween-20, 5% skim milk, and 2% BSA (blocking buffer) for 1 hr at room temperature. Plates were washed again with washing buffer. Known concentrations of purified gH/gL or gp42 mAb were used as a standard. Control wells were incubated with blocking buffer without any serum or mAb. Plates were incubated with mouse sera, mouse plasma, or control mAb for 1 hr at room temperature and washed 6 times with washing buffer. Following washing, a 1:8000 dilution of goat anti-human IgG-HRP (Southern Biotech, Birmingham, AL) in blocking buffer was added to each well, including mAb control wells, and incubated at room temperature for 1 hr. Plates were washed with washing buffer and 100 µl of SureBlue Reserve TMB Microwell Peroxidase substrate was added. 100 µl of 1 N sulfuric acid was added to each well after 3 min to stop the reaction and the absorbance of yellow color was read at $A_{450}$. All assays were performed in duplicate and samples were corrected to subtract the background level (averaged $A_{450}$ values of control wells). A standard curve was generated by plotting corrected averaged $A_{450}$ values to known concentration of gH/gL or gp42 mAb by fitting data to sigmoidal dose-response curve using GraphPad PRISM software.

### 7.19 Construction of bispecific mAb

EBV bispecific mAb was constructed in the format of CrossMab$^{CH1\text{-}CL}$ where the CH1 heavy chain and constant region light chain of gp42 mAb A10 were swapped; no changes were made for Fab region of gH/gL mAb B10. Backbone plasmids for heavy and light chains of antibodies 1 and 2 were generously provided by the Vaccine Research Center, NIAID, NIH. A variable region of gH/gL mAb B10 heavy chain and variable regions of heavy and light chains of gp42mAb A10 were cloned into the backbone plasmids, VRC 4193, VRC 4192, and VRC3778, respectively. No changes were made for light chain of gH/gL mAb B10. For knob-into-hole mutations, S354C and T366W were introduced in the heavy chain of gH/gL mAb B10, and Y349C, T366S, L368A, and Y407V mutations were introduced in the heavy chain of gp42 mAb A10. M428L and N434S mutations were engineered into the Fc region to increase half-life of the bispecific mAb.

### 7.20 Production and purification of bispecific mAb

Heavy and light chains of gH/gL mAb B10 and gp42 mAb A10 were diluted to a concentration of 300 ng/μL. Heavy and light chain plasmids were mixed at a 1:2 ratio for both mAbs. Expi293F cells were transfected with a 1:3 ratio with above heavy and light chain mixed gH/gL mAb B10 and gp42 mAb A10, respectively. Transfected cells were incubated for 5 days, and supernatant was loaded onto a HiTrap MabSelect PrismA protein A column (Cytiva). The antibody was eluted from the column using Pierce IgG elution buffer (Thermo Scientific). Purified bispecific mAb was dialyzed to 1X PBS and stored at -80°C for long term storage.

### 7.21 SDS-PAGE gels

EBV mAbs and bispecific mAb were evaluated for protein sizes using SDS-PAGE gels under reducing and non-reducing conditions. For non-reducing gels, mAbs were mixed with NuPAGE LDS sample buffer 4X (Invitrogen). For reducing gels, mAbs were mixed with NuPAGE LDS sample buffer 4X with 10% β-mercaptoethanol and heated at 95°C for 5 min. Sample buffer was added to the mAbs and they were loaded onto NuPAGE 4-12% Bis-Tris gels (Invitrogen) and electrophoresis was performed at 200V for 40 min. Gels were stained with coomassie blue and imaged with a gel imager.

### 7.22 Size exclusion chromatography

To confirm the purity of purified mAbs and the bispecific mAb, size-exclusion chromatography was performed. Superdex 200 increase 100/300 GI columns (Cytiva) were equilibrated with 1X PBS before use. Purified mAbs or bispecific mAb that were concentrated to a volume of 700 µl were loaded onto columns and eluted with 1X PBS.

### 7.23 Digestion to yield Fab or $F(ab)_2$ fragments of EBV mAbs and a bispecific mAb

An HRV-3C protease site was introduced in the middle of the hinge region in the heavy chains of gH/gL mAb B10 and gp42 mAb A10 plasmids to produce Fab fragments while the protease site was introduced below the hinge region for heavy chains of bispecific gH/gL mAb B10 and gp42 mAb A10 plasmids to produce a $F(ab)_2$ fragment. Expi293F cells were transfected as described above for EBV mAbs or bispecific mAb production but using heavy chain plasmids with a protease site. EBV mAbs and bispecific mAb with a protease site was purified in the same method as regular EBV mAbs or bispecific mAb. 1 µg of protease was added to 50 µg of purified

EBV mAbs or bispecific mAb with a protease site and digested overnight at 4°C. Protease digestion was confirmed by SDS-PAGE gel and the digested material was loaded on a HiTrap rProtein A FF column (Cytiva) that was connected to a GSTrap FF column (Cytiva). Fab or $F(ab)_2$ fragments were eluted from the connected columns with 1X PBS and purity was confirmed using size exclusion chromatography SEC.

### 7.24 Sequential binding of bispecific mAb by biolayer interferometry

Streptavidin biosensors (ForteBio) were equilibrated with 1X PBS for 60 sec and biotinylated gp42-del or gH/gL protein (10 μg/mL) was immobilized onto the biosensors for 300 sec. The sensors were placed in 1X PBS for 30 seconds (baseline measurement) followed by dipping in 75 μg/mL of either gp42 mAb A10, gH/gL mAb B10, bispecific mAb $F(ab)_2$ fragment, or non-specific gp350 mAb A9 for 300 sec. The sensors were dipped in 1X PBS for 30 sec (second baseline) and then placed in 75 μg/mL of gH/gL or gp42-del for 300 sec. The sensors were then placed into 1X PBS for 300 sec to measure dissociation.

### 7.25 Quantification of surface CD21 expression levels by flow cytometry

To quantify the level of CRD21 expression on Raji, BL41, BL30, and DG75 cells, 0.5 x $10^6$ cells were harvested and stained with anti-CD3-V421, anti-CD19/20-A488, or anti-CD21-APC antibody, and live/dead-near infrared antibodies for 30 min at 4°C. Cells were washed with 1X PBS and fixed in 0.5% paraformaldehyde. Using a Fortessa flow cytometer (BD Biosciences), the live cell population was selected by live/dead staining, and then the $CD20^+$ cell population was gated based on CD3 and CD20 antibody staining. The $CD21^+$ high expressing $CD20^+$ B cells were quantified and the % of B cells expressing CD21 was determined.

# Bibliography


Abbas, A.K., Lichtman, A.H., and Pillai, S. (2012). Antibodies and Antigens. *Cellular and Molecular Immunology* e-book 7th ed. Elsevier Saunders. 89-107.

Abbas, A.K., Lichtman, A.H., and Pillai, S. (2012). Effector Mechanisms of Humoral Immunity. *Cellular and Molecular Immunology* e-book 7th ed. Elsevier Saunders. 269-292.

Ahearn, J.M., Hayward, S.D., Hickey, J.C., and Fearon, D.T. (1988). Epstein-Barr virus (EBV) infection of murine L cells expressing recombinant human EBV/C3d receptor. *Proc. Natl. Acad. Sci. U.S.A.* 85(23), 9307-9311.

Allen, T.M., Brehm, M.A., Bridges, S., Ferguson, S., Kumar, P., Mirochnitchenko, O., Palucka, K., Pelanda, R., Sanders-Beer, B., Shultz, L.D., Su, L., and PrabhuDas, M. (2019). Humanized immune system mouse models: progress, challenges and opportunities. *Nat Immunol.* 20**,** 770–774.

Al-Mansour, Z., Nelson, B. P., & Evens, A. M. (2013). Post-transplant lymphoproliferative disease (PTLD): risk factors, diagnosis, and current treatment strategies. *Curr Hematol Malig Rep*. *8*(3), 173–183.

Bjornevik, K., Cortese, M., Healy, B.C., Kuhle, J., Mina, M.J., Leng, Y., Elledge, S.J., Niebuhr, D.W., Scher, A.I., Munger, K.L., and Ascherio, A. (2022). Longitudinal analysis reveals high prevalence of Epstein-Barr virus associated with multiple sclerosis. *Science.* 375(6578):296-301.

Bu, W., Joyce, G.M., Nguyen, H., Banh, D.V., Aguilar, F., Tariq, Z., Yap, M.L., Tsujimura, Y., Gillespie, R.A., Tsybovsky, Y., Andrews, S.F., Narpala, S.R., McDermott, A.B., Rossmann, M.G., Yasutomi, Y., Nabel, G.J., Kanekiyo, and M., Cohen, J.I. (2019). Immunization with Components of the Viral Fusion Apparatus Elicits Antibodies That Neutralize Epstein-Barr Virus in B Cells and Epithelial Cells. *Immunity.* 50(5), 1305-1316.

Brezski, R.J., and Georgiou, G. (2016). Immunoglobulin isotype knowledge and application to Fc engineering. *Curr Opin Immunol*. 40:62-9.

Brinkmann, U., and Kontermann, R.E. (2017). The making of bispecific antibodies. *mAbs*. 9:2, 182-212.

Carr, C.M., and Kim, P.S. (1993). A spring-loaded mechanism for the conformational change of influenza hemagglutinin. *Cell*. 73, 823-832.

Chen, J., Sathiyamoorthy, K., Zhang, X., Schaller, S., Perez White, B.E., Jardetzky, T.S., and Longnecker, R. (2018). Ephrin receptor A2 is a functional entry receptor for Epstein-Barr virus. *Nat Microbiol*. 3, 172–180

Chesnokova, L.S., Nishimura, S.L., and Hutt-Fletcher, L.M. (2009). Fusion of epithelial cells by Epstein-Barr virus proteins is triggered by binding of viral glycoproteins gHgL to integrins alphavbeta6 or alphavbeta8. *Proc. Natl. Acad. Sci. USA*. 106, 20464–20469.

Chiu, M.L., Goulet, D.R., Teplyakov, A., and Gilliland, G.L. (2019). Antibody Structure and Function: The Basis for Engineering Therapeutics. *Antibodies (Basel, Switzerland)*. *8*(4), 55.

Cho, H., Gonzales-Wartz, K.K., Huang, D., Yuan, M., Peterson, M., Liang, J., Beutler, N., Torres, J.L., Cong, Y., Postnikova, E., Bangaru, S., Talana, C.A., Shi, W., Yang, E.S., Zhang, Y., Leung, K., Wang, L., Peng, L., Skinner, J., Li, S., Wu, N.C., Liu, H., Dacon, C., Moyer, T., Cohen, M., Zhao, M., Lee, F.E., Weinberg, R.S., Douagi, I., Gross, R., Schmaljohn, C., Pegu, A., Mascola, J.R., Holbrook, M., Nemazee, D., Rogers, T.F., Ward, A.B., Wilson, I.A., Crompton, P.D., and Tan, J. (2021). Ultrapotent bispecific antibodies neutralize emerging SARS-CoV-2 variants. *Sci Transl Med.*13(616).

Cho, Y., Gordadze, A.V., Ling, P.D., and Wang, F. (1999). Evolution of Two Types of Rhesus Lymphocryptovirus Similar to Type 1 and Type 2 Epstein-Barr Virus. *J Virol*. 73(11), 9206–9212.

Clemens, M.J., Laing, K.G., Jeffrey, I.W., Schofield, A., Sharp, T.V., Elia, A., Matys, V., James, M.C., and Tilleray, V.J. (1994). Regulation of the interferon-inducible eIF-2 alpha protein kinase by small RNAs. *Biochimie*. 76(8):770-8.

Cohen, J.I., Wang, F., Mannick, J., and Kieff, E. (1989) Epstein-Barr virus nuclear protein 2 is a key determinant of lymphocyte transformation. *Proc Natl Acad Sci U S A*. 86(23):9558-62.

Cohen, J.I. (2000). Epstein-Barr virus infection. *N Engl J Med*. 17;343(7):481-92.

Cohen, J.I., Fauci, A.S., Varmus, H., and Nabel, G.J. (2011). Epstein-Barr virus: an important vaccine target for cancer prevention. *Sci. Transl. Med*. 3, 1-3.

Cohen, J.I. (2015). Primary Immunodeficiencies Associated with EBV Disease. *Curr. Top. Microbiol. Immunol*. 390, 241-265.

De Gasparo, R., Pedotti, M., Simonelli, L., Nickl, P., Muecksch, F., Cassaniti, I., Percivalle, E., Lorenzi, J.C.C., Mazzola, F., Magri, D., Michalcikova, T., Haviernik, J., Honig, V., Mrazkova, B., Polakova, N., Fortova, A., Tureckova, J., Iatsiuk, V., Di Girolamo, S., Palus M., Zudova, D., Bednar, P., Bukova, I., Bianchini, F., Mehn, D., Nencka, R., Strakova, P., Pavlis, O., Rozman, J., Gioria, S., Sammartino, J.C., Giardina, F., Gaiarsa, S., Pan-Hammarstrom, Q., Barnes, C.O., Bjorkman, P., Calnolai, L., Piralla, A., Baldati, F., Nussenzweig, M.C., Bieniasz, P.D., Hatziioannou, T., Prochazka, J., Sedlacek, R., Robbiani, D., Ruzek, D., and Varani, L. (2021). Bispecific IgG neutralizes SARS-CoV-2 variants and prevents escape in mice. *Nature.* 593, 424–428.

Delecluse, H.J., Hilsendegen, T., Pich, D., Zeidler, R., Hammerschmidt, W. (1998). Propagation and recovery of intact, infectious Epstein-Barr virus from prokaryotic to human cells. *Proc. Natl. Acad. Sci. U.S.A*. 95, 8245–8250.

Dharnidharka, V.R., Tejanim A.H., Hom P.L., and Harmonm W.E. (2002). Post-transplant lymphoproliferative disorder in the United States: young Caucasian males are at highest risk. *Am J Transplant*. 2(10):993-8.

Dreyfus, C., Laursen, N.S., Kwaks, T., Zuijdgeest, D., Khayat, R., Ekiert, D.C., Lee, J.H., Metlagel, Z., Bujny, M.V., Jongeneelen, M., van der Vlugt, R., Lamrani, M., Korse, H.J., Geelen, E., Sahin, O., Sieuwerts, M., Brakenhoff, J.P., Vogels, R., Li, O.T., Poon, L.L., Peiris, M., Koudstaal, W., Ward, A.B., Wilson, I.A., Goudsmit, J., and Friesen, R.H. (2012). Highly conserved protective epitopes on influenza B viruses. *Science.* 337:1343–1348.

Dunmire, S.K., Hogquist, K.A., Balfour, H.H. (2015). Infectious Mononucleosis. In: Münz, C. (eds) Epstein Barr Virus Volume 1. *Current Topics in Microbiology and Immunology*, vol 390. Springer, Cham.

Edelman, D.C. (2005). Human herpesvirus 8--a novel human pathogen. *Virol J.* 2, 78.

Espinosa, D., Mendy, J., Manayani, D., Vang, L., Wang, C., Richard, T., Guenther, B., Aruri, J., Avanzini, J., Garduno, F., Farness, P., Gurwith, M., Smith, J., Harris, E., and Alexander, J. (2018). Passive Transfer of Immune Sera Induced by a Zika Virus-Like Particle Vaccine Protects AG129 Mice Against Lethal Zika Virus Challenge. *EBioMedicine*. 27:61-70.

Fan, G., Wang, Z., Hao, M., and Li, J. (2015). Bispecific antibodies and their applications. *J Hematol Oncol*. *8*, 130.

Fingeroth, J.D., Weis, J.J., Tedder, T.F., Strominger, J.L., Biro, P.A., and Fearon, D.T. (1984). Epstein-Barr virus receptor of human B lymphocytes is the C3d receptor CR2. *Proc Natl Acad Sci U S A*. 81(14), 4510–4514.

Forthal, D.N. (2014). Functions of Antibodies. *Microbiol Spectr*. 2(4), 1–17.

Frade, R., Barel, M., Ehlin-Henriksson, B., and Klein, G. (1985). gp140, the C3d receptor of human B lymphocytes, is also the Epstein-Barr virus receptor. *Proc Natl Acad Sci USA*. 82: 1 490–1 493.

Frei, J., Nyakatura, E., Zak, S., Bakken, R.R., Chandran, K., Dye, J.M., Lai, J.R. (2016). Bispecific Antibody Affords Complete Post-Exposure Protection of Mice from Both Ebola (Zaire) and Sudan Viruses. *Sci Rep.* 6, 19193

Fujimoto, A., and Suzuki, R. (2020). Epstein-Barr Virus-Associated Post-Transplant Lymphoproliferative Disorders after Hematopoietic Stem Cell Transplantation: Pathogenesis, Risk Factors and Clinical Outcomes. *Cancers (Basel).* 12, 328.

Fujiwara, S., Imadome, KI. and Takei, M. (2015). Modeling EBV infection and pathogenesis in new-generation humanized mice. *Exp Mol Med.* 47, e135.

Gewurz, B. E., Longnecker, R., and Cohen, J.I. (2022). Epstein-Barr Virus. *Field's Virology 7th ed*. Wolters Kluwer. 324-388.

Gires, O., Kohlhuber, F., Kilger, E., Baumann, M., Kieser, A., Kaiser, C., Zeidler, R., Scheffer, B., Ueffing, M., and Hammerschmidt, W. (1999). Latent membrane protein 1 of Epstein-Barr virus interacts with JAK3 and activates STAT proteins. *EMBO J*. 18(11), 3064–3073.

Gottschalk, S., Ng, C.Y., Perez, M., Smith, C.A., Sample, C., Brenner, M.K., Heslop, H.E., and Rooney, C.M. (2001). An Epstein-Barr virus deletion mutant associated with fatal lymphoproliferative disease unresponsive to therapy with virus-specific CTLs. *Blood*. 97(4):835-43.

Haque, T., Johannessen, I., Dombagoda, D., Sengupta, C., Burns, D.M., Bird, P., Hale, G., Mieli-Vergani, G., and Crawford, D.H. (2006). A mouse monoclonal antibody against Epstein-Barr virus envelope glycoprotein 350 prevents infection both in vitro and in vivo. *J Infect Dis*. 194(5), 584-587.

Hatton, O.L., Harris-Arnold, A., Schaffert, S., Krams, S.M., and Martinez, O.M. (2014). The interplay between Epstein-Barr virus and B lymphocytes: implications for infection, immunity, and disease. *Immunol Res*. 58(2-3):268-76.

Herrman, M., Mühe, J., Quink, C., and Wang, F. (2016). Epstein-Barr virus gp350 can functionally replace the rhesus lymphocryptovirus major membrane glycoprotein and does not restrict infection of rhesus macaques. *J Virol*. 90,1222–1230

Howard, M.K., Sabarth, N., Savidis-Dacho, H., Portsmouth, D., Kistner, O., Kreil, T.R., Ehrlich, H.J., and Barrett, P.N. (2011). H5N1 whole-virus vaccine induces neutralizing antibodies in humans which are protective in a mouse passive transfer model. *PLoS One*. 6(8):e23791.

Humar, A., Hébert, D., Davies, H.D., Humar, A., Stephens, D., O'Doherty, B., Allen, U. (2006). A randomized trial of ganciclovir versus ganciclovir plus immune globulin for prophylaxis against Epstein-Barr virus related posttransplant lymphoproliferative disorder. *Transplantation*. 81(6), 856-861.

Ito, R., Takahashi, T., Ito, M. (2017). Humanized mouse models: application to human diseases. *J Cell Physiol*. 233 (5), 3723-3728.

Janeway, C.A. Jr, Travers, P., Walport, M., and Shlomchik, M. (2001). The distribution and functions of immunoglobulin isotypes. *Immunobiology: The Immune System in Health and Disease*. Garland Science.

Janz, A., Oezel, M., Kurzeder, C., Mautner, J., Pich, D., Kost, M., Hammerschmidt, W., Delecluse, H.J. (2000). Infectious Epstein-Barr virus lacking major glycoprotein BLLF1 (gp350/220) demonstrates the existence of additional viral ligands. *J Virol*. 74, 10142-10152.

Kamen, L., Myneni, S., Langsdorf, C., Kho, E., Ordonia, B., Thakurta, T., Zheng, K., Song, A., and Chung, S. (2019). A novel method for determining antibody-dependent cellular phagocytosis. *J Immunol Methods*. 468:55-60.

Kanekiyo, M., Bu, W., Joyce, M.G., Meng, G., Whittle, J.R., Baxa, U., Yamamoto, T., Narpala, S., Todd, J.P., Rao, S.S., McDermott, A.B., Koup, R.A., Rossmann, M.G., Mascola, J.R., Graham, B.S., Cohen, J.I., and Nabel, G.J. (2015). Rational Design of an Epstein-Barr Virus Vaccine Targeting the Receptor-Binding Site. *Cell*. 162(5):1090-100.

Kang, M.S., and Kieff, E. (2015). Epstein-Barr virus latent genes. *Exp Mol Med*. 47(1):e131.

Kim, J., Bu, W., Mine, S., Tariq, Z., Nguyen, H., Wang, Y., Tolman, C., Mond, J., and Cohen, J.I. (2021). Epstein-Barr virus (EBV) hyperimmune globulin isolated from donors with high gp350 antibody titers protect humanized mice from challenge with EBV. *Virology*. 561:80-86

Kirschner, A.N., Lowrey, A.S., Longnecker, R., and Jardetzky, T.S. (2007). Binding-site interactions between Epstein-Barr virus fusion proteins gp42 and gH/gL reveal a peptide that inhibits both epithelial and B-cell membrane fusion. *J. Virol*. 81, 9216–9229

Klein, C., Schaefer, W., and Regula, J.T. (2016). The use of CrossMAb technology for the generation of bi- and multispecific antibodies. *MAbs*. 8(6):1010-20.

Ko, S.Y., Pegu, A., Rudicell, R., Yang, Z.Y., Joyce, M.G., Chen, X., Wang, K., Bao, S., Kraemer, T.D., Rath, T., Zeng, M., Schmidt, S.D., Todd, J.P., Penzak, S.R., Saunders, K.O., Nason, M.C., Haase, A.T., Rao, S.S., Blumberg, PS., Mascola, J.R., and Nabel, G.J. (2014). Enhanced neonatal Fc receptor function improves protection against primate SHIV infection. *Nature*. 514, 642–645.

Krah, S., Kolmar, H., Becker, S., and Zielonka, S. (2018). Engineering IgG-like bispecific antibodies-an overview. *Antibodies*. 7, 28.

Labrijn, A.F., Janmaat, M.L., Reichert, J.M., and Parren, P.W.H.I. (2019). Bispecific antibodies: a mechanistic review of the pipeline. *Nat Rev Drug Discov.* 18, 585–608.

Lanz, T.V., Brewer, R.C., Ho, P.P., Moon, J.S., Jude, K.M., Fernandes, D., Fernandes, R.A., Gomez, A.M., Nadj, G.S., Bartley, C.M., Schubert, R.D., Hawes, I.A., Vazquez, S.E., Lyer, M., Zuchero, B., Teegen, B., Dunn, J.E., Lock, C.B., Kipp, L.B., Cotha,, V.C., Ueberheide, B.M., Aftab, B.T., Anderson, M.S., DeRisi, J.L., Wilson, M.R., Bashford-Rogers, R.J.M., Platten, M., Garcia, K.C., Steinman, L., and Robinson, W.H (2022). Clonally expanded B cells in multiple sclerosis bind EBV EBNA1 and GlialCAM. *Nature*. 603, 321–327.

Laoprasopwattana, K., Libraty, D.H., Endy, T.P., Nisalak, A., Chunsuttiwat, S., Ennis, F.A., Rothman, A.L., and Green, S. (2007). Antibody-dependent cellular cytotoxicity mediated by plasma obtained before secondary dengue virus infections: potential involvement in early control of viral replication. *J Infect Dis*.195(8):1108-16.

Le, Q.T., Jones, C.D., Yau, T.K., Shirazi, H.A., Wong, P.H., Thomas, E.N., Patterson, B.K., Lee, A.W., Zehnder, J.L. (2005). A comparison study of different PCR assays in measuring circulating plasma epstein-barr virus DNA levels in patients with nasopharyngeal carcinoma. *Clin Cancer Res*. 11(16):5700-7.

Li, S.S., Gilbert, P.B., Tomaras, G.D., Kijak, G., Ferrari, G., Thomas, R., Pyo, C.W., Zolla-Pazner, S., Montefiori, D., Liao, H.X., Nabel, G., Pinter, A., Evans, D.T., Gottardo, R., Dai, J.Y., Janes, H., Morris, D., Fong, Y., Edlefsen, P.T., Li, F., Frahm, N., Alpert, M.D., Prentice, H., Rerks-Ngarm, S., Pitisuttithum, P., Kaewkungwal, J., Nitayaphan, S., Robb, M.L., O'Connell, R.J., Haynes, B.F., Michael, N.L., Kim, J.H., McElrath, M.J., and Geraghty, D.E. (2014). FCGR2C polymorphisms associate with HIV-1 vaccine protection in RV144 trial. *J Clin Invest.*124(9):3879-90.

Li, Q.X., Young, L.S., Niedobitek, G., Dawson, C.W., Birkenbach, M., Wang, F., and Rickinson, A.B. (1992). Epstein-Barr virus infection and replication in a human epithelial cell system. *Nature*. 356(6367):347-50.

Lin, J., Johannsen, E., Robertson, E., and Kieff, E. (2002). Epstein-Barr virus nuclear antigen 3C putative repression domain mediates coactivation of the LMP1 promoter with EBNA-2. *J Virol*. 76(1):232-42.

Liu, F., Marquardt, G., Kirschner, A.N., Longnecker, R., and Jardetzky, T.S. (2010). Mapping the N-terminal residues of Epstein-Barr virus gp42 that bind gH/gL by using fluorescence polarization and cell-based fusion assays. *J Virol*. 84(19):10375-85.

Liu, Q., Fan, C., Li, Q., Zhou, S., Huang, W., Wang, L., Sun, C., Wang, M., Wu, X., Ma, J., Li, B., Xie, L., and Wang, Y. (2017). Antibody-dependent-cellular-cytotoxicity-inducing antibodies significantly affect the post-exposure treatment of Ebola virus infection. *Sci Rep*. 7:45552.

Litman, G.W., Rast, J.P., Shamblott, M.J., Haire, R.N., Hulst, M., Roess, W., Litman, R.T., Hinds-Frey, K.R., Zilch, A., and Amemiya, C.T. (1993). Phylogenetic diversification of immunoglobulin genes and the antibody repertoire. *Mol Biol Evol*. 10(1):60-72.

Longnecker, R. (2000). Epstein-Barr virus latency: LMP2, a regulator or means for Epstein-Barr virus persistence? *Adv Cancer Res*. 79:175-200.

Longnecker, R., Kieff, E., and Cohen, J.I. (2013). Epstein-Barr Virus. *Field's Virology*. Lippincott Williams & Wilkins. 1898-1959.

Lu, L.L., Suscovich, T J., Fortune, S.M., and Alter, G. (2018). Beyond binding: antibody effector functions in infectious diseases. *Nat Rev Immunol*. 18(1), 46–61.

Lucchesi, W., Brady, G., Dittrich-Breiholz, O., Kracht, M., Russ, R., and Farrell, P.J. (2008). Differential gene regulation by Epstein-Barr virus type 1 and type 2 EBNA2. *J Virol*. 82 (15), 7456-7466.

Ma, J., Mo, Y., Tang, M., Shen, J., Qi, Y., Zhao, W., Huang, Y., Xu, Y., and Qian, C. (2021). Bispeific antibodies: from research to clinical application. *Front Immunol*. 12:626616.

Mannick, J.B., Cohen, J.I., Birkenbach, M., Marchini, A., and Kieff, E. (1991). The Epstein-Barr virus nuclear protein encoded by the leader of the EBNA RNAs is important in B-lymphocyte transformation. *J Virol*. 65(12):6826-37.

McShane, M.P., and Longnecker, R. (2004). Cell-surface expression of a mutated Epstein-Barr virus glycoprotein B allows fusion independent of other viral proteins. *Proc Natl Acad Sci U S A*. 101(50):17474-9.

Miller, C.L., Burkhardt, A.L., Lee, J.H., Stealey, B., Longnecker, R., Bolen, J.B., and Kieff, E. (1995). Integral membrane protein 2 of Epstein-Barr virus regulates reactivation from latency through dominant negative effects on protein-tyrosine kinases. *Immunity*. 2(2):155-66.

Mullard, A. (2021). FDA approves 100th monoclonal antibody product. *Nat Rev Drug Discov.* **20,** 491-495.

Munz, C. (2017). Humanized mouse models for Epstein Barr virus infection. *Curr Opin Virol*. 25, 113-118.

Munz, C. (2019). Latency and lytic replication in Epstein-Barr virus-associated oncogenesis. *Nat Rev Microbiol.* 17, 691–700.

Mutsvunguma, L.Z., Rodriguez, E., Escalante, G.M., Muniraju, M., Williams, J.C., Warden, C., Qin, H., Wang, J., Wu, X., Barasa, A., Mulama, D.H., Mwangi, W., Ogembo, J.G. (2019). Identification of multiple potent neutralizing and non-neutralizing antibodies against Epstein-Barr virus gp350 protein with potential for clinical application and as reagents for mapping immunodominant epitopes. *Virology*. 536, 1-15.

Nanbo, A., and Takada, K. (2002). The role of Epstein-Barr virus-encoded small RNAs (EBERs) in oncogenesis. *Rev Med Virol*. 12(5):321-6.

Nelson, C.S., Huffman, T., Jenks, J.A., Cisneros de la Rosa, E., Xie, G., Vandergrift, N., Pass, R.F., Pollara, J., and Permar, S.R. (2018). HCMV glycoprotein B subunit vaccine efficacy mediated by nonneutralizing antibody effector functions. *Proc Natl Acad Sci U S A*.115(24):6267-6272.

Nemerow, G.R., Mold, C., Schwend, V.K., Tollefson, V., Cooper, N.R. (1987). Identification of gp350 as the viral glycoprotein mediating attachment of Epstein-Barr virus (EBV) to the EBV/C3d receptor of B cells: sequence homology of gp350 and C3 complement fragment C3d. *J Virol*. 61(5), 1416-1420.

Neuhierl, B., Feederle, R., Hammerschmidt, W., Delecluse, H.J. (2002). Glycoprotein gp110 of Epstein-Barr virus determines viral tropism and efficiency of infection. *Proc. Natl. Acad. Sci. U.S.A*. 99, 15036–15041.

Ogembo, J.G., Kannan, L., Ghiran, I., Nicolson-Weller, A., Finberg, R., Tsokos, G.C., Fingeroth, J.D. (2013). Human complement receptor type 1/CD35 is an Epstein-Barr virus receptor. *Cell Rep*. 3(2), 371-385.

Omerović, J., Lev, L., and Longnecker, R. (2005). The amino terminus of Epstein-Barr virus glycoprotein gH is important for fusion with epithelial and B cells. *J Virol. 79*(19), 12408–12415.

Orange, J.S., Hossny, E.M., Weiler, C.R., Ballow, M., Berger, M., Bonilla, F.A., Buckley, R., Chinen, J., El-Gamal, Y., Mazer, B.D., Nelson, R.P., Patel, D.D., Secord, E., Sorensen, R.U., Wasserman, R.L, Cunningham-Rundles, C. (2006). Use of intravenous immunoglobulin in human disease a review of evidence by members of the primary immunodeficiency committee of the American Academy of Allergy, Asthma, and Immunology. *J Allergy Clin Immunol*. 117, S525-553.

Paine, E., Scheinman, R.I., Baldwin, A.S. Jr, and Raab-Traub, N. (1995). Expression of LMP1 in epithelial cells leads to the activation of a select subset of NF-kappa B/Rel family proteins. *J Virol*. 69(7):4572-6.

Panchal, N., Booth, C., Cannons, J.L., Schwartzberg, P.L. (2018). X-Linked Lymphoproliferative Disease Type 1: A Clinical and Molecular Perspective. *Front Immunol*. 9:666.

Pearson, T., Greiner, D.L., and Shultz, L.D. (2008). Creation of "humanized" mice to study human immunity. *Curr Protoc Immunol.* Chapter 15, Unit–15.21.

Preiksaitis, J.K. Cockfield, S.M. (1998). Epstein-Barr virus and lymphoproliferative disease after transplantation. In: Bowden, R.A., Ljungman, P., Pava, C.V. (Eds.) *Transplant infections*. Lippincott-Raven, Philadelphia, pp. 245-263.

Ray, U., Cinque, P., Gerevini, S., Longo, V., Lazzarin, A., Schippling, S., Martin, R., Buck, C. B., and Pastrana, D. V. (2015). JC polyomavirus mutants escape antibody-mediated neutralization. *Sci Transl Med*. *7*(306), 306ra151.

Rechsteiner, M.P., Berger, C., Zauner, L., Sigrist, J.A., Weber, M., Longnecker, R., Bernasconi, M., and Nadal, D. (2008). Latent membrane protein 2B regulates susceptibility to induction of lytic Epstein-Barr virus infection. *J Virol.* 82(4):1739-47.

Roopenian, D., and Akilesh, S. (2007). FcRn: the neonatal Fc receptor comes of age. *Nat Rev Immunol.* 7, 715–725.

Rosa, M.D., Gottlieb, E., Lerner, M.R., and Steitz, J.A. (1981). Striking similarities are exhibited by two small Epstein-Barr virus-encoded ribonucleic acids and the adenovirus-associated ribonucleic acids VAI and VAII. *Mol Cell Biol*. 1(9):785-96.

San-Juan, R., Comoli, P., Caillard, S., Moulin, B., Hirsch, H.H., and Meylan, P. (2014). Epstein-Barr virus related post-transplant proliferative disorder in solid organ transplant recipients. *Clin Microbiol Infect*. 20, 109–118.

Sashihara, J., Burbelo, P.D., Savoldo, B., Pierson, T.C., and Cohen, J.I. (2009). Human antibody

titers to Epstein-Barr Virus (EBV) gp350 correlate with neutralization of infectivity better than antibody titers to EBV gp42 using a rapid flow cytometry-based EBV neutralization assay. *Virology*. 391(2), 249–256.
Sedykh, S.E., Prinz, V.V., Buneva, V.N., and Nevinsky, G.A. (2018). Bispecific antibodies: design, therapy, perspectives. *Drug Des Devel Ther*. 12, 195–208.

Seemayer, T.A., Gross, T.G., Egeler, R.M., Pirruccello, S.J., Davis, J.R., Kelly, C.M., Okano, M., Lanyi, A., Sumegi, J. (1995). X-linked lymphoproliferative disease: twenty-five years after the discovery. *Pediatr Res*. 38, 471-478.

Shannon-Lowe, and C., Rowe, M. (2014). Epstein Barr virus entry; kissing and conjugation. *Curr Opin Virol*. 4:78-84.

Shi, X., Deng, Y., Wang, H., Ji, G., Tan, W., Jiang, T., Li, X., Zhao, H., Xia, T., Meng, Y., Wang, C., Yu, X., Yang, Y., Li, B., Qin, E.D., Dai, J., Qin, C.F., and Guo, Y. (2016). A bispecific antibody effectively neutralizes all four serotypes of dengue virus by simultaneous blocking virus attachment and fusion. *MAbs.* 8:574–584.

Singh, S., Homad, L.J., Akins, N.R., Stoffers, C.M., Lackhar, S., Malhi, H., Wan, Y.H., Rawlings, D.J., McGuire, A.T. (2020). Neutralizing antibodies protect against oral transmission of lymphocryptovirus. *Cell Rep Med*. 1, 100033.

Sivachandran, N., Wang, X., and Frappier, L. (2012). Functions of the Epstein-Barr virus EBNA1 protein in viral reactivation and lytic infection. *J Virol*. 86(11):6146-58.

Skare, J., Edson, C., Farley, J., & Strominger, J. L. (1982). The B95-8 isolate of Epstein-Barr virus arose from an isolate with a standard genome. *J Virol*. *44*(3), 1088–1091.

Skelton, J.K, Ortega-Prieto, A.M., and Dorner, M. (2018). A hitchhiker's guide to humanized mice: new pathways to studying viral infections. *Immunology*. 154(1):50-61.

Slifka, J. Amanna, I.J. (2017). Passive Immunization. In: Plotkin, S., Orenstein, W., Offit, P. Edwards, K.M. (Eds.) *Vaccines.* 7th. Elsevier, Philadelphia, pp. 84-95.

Snijder, J., Ortego, M.S., Weidle, C., Stuart, A.B., Gray, M.D., McElrath, M.J., Pancera, M., Veesler, D., McGuire, A.T. (2018). An Antibody Targeting the Fusion Machinery Neutralizes Dual-Tropic Infection and Defines a Site of Vulnerability on Epstein-Barr Virus. *Immunity*. 48(4):799-811.

Sokal, E.M., Hoppenbrouwers, K., Vandermeulen, C., Moutschen, M., Leonard, P., Moreels, A., Haumont, M., Bollen, A., Smets, F., Denis, M. (2007). Recombinant gp350 vaccine for infectious mononucleosis: a phase 2, randomized, double-blind, placebo-controlled trial to evaluate the safety, immunogenicity, and efficacy of an Epstein-Barr virus vaccine in healthy young adults. *J Infect Dis*. 196(12), 1749-1753.

Speck, P., and Longnecker, R. (1999). Epstein-Barr virus (EBV) infection visualized by EGFP expression demonstrates dependence on known mediators of EBV entry. *Arch Virol*. 144(6):1123-37.

Spriggs, M.K., Armitage, R.J., Comeau, M.R., Strockbine, L., Farrah, T., Macduff, B., Ulrich, D., Alderson, M.R., Müllberg, J., and Cohen, J.I. (1996). The extracellular domain of the Epstein-Barr virus BZLF2 protein binds the HLA-DR beta chain and inhibits antigen presentation. *J Virol*. 70(8):5557-63.

Stanfield, R., and Wilson, I.A. (2014). Antibody structure. *Microbiol Spectr*. 2(2).

Strnad, B.C., Schuster, T., Klein, R., Hopkins, R.F., Witmer, T., Neubauer, R H., and Rabin, H. (1982). Production and characterization of monoclonal antibodies against the Epstein-Barr virus membrane antigen. *J Virol. 41*(1), 258–264.

Strowig, T., Gurer, C., Ploss, A., Liu, Y., Arrey, F., Sashihara, J., Koo, G., Rice, C.M., Young, J.W., Chadburn, A., Cohen, J.I., Munz, C. (2009). Priming of protective T cell responses against virus-induced tumors in mice with human immune system components. *J Exp Med*. 206, 1423-1434.

Su, H., Ye, X., Freed, D.C., Li, L., Ku, Z., Xiong, W., Gao, P., Liu, X., Montgomery, D., Xu, W., Espeseth, A.S., Wang, D., Ma, N., Fu, T.M., Zhang, N., and An, Z. (2021). Potent Bispecific Neutralizing Antibody Targeting Glycoprotein B and the gH/gL/pUL128/130/131 Complex of Human Cytomegalovirus. *Antimicrob Agents Chemother*. 65(3).

Sung, J.A., Pickeral, J., Liu, L., Stanfield-Oakley, S.A., Lam, C.Y., Garrido, C., Pollara, J., LaBranche, C., Bonsignori, M., Moody, M.A., Yang, Y., Parks, R., Archin, N., Allard, B., Kirchherr, J., Kuruc, J.D., Gay, C.L., Cohen, M.S., Ochsenbauer, C., Soderberg, K., Liao, H.X., Montefiori, D., Moore, P., Johnson, S., Koenig, S., Haynes, B.F., Nordstrom, J.L., Margolis, D.M., and Ferrari, G. (2015). Dual-affinity re-targeting proteins direct T cell-mediated cytolysis of latently HIV-infected cells. *J Clin Invest.* 125:4077–4090

Sutton, B.J., Davies, A.M., Bax, H.J., Karagiannis, S.N. (2019). IgE antibodies: from structure to function and clinical translation. *Antibodies*. 8(1):19.

Tan, W., Meng, Y., Li, H., Chen, Y., Han, S., Zeng, J., Huang, A., Li, B., Zhang, Y., and Guo, Y. (2013) A bispecific antibody against two different epitopes on hepatitis B surface antigen has potent hepatitis B virus neutralizing activity. *MAbs*. 5(6); 946-55.

Tanner, J.E., Hu, J., Alfieri, C. (2018). Construction and characterization of a humanized anti-Epstein- Barr virus gp350 antibody with neutralizing activity in cell culture. *Cancers.* 10(4), 112.

Tay, M.Z., Wiehe, K., and Pollara, J. (2019). Antibody-Dependent Cellular Phagocytosis in Antiviral Immune Responses. *Front Immunol*. 10, 332.

Thorley-Lawson, D.A., Poodry, C.A. (1982). Identification and isolation of the main component (gp350-gp220) of Epstein-Barr virus responsible for generating neutralizing antibodies in vivo. *Journal of virology*. 43(2), 730–736.

Tsai, M.H., Raykova, A., Klinke, O., Bernhardt, K., Gartner, K., Leung, C.S., Geletneky, K., Sertel, S., Munz, C., Feederle, R. and Delecluse, H.J. (2013). Spontaneous lytic replication and epitheliotropism define an Epstein-Barr virus strain found in carcinomas. *Cell reports*. 5:458-470.

Tsai, M.H., Lin, X., Shumilov, A., Bernhardt, K., Feederle, R., Poirey, R., Kopp-Schneider, A., Pereira, B., Almeida, R., and Delecluse, H.J. (2017). The biological properties of different Epstein-Barr virus strains explain their association with various types of cancers. *Oncotarget*. 8(6):10238-10254.

Tugizov, S.M., Berline, J.W., and Palefsky, J.M. (2003). Epstein-Barr virus infection of polarized tongue and nasopharyngeal epithelial cells. *Nat Med.* 9(3):307-14.

van Meerten, T., van Rijn, R.S., Hol, S., Hagenbeek, A., and Ebeling, S.B. (2006). Complement-induced cell death by rituximab depends on CD20 expression level and acts complementary to antibody-dependent cellular cytotoxicity. *Clin Cancer Res*. 12(13):4027-35

Walsh, N.C., Kenney, L.L., Jangalwe, S., Aryee, K.E., Greiner, D.L., Brehm, M.A., and Shultz, L.D. (2017). Humanized Mouse Models of Clinical Disease. *Annu Rev Pathol.* 12, 187–215.

Wang, J., Bardelli, M., Espinosa, D.A., Pedotti, M., Ng, T.S., Bianchi, S., Simonelli, L., Lim, E.X.Y., Foglierini, M., Zatta, F., Jaconi, S., Beltramello, M., Cameroni, E., Fibriansah, G., Shi, J., Barca, T., Pagani, I., Rubio, A., Broccoli, V., Vicenzi, E., Graham, V., Pullan, S., Dowall, S., Hewson, R., Jurt, S., Zerbe, O., Stettler, K., Lanzavecchia, A., Sallusto, F., Cavalli, A., Harris, E., Lok, S.M., Varani, L., and Corti, D. (2017). A human bi-specific antibody against Zika virus with high therapeutic potential. *Cell*. 171:229–241.e15

Wei, C.J., Bu, W., Nguyen, L.A., Batchelor, J., Kim, J.H., Pittaluga, S., Fuller, J., Nguyen, H., Chou, T.H., Cohen, J.I., Nabel, G.J. (2022) A bivalent Epstein-Barr virus vaccine induces neutralizing antibodies that block infection and confer immunity in humanized mice. *Science Translational Medicine.* 14 (643): eabf3685

Wistinghausen, B., Gross, T.G., and Bollard, C. (2013). Post-transplant lymphoproliferative disease in pediatric solid organ transplant recipients. *Pediatr Hematol Oncol*. 6, 520-531.

Woof, J.M., Kerr, M.A. (2006). The function of immunoglobulin A in immunity. *J Pathology*. 208(2), 270-282.

Wu, C.R., Kim, H.J., Sun, C.P., Chung, C.Y., Lin, Y.Y., Tao, M.H., Kim, J.H., Chen, D.S., Chen, P.J. (2021). Mapping the conformational epitope of a therapeutic monoclonal antibody against HBsAg by in vivo selection of HBV escape variants. *Hepatology*. 2021 Dec 27.

Wu, L., Hutt-Fletcher, L.M. (2007). Point mutations in EBV gH that abrogate or differentially

affect B cell and epithelial cell fusion. *Virology*. 363(1), 148-155.

Xu, Y., Xu, L., Zhao, M., Xu, C., Fan, Y., Pierce, S.K., and Liu, W. (2014). No receptor stands alone: IgG B-cell receptor intrinsic and extrinsic mechanisms contribute to antibody memory. *Cell Res.* 24, 651–664.

Yajima, M., Imadome, K., Nakagawa, A., Watanabe, S., Terashima, K., Nakamura, H., Ito, M., Shimizu, N., Honda, M., Yamamoto, N., and Fujiwara, S. (2008). A New Humanized Mouse Model of Epstein-Barr Virus Infection That Reproduces Persistent Infection, Lymphoproliferative Disorder, and Cell-Mediated and Humoral Immune Responses. *J Infect Dis*. 198(5), 673– 682.

Yong, K., Her, Z., and Chen, Q. (2018). Humanized Mice as Unique Tools for Human-Specific Studies. *Arch Immunol Ther Exp*. 66(4), 245–266.

Young, L.S., and Murray, P.G. (2003). Epstein-Barr virus and oncogenesis: from latent genes to tumours. *Oncogene.* 22(33):5108-21.

Zhang, H., Li, Y., Wang, H.B., Zhang, A., Chen, M.L., Fang, Z.X., Dong, X.D., Li, S.B., Du, Y., Xiong, D., He, J.Y., Li, M.Z., Liu, Y.M., Zhou, A.J., Zhong, Q., Zeng, Y.X., Kieff, E., Zhang, Z., Gewurz, B.E., Zhao, B., and Zeng, M.S. (2018). Ephrin receptor A2 is an epithelial cell receptor for Epstein-Barr virus entry. *Nat Microbiol*. 3(2):1-8.

Zhu, Q.Y., Shan, S., Yu, J., Peng, S.Y., Sun, C., Zuo, Y., Zhong, L.Y., Yan, S.M., Zhang, X., Yang, Z., Peng, Y.J., Shi, X., Cao, S.M., Wang, X., Zeng, M.S., and Zhang, L. (2021). A potent and protective human neutralizing antibody targeting a novel vulnerable site of Epstein-Barr virus. *Nat Commun.* 12, 6624.